MECHANISMS OF DRUG-INDUCED OXIDATIVE STRESS IN THE HEPATOCYTE INFLAMMATION MODEL

By

Shahrzad Tafazoli

A thesis submitted in conformity with the requirements
for the degree of Doctor of Philosophy
Graduate Department of Pharmaceutical Sciences
University of Toronto

Your file Votre référence
ISBN: 978-0-494-58098-1
Our file Notre référence
ISBN: 978-0-494-58098-1

Abstract

Mechanisms of drug-induced oxidative stress in the hepatocyte inflammation model
Doctor of Philosophy, 2008
Shahrzad Tafazoli
Department of Pharmaceutical Sciences
University of Toronto

Drug induced idiosyncratic agranulocytosis has been attributed to oxidation by hypochlorite formed by bone marrow myeloperoxidase (MPO). Idiosyncratic liver toxicity could also involve drug oxidative activation by cytochrome P450 (in hepatocytes) or MPO (in Kupffer cells or infiltrating neutrophil/macrophages). Such drug reactive metabolites could cause cytotoxicity or release "danger signals" that attract immune cells which release H_2O_2 resulting from nicotinamide adenine dinucleotide phosphate oxidase (NADPH oxidase) activation. *In vivo* animal studies have shown that low level tissue inflammation markedly increased drug-induced tissue toxicity which was prevented by immune cell inhibitors and increased by cell activators. It is suggested that idiosyncratic drugs are much more toxic, taken during symptomless inflammation periods. Furthermore, it is hypothesized that hepatocytes are much more susceptible to some idiosyncratic drugs if they are exposed to hydrogen peroxide (H_2O_2)/myeloperoxidase or cytokines released by inflammatory cells. A hepatocyte inflammation model, in which hepatocytes were exposed to a non-toxic H_2O_2 generating system and peroxidase, was found to be much more vulnerable to four idiosyncratic drugs e.g., troglitazone, isoniazid, hydralazine and amodiaquine. The molecular cytotoxic mechanisms for this marked increase in cytotoxicity were investigated as follows: 1) A P450/H_2O_2-catalyzed pathway not involving oxidative stress e.g., hydralazine and isoniazid; 2) A P450/H_2O_2-catalyzed oxidative stress-mediated cytotoxic pathway e.g., hydrazine (an isoniazid metabolite) and hydralazine; and 3) A peroxidase/H_2O_2-catalyzed oxidative stress-mediated cytotoxic pathway e.g,, hydralazine, amodiaquine and troglitazone. Before cytotoxicity ensued, GSH oxidation, protein carbonyl formation and often lipid peroxidation occurred followed by a decrease in mitochondrial membrane potential indicating that oxidative stress was the molecular mechanism of cytotoxicity. In summary, a H_2O_2-enhanced hepatocyte system in the presence and absence of peroxidase may prove useful for a more robust screening of drugs for assessing the enhanced drug toxicity risk associated with taking drugs during periods of inflammation.

Acknowledgments

I would like to dedicate this work with my heartfelt gratitude to my parents, Simin and Jahan for their love and support. Their words of wisdom while they were miles away from me, in times of stress and frustration, afforded me the enthusiasm to press forward. My special acknowledgment and deepest thank you goes to my beloved husband Giuseppe for his constant support and inspiration without which I would not have been able to write this dissertation.

I would like to express my sincerest gratitude to my supervisor, Dr. Peter J. O'Brien, for his inspiring supervision and patient guidance throughout the course of my study and for leading me into the world of life sciences. His broad knowledge and enthusiasm has set an example for me.

I would like to acknowledge Dr. W. Robert Bruce, Dr. A. Michael Rauth and Dr. Peter Pennefather who have been an essential part of my advisory committee and their suggestions and advice helped in shaping my research. Most notably, I would like to extend my gratitude to Dr. Rauth for giving his time to meticulously appraise my thesis. I would like to thank Dr. Deborah A. Nicoll-Griffith, my external appraiser, and Dr. David Riddick for taking the time to be part of my defense committee.

My experience during my research in Dr. O'Brien's laboratory was enhanced by many stupendous people, without which completion of this dissertation would not have been possible. I am indebted to all of them. Most notably, I would like to extend my thanks to Katie Chan and Rhea Mehta whose support and thoughtfulness and above all, friendship helped make my stressful research moments tolerable and my laboratory experience memorable. I will always cherish our coffee breaks!

Thank you all for your support. Each of you has made a valuable contribution to this work. In the end, though, maybe we must all give up just trying to pay back the people in this world who sustain our lives:

"Maybe it is wise to surrender before the miraculous scope of human generosity and to just keep saying thank you, forever and sincerely, for as long as we have voices." –Elizabeth Gilbert

Table of Contents

List of Abbreviations

ACMS	Accelerated cytotoxic mechanism screening (ACMS)
ADRs	Adverse drug reactions
ALT	Alanine aminotransferase
ANOVA	Analysis of variance
$AscH_2$	Ascorbate
AST	Aspartate aminotransferase
ATP	Adenosine triphosphate
BDE	Bond dissociation energy
BHA	Butylated hydroxyanisole
t-BHP	*tert*-Butyl hydroperoxide
BNPP	bis-*p*-Nitrophenyl phosphate
BSA	Bovine serum albumin
CuZnSOD	Copper/zinc superoxide dismutase
CYP	Cytochrome P450
CYP1A2, CYP2C8	Cytochrome P450 1A2, Cytochrome P450 2C8
DCFH	2',7'-Dichlorofluorescein
DCFH-DA	2',7'-Dichlorofluorescein diacetate
DETAPAC	Diethylenetriamine penta-acetic acid
DMSO	Dimethylsulfoxide
DNA	Deoxyribonucleic acid
DNFB	2′,4′-Dinitrofluorobenzene
DNPH	2',4'-Dinitrophenylhydrazine
DTNB	5,5′-Dithiobis-(2-nitrobenzoic acid) (Ellman's reagent)
ECSOD	Extracellular superoxide dismutase
E_{HOMO}	Energy of the highest occupied molecular orbital
ELISA	Enzyme-linked immunosorbent assay
EPR	Electron paramagnetic resonance
ESR	Electron spin resonance

ER	Endoplasmic reticulum
F	Fischer value, An overall indicator of significance, where the greater the value corresponds to better regression.
FAD	Flavin adenine dinucleotide
FMN	Flavin mononucleotide
FOX 1 reagent	Ferrous oxidation of xylenol orange
G	Glucose
GI	Gastrointestinal tract
GO	Glucose oxidase
GPx	Glutathione peroxidase
GSH	Reduced glutathione
GSSG	Glutathione disulfide (oxidized glutathione)
H_2O_2	Hydrogen peroxide
HEPES	4-(2-Hydroxyethyl)-1-piperazineethanesulfonic acid
$HO_2^{\bullet}$	Hydroperoxyl radical
HOCl	Hypochlorous acid
HPLC	High pressure liquid chromatography
HRP	Horseradish peroxidase
IAA	Indole-3-acetic acid
IDRs	Idiosyncratic drug reactions
LD_{50}/LC_{50}	Dose/concentration of a chemical that produces 50% death of the population (e.g., cells) under study
Log P	Logarithm of partition coefficient
Log LPO	Logarithm of lipid peroxidation
LPS	Lipopolysaccharide
MDA	Malondialdehyde
MnSOD	Manganese Superoxide Dismutase
MOPAC	Molecular orbital package
MPO	Myeloperoxidase
n	Number of observations
NAD	Oxidized nicotinamide adenine dinucleotide

NADH	Reduced nicotinamide adenine dinucleotide
NAD(P)H	Reduced nicotinamide adenine dinucleotide phosphate
NQO	NAD(P)H/quinone oxidoreductase
NSAIDs	Nonsteroidal anti-inflammatory drugs
$O_2^{\bullet-}$	Superoxide anion
$OH^{\bullet}$	Hydroxyl radical
p	Probability, represents statistical significance
$PhO^{\bullet}$	Phenoxyl radical
PhOH	Phenolic compound
PHS	Prostaglandin H synthase
PMC	2,2,5,7,8-Pentamethyl-6-hydroxychromane
PTU	6-*n*-propyl-thiouracil
PUFA	Polyunsaturated fatty acids
$PUFA^{\bullet}$	Lipid radical
$PUFAOO^{\bullet}$	Lipid peroxy radical
$R^{\bullet}$	Reactive free radical
r^2	r-Squared, Statistical measure of how well a regression line approximates real data points; an r-squared of 1.0 (100%) indicates a perfect fit.
ROS	Reactive oxygen species
s	Standard error of the estimate
SARs	Structure-activity relationships
SEM	Standard error of mean
SOD	Superoxide dismutase
TBARS	Thiobarbituric acid reactive substances
TCA	Trichloroacetic acid
TEMPOL	4-Hydroxy-2,2,6,6-tetramethylpiperidene-1-oxyl
TNB	2-Nitro-5-thiobenzoic acid
TNB^{2-}	2-Nitro-5-thiobenzoic acid dianion
$UQ^{\bullet-}$	Ubisemiquinone anion radical
UV	Ultraviolet

List of Tables

List of Figures

Appendix III

List of Publications Relevant to Thesis

1) **<u>Tafazoli, S</u>**. and O'Brien, P. J., 2005. Peroxidases: a role in the metabolism and side effects of drugs. *Drug Discov. Today* 10, 617-625.

This review was an introduction to the hepatocyte inflammation model and has been cited throughout this thesis, but has not been used in its entirety in the thesis. This review was written as per an invitation by the journal *Drug Discovery Today*. The work cited in the review and the major part of the manuscript was written by me.

2) **<u>Tafazoli, S.,</u>** Spehar, D. D., and O'Brien, P. J., 2005. Oxidative stress mediated idiosyncratic drug toxicity. *Drug Metab Rev*. 37, 311-325.

This article was our first attempt to optimize the hepatocyte inflammation model for use in screening hepatotoxic drugs. It has been cited throughout this thesis, but has not been used in its entirety in the thesis. My contribution to this manuscript was carrying out the majority of the experiments and writing the manuscript.

3)* **<u>Tafazoli, S.,</u>** Wright, J. S., and O'Brien, P. J., 2005. Prooxidant and antioxidant activity of vitamin E analogues and troglitazone. *Chem. Res. Toxicol.* 18, 1567-1574.

This work was reproduced with the permission from *Chemical Research in Toxicology* (Chapter 2). My contribution to this study was carrying out the research and writing the manuscript.

4) O'Brien, P. J., **<u>Tafazoli, S.,</u>** Chan, K., Mashregi, M., Mehta, R., and Shangari, N., 2007. A hepatocyte inflammation model for carbonyl induced liver injury: drugs, diabetes, solvents, chlorination. In: Weiner, H., Maser, E., Lindahl, R, and Plapp, B. (Eds.), Purdue University Press. West Lafayette, Indiana, pp. 105-112

This manuscript constitutes the study on some therapeutic drugs forming carbonyl metabolites in the hepatocyte inflammation model. This review was written in combination with an invited oral presentation given at the *Enzymology and Molecular Biology of Carbonyl Metabolism* conference at Nashville, Indiana in July 2006. This manuscript has been cited throughout this thesis, but has not been used in its entirety in the thesis. My contribution to this manuscript was carrying out the experiments on alcohols in the inflammation model and writing parts of the manuscript.

5)* **Tafazoli, S.,** Mashregi, M., and O'Brien, P. J., 2008. Role of hydrazine in isoniazid-induced hepatotoxicity in a hepatocyte inflammation model. *Toxicol. Appl. Pharmacol.* 229, 94-101.

This work was reproduced with the permission from *Toxicology and Applied Pharmacology* (Chapter 3). My contribution to this study was carrying out the research, doing all the analysis and writing the manuscript.

6)* **Tafazoli, S**. and O'Brien, P. J., 2008. Accelerated cytotoxic mechanism screening of hydralazine using an *in vitro* hepatocyte inflammatory cell peroxidase model. *Chem. Res. Toxicol*. 21, 904-910.

This work was reproduced with the permission from *Chemical Research in Toxicology* (Chapter 4). My contribution to this study was carrying out the research, doing all the analysis and writing the manuscript.

7) ***Tafazoli, S**. and O'Brien, P. J., Amodiaquine-induced oxidative stress in a hepatocyte inflammation model. Submitted to *Toxicology*.

My contribution to this study was carrying out the research, doing all the analysis and writing the manuscript (Chapter 5).

* References that are used as Chapters in the thesis.

Chapter 1

General Introduction

This introduction covers four major topics. The first part introduces “Accelerated Cytotoxic Mechanism Screening (ACMS)”, as a screening system to determine the molecular cytotoxic mechanism of drugs or xenobiotics when they are incubated with freshly isolated hepatocytes from Sprague-Dawley male rats. The second topic, deals with drug or xenobiotic-induced reactive oxygen species (ROS), their sources of production within hepatocytes, the hepatocyte defense mechanisms against ROS-mediated injuries and also ROS as mediators of oxidative stress and lipid peroxidation. The theme of ROS-mediated oxidative stress is carried out throughout all the chapters of the thesis. The third part of the introduction covers the role of Kupffer cells and inflammation in mediating adverse drug reactions with a focus on idiosyncratic drug reaction. This leads to the last part of the introduction which introduces the use of hepatocytes in an *in vitro* inflammation model, which can be used as a tool for screening the cytotoxic mechanism of some drugs known for idiosyncratic hepatotoxicity.

1.1 Isolated hepatocytes in studying drug-induced hepatotoxicity

The liver is the chief organ involved in the metabolism of xenobiotics. Xenobiotic compounds are taken up by hepatocytes and metabolized to pharmacologically inactive, active or sometimes toxic products. Liver parenchymal cells are richly endowed with drug-metabolizing enzymes which are conveniently divided into two groups. Phase I reactions generally include oxidative, reductive and hydrolytic processes. Oxidation is usually catalyzed by cytochrome P450-dependent monooxygenases located in the endoplasmic reticulum (ER). Phase I reactions provide the necessary functional group for Phase II reactions, which are generally conjugations with sulfate or glucuronic acid (Guillouzo et al, 1993). The complexity of hepatic metabolic processes makes it difficult to distinguish the primary effects of a compound. This explains why many investigators have turned to simpler models than the whole animal for studying drug metabolism and other liver functions. The most frequently used and simpler liver preparations include isolated perfused organs, subcellular fractions and isolated hepatocytes.

Isolated hepatocytes and hepatocyte suspensions are a successful example of a cellular model that is used routinely during the development of new drugs and in the investigation of metabolic or toxic effects of xenobiotics (Castell et al, 2006; Davila and Morris, 1999; LeCluyse, 2001). Primary hepatocytes represent a unique system since they are able to retain Phase I and II enzyme activities, as well as the inducibility of Phase I and II enzymes by xenobiotics (Davila and Morris, 1999).

1.2 Accelerated cytotoxic mechanism screening (ACMS) with hepatocytes

The accelerated cytotoxicity mechanism screening (ACMS) method determines the molecular cytotoxic mechanisms of drugs or xenobiotics when incubated for 2 hours with freshly isolated hepatocytes from Sprague-Dawley male rats. ACMS is useful for identifying the hepatocyte metabolizing enzymes by comparing the effects of specific inhibitors of metabolizing enzymes in modulating the loss of cell viability caused by the drug/xenobiotic being investigated. This functionomic approach is useful for understanding the molecular cytotoxic mechanism, e.g., the effects of metabolizing enzyme inhibitors or substrates on the loss of cell viability induced by the drug/xenobiotic were investigated. The following procedures have been used:

1) Determine the concentration of drug/xenobiotics required to induce a 50% loss of membrane integrity (LD_{50}) of freshly isolated rat hepatocytes in 2 hrs using the trypan blue exclusion assay. A major assumption with ACMS was that high dose/short time (*in vitro*) exposure simulates low dose/long time (*in vivo*) exposure. With 24 halobenzenes, it was found that the relative LD_{50}

concentration required to cause 50% cytotoxicity in 2 hrs determined with hepatocytes isolated from phenobarbital-induced Sprague-Dawley rats correlated with hepatotoxicity *in vivo* at 24-54 h (Chan et al, 2007). Moreover, using these techniques the molecular hepatocytotoxic mechanisms found *in vitro* for seven classes of xenobiotics/drugs were found to be similar to the rat hepatotoxic mechanisms reported *in vivo* (O'Brien et al, 2004).

2) The effect on the cytotoxic effectiveness of xenobiotics by inhibiting or inducing metabolizing enzymes which activate or detoxify the xenobiotic was then determined. In this way, the major metabolic pathways and metabolizing enzymes of xenobiotics can be rapidly identified. Although it is generally agreed that hepatocytes are the gold standard for hepatic drug metabolism, ACMS techniques were used to show that the drug metabolic pathways at cytotoxic drug concentrations *in vitro* in 2 hrs were similar to those that occur *in vivo* in 24-36 hrs (Chan et al, 2007; O'Brien et al, 2004).

3) The hepatocyte molecular cytotoxic mechanism of xenobiotics is determined by following the changes in bioenergetics (ATP, mitochondrial membrane potential, respiration, glycogen depletion), oxidative stress (GSH/GSSG levels, lactate/pyruvate ratio, and ROS formation), and electrophile stress (GSH conjugates, protein/DNA adducts). If oxidative stress caused the cytotoxicity, then it should precede cytotoxicity and antioxidants, ROS scavengers or redox therapy should prevent or delay the cytotoxicity. If not, then the oxidative stress likely occurred as a secondary result of the cytotoxicity. If mitochondrial toxicity caused the cytotoxicity, then glycolytic substrates should be protective and the membrane potential should be restored.

1.3 Biochemistry of Reactive Oxygen Species (ROS)

The term “free radical” describes a chemical species that has one or more unpaired electrons. Oxygen readily reacts to form partially reduced species, which are generally short-lived and highly reactive. Oxygen free radicals are products of many biological redox reactions. ROS include radical species, such as 1) Superoxide anion ($O_2^{\bullet-}$), formed through one electron reduction of O_2:

$$O_2 + e^- \rightarrow O_2^{\bullet-}$$

2) Hydrogen peroxide (H_2O_2), which is the non radical oxidant (it has no unpaired electrons), is formed by several metabolic reactions. For instance, the dismutation reaction of $O_2^{\bullet-}$ catalyzed by superoxide dismutases (SOD), which has as an intermediate the hydroperoxyl radical ($HO_2^{\bullet}$):

$$O_2^{\bullet-} + H^+ \rightarrow HO_2^{\bullet}$$

$$2HO_2^{\bullet} \rightarrow H_2O_2 + O_2$$

3) The hydroxyl radical ($OH^{\bullet}$) that can be formed from either the superoxide anion (Haber-Weiss reaction) or from H_2O_2:

$$O_2^{\bullet-} + H_2O_2 \rightarrow O_2 + OH^- + OH^{\bullet} \quad \text{(Haber-Weiss reaction)}$$

$$Fe^{2+} + H_2O_2 \rightarrow Fe^{3+} + OH^- + OH^{\bullet} \quad \text{(Fenton reaction)}$$

Although other transition metal ions are capable of catalyzing this reaction, the iron-catalyzed Fenton reaction is now considered to be the major mechanism by which the highly reactive hydroxyl radical is generated in biological systems (Liochev, 1999). $OH^{\bullet}$ is, perhaps, the most toxic from of oxygen as it is highly reactive; therefore it reacts indiscriminately at, or close to, the site of its formation with most molecules that it encounters (Yu, 1994). This is why this radical is unlikely to function as a signaling molecule, while both $O_2^{\bullet-}$ and H_2O_2, which are less reactive and therefore longer-lived, are more appropriate for intra- and even extracellular signaling (Bright and Porter, 1975; Saran et al, 2000).

In addition to H_2O_2, some non-radical species also ascribed to ROS, are hypochlorous acid (HOCl), a powerful antimicrobial agent, fatty acid hydroperoxides and reactive aldehydes (Halliwell and Gutteridge, 1985).

1.4 Sources of ROS

ROS can be derived from numerous sources *in vivo.* These include autooxidation, photochemical and enzymatic reactions, and may involve both endogenous compounds and various xenobiotics. For example, quinones can undergo redox cycling, generating large amounts of ROS without themselves being degraded (O'Brien, 1991). Enzymatic sources include NADPH oxidases located on the cell membrane of polymorphonuclear cells, macrophages and endothelial cells (Babior, 2000) and cytochrome P450 (CYP)-dependent oxygenases (Coon et al, 1992). The proteolytic conversion of xanthine dehydrogenase to xanthine oxidase during the ischemic period provides another enzymatic source for both $O_2^{\bullet-}$ and H_2O_2 (Parks et al, 1988), and has been proposed to mediate deleterious processes *in vivo* (Yokoyama et al, 1990). Other endogenous and exogenous sources of ROS are described below.

1.4.1 Mitochondrial sources of ROS

Perhaps the most important *in vivo* source of ROS is the mitochondrion (Boveris and Cadenas, 1975; Loschen et al, 1971). The mitochondrial electron transport chain contains several redox centers, which may leak electrons to molecular oxygen, serving as the primary source for $O_2^{\bullet-}$ production in most tissues (Ott et al, 2007). Mitochondrial electron transport generates $O_2^{\bullet-}$ as an inevitable by-product and primary ROS at two complexes, Complex I and III (Brand et al, 2004; Cadenas and Davies, 2000). There is growing evidence that most of the $O_2^{\bullet-}$ generated by intact mammalian mitochondria *in vitro* is produced by Complex I (NADH-coenzyme Q). This $O_2^{\bullet-}$ production occurs primarily on the matrix side of the inner mitochondrial membrane (de Vries, 1986). Significant $O_2^{\bullet-}$ production in Complex I was observed with succinate in the absence of endogenous Complex I substrates. This ROS formation was due to reversed electron transfer (Kushnareva et al, 2002; Liu et al, 2002b) and was inhibited by rotenone, an inhibitor of Complex I (Lambert and Brand, 2004a; Lambert and Brand, 2004b). Complex III contributed to $O_2^{\bullet-}$ generation by auto-oxidation of the ubisemiquinone anion radical ($UQ^{\bullet-}$), in which one-electron reduction of oxygen by $UQ^{\bullet-}$ causes $O_2^{\bullet-}$ formation. Complex III releases $O_2^{\bullet-}$ to both sides of the inner membrane (Cadenas and Davies, 2000; Muller et al, 2004).

1.4.2 Cytochrome P450 enzymes

Another major source of ROS, especially in the liver, is a group of enzymes called the CYP mixed function oxidases. These are membrane bound terminal oxidases present mainly in the endoplasmic reticulum (ER) as components of a multi-enzyme system, which also includes the flavin adenine dinucleotide/flavin mononucleotide (FAD/FMN)-containing NADPH-P450 reductase and cytochrome *b5.* They provide substrate oxidation reactions (oxidation, peroxidation, and/or reduction in O_2 and NADPH-dependent manner) of a structurally diverse group of xenobiotics and endogenous substances (Ortiz de Montellano, 1995).

Active cytochromes (CYPs) produce ROS, namely $O_2^{\bullet-}$ and H_2O_2, that may arise in two ways. The first possibility is the formation of ROS as intermediates in the CYP-mediated catalytic cycle, where O_2 is reduced instead of being added to the substrate (Jezek and Hlavata, 2005). The second possibility is that an electron can escape to O_2 from flavins in the NADPH:P450 reductase enzyme (Jezek and Hlavata, 2005). Therefore, CYPs should also be considered as a significant source of ROS and intracellular signals, not only via participation in metabolic pathways, but also via ROS-mediated signaling (Jezek and Hlavata, 2005).

1.4.3 Peroxisomes

Peroxisomes are subcellular, single, membrane-bound respirator organelles that are present in virtually all eukaryotic cells, and carry out a wide range of essential functions, including β-oxidation of fatty acids, biosynthesis of cholesterol, bile acids, and metabolism of ROS (van den Bosch et al, 1992). Peroxisomes were characterized initially by the presence of several H_2O_2-generating flavine oxidase, together with H_2O_2-degrading catalase (Singh, 1997). In contrast to mitochondria, peroxisomal β-oxidation is not coupled with oxidative phosphorylation. Rather, oxygen is stoichiometrically converted into H_2O_2, and peroxisomal oxidase activity has been estimated to consume between 10-30% of the oxygen consumed by the liver (De Duve and Baudhuin, 1966). Over 90% of oxygen consumed by mitochondrial cytochrome oxidase is reduced by a $4e^-$ reduction to form H_2O with the rest forming $O_2^{\bullet-}$. By contrast, the oxygen consumed by peroxisomes is mostly converted to H_2O_2 and a relatively small amount to $O_2^{\bullet-}$ with no H_2O formed (Singh, 1996). If catalase is not efficient then H_2O_2 may escape from peroxisomes. The morphological and biochemical changes that occur during peroxisomal proliferation are thought to result from such an increase in the synthesis of H_2O_2 with only a small increase in H_2O_2 degradation by catalase (Singh, 1996). This process can happen under various other conditions. For example, during aging, peroxisomal ROS increases, while its catalase function may decrease, so that peroxisomes may become a source of cytosolic ROS (Singh, 1996).

1.4.4 Phagocytic NADPH oxidase

Activated macrophages and neutrophils can produce large amounts of $O_2^{\bullet-}$, H_2O_2 and its derivatives via the phagocyte isoform of NADPH oxidase. The enzyme is a heme-containing protein complex illustrated schematically in Figure1.1:

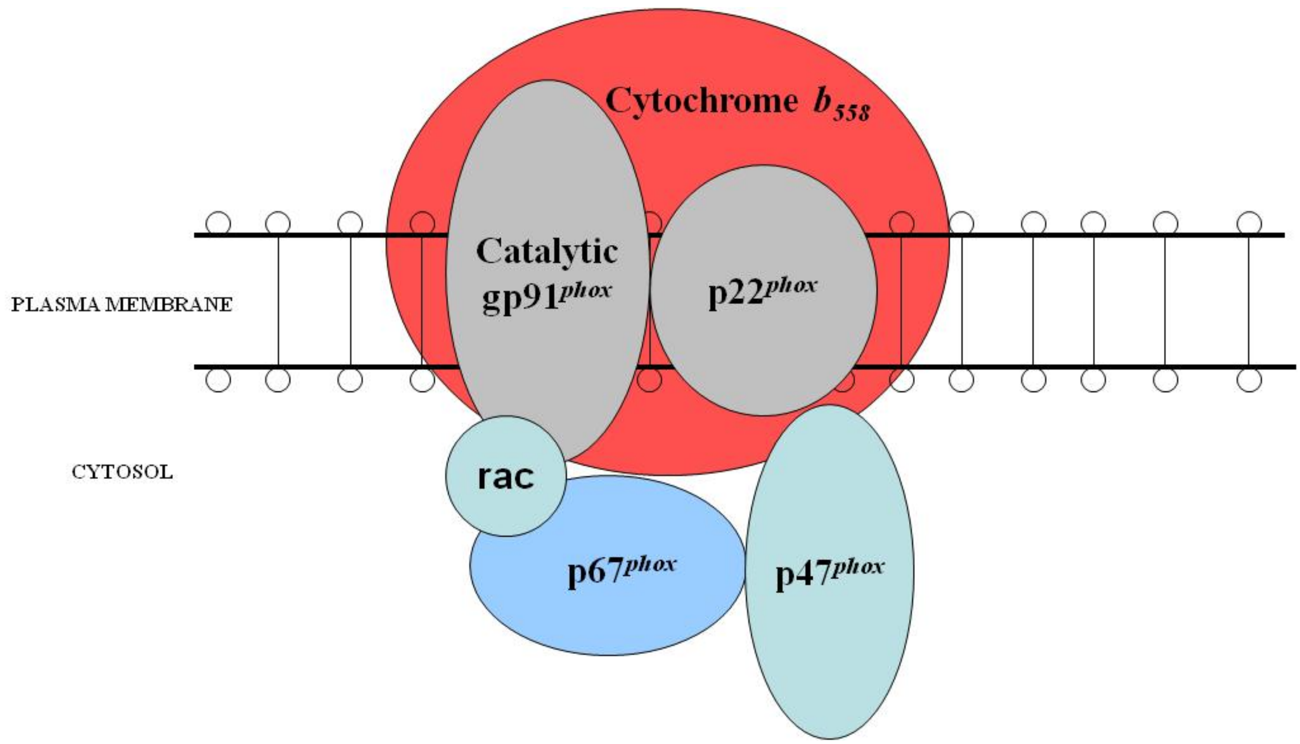

Figure 1.1 Structure of neutrophil NAD(P)H oxidase
The enzyme consists of the membrane-bound cytochrome b_{558} complex comprising gp91^{phox} and p22^{phox}, the cytosolic proteins p47^{phox} and p67^{phox}, and a low-molecular weight G protein of the rac family (Droge, 2002; Griendling et al, 2000).

In an inflammatory response H_2O_2 is produced by activated macrophages at an estimated rate of 2-6 × 10^{-14} mol.h^{-1} $cell^{-1}$ and may reach a concentration of 10-100 μM in the vicinity of these cells (Keisari et al, 1983; Nathan and Root, 1977). The massive production of antimicrobial ROS in an inflammatory environment is called the "respiratory burst" and plays an important role as a first line of defense against environmental pathogens. Phagocytic NADPH oxidase becomes activated upon translocation of cytosolic p47^{phox}, p67^{phox} and a G protein of the rac family to the membrane-bound cytochrome b_{558} complex. The cytochrome b_{558} complex carries a flavin-adenine dinucleotide (FAD) and two heme prosthetic groups that catalyze the NADPH-dependent reduction of O_2 to from $O_2^{\bullet-}$. The flavocytochrome b_{558} comprises two protein subunits, the larger of the two is gp91^{phox} and the smaller is referred to as p22^{phox} (Griendling et al, 2000; Lambeth et al, 2000; Shatwell and Segal, 1996). The physiological relevance of NADPH oxidase as a defense enzyme is suggested by the observation that mice lacking the NADPH oxidase components gp91^{phox} or p47^{phox} exhibit reduced resistance to infection (Dinauer et al, 1997). The activation of phagocytic NADPH oxidase can be induced by microbial products such as bacterial lipopolysaccharide (LPS), lipoproteins, or by cytokines such as interferon-γ or interleukin-1β (Bonizzi et al, 2000).

The combined activities of NADPH oxidase and myeloperoxidase (MPO), in phagocytes leads to the production of hypochlorous acid (HClO), the strongest physiological oxidant and antimicrobial agent (Hampton et al, 1998).

The major endogenous and exogenous sources of ROS have been summarized in Figure 1.2:

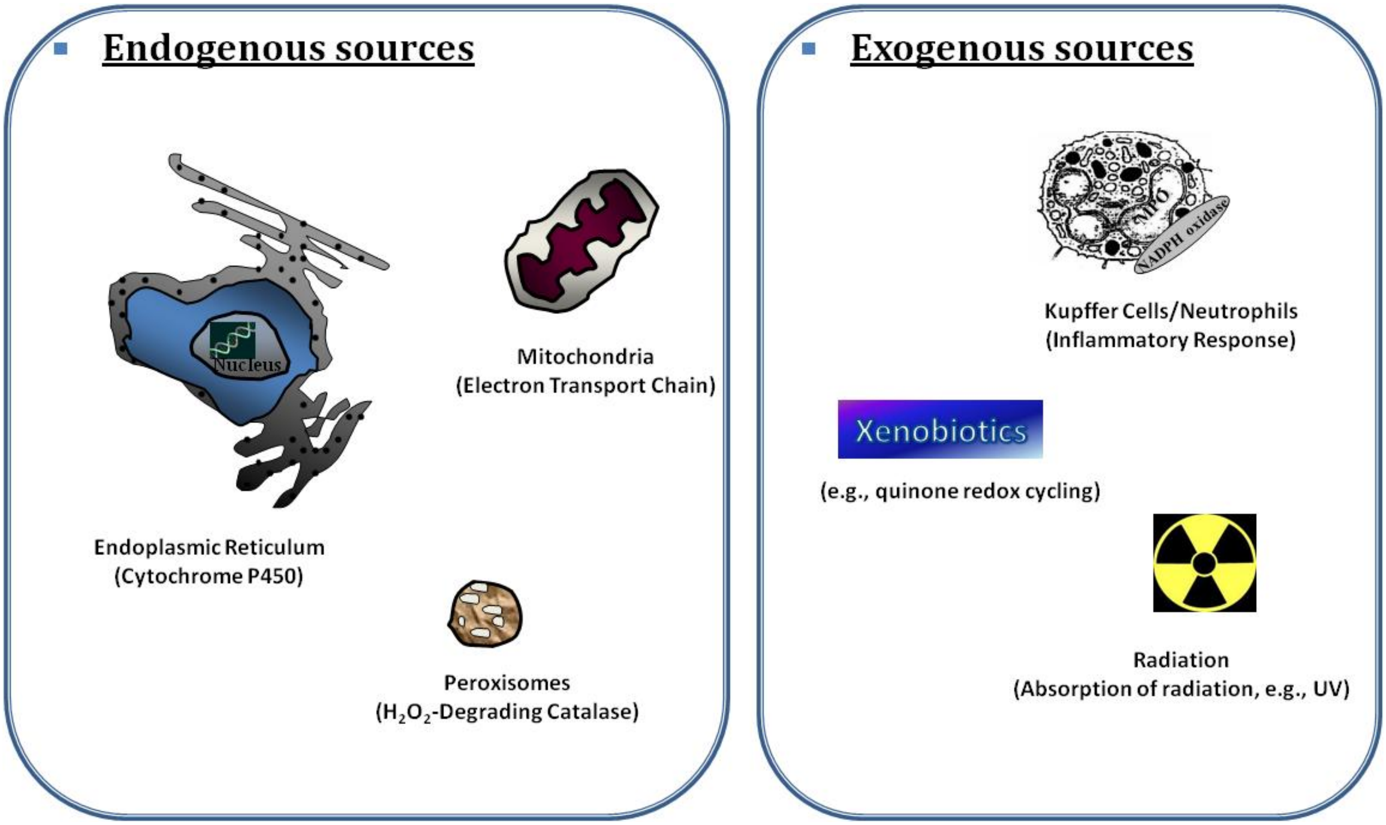

Figure 1.2 Endogenous and exogenous sources of ROS production
ROS can be produced by both endogenous and exogenous sources. The endogenous sources of ROS are peroxisomes (the H_2O_2 detoxyfying process by catalase), mitochondrial electron transport chain, cytochrome P450 and inflammatory cells. The exogenous sources of ROS are radiation, and xenobiotics.

1.5 ROS detoxification

ROS have been implicated in a variety of pathologies, including cancer, atherosclerosis, chronic inflammatory processes, and multiple neurodegenerative diseases (Droge, 2002). In addition, they play a regulatory role in cellular metabolic processes by activation of various enzymatic cascades as well as several transcription factors (Khan and Wilson, 1995). Free radicals and reactive non-radical species derived from radicals exist in biological cells and tissues at low but measurable concentrations (Halliwell and Gutteridge, 2002). Low levels of ROS can modulate gene expression, growth factor and second messenger signaling during cellular activation (Droge, 2002; Remacle et al, 1995). Their concentrations are determined by the balance between their rates of production and clearance by various antioxidant compounds and enzymes. Antioxidants have been defined as substances that are able, at relatively low concentrations, to compete with other oxidizable substrates and thus, to significantly delay or inhibit the oxidation of these substrates (Halliwell and Gutteridge, 1985). These substances are divided into enzymatic and non-enzymatic antioxidants. This definition includes the following enzymes:

1) Superoxide dismutase (SOD) is one of the body's most important defense mechanisms against free-radical damage. There are three forms of SOD: the manganese containing SOD (MnSOD) which is located in the mitochondrial matrix and the more ubiquitous SOD, containing copper and zinc (CuZnSOD) located in the cytosol, the extracellular space and the mitochondtial inner membrane (Fridovich, 1995). The third form and the so-called extracellular SOD (ECSOD) is present on the surface of the cells and also contains a copper-zinc prosthetic group (Fridovich, 1995). SOD catalyzes the dismutation of $O_2^{\bullet-}$ to form H_2O_2 as shown below:

$$2O_2^{\cdot -} + 2H^+ \xrightarrow{SOD} H_2O_2 + O_2$$

2) Glutathione peroxidase (GPx) with six isoenzymes (GPx-1 - GPx-6), is a selenium-dependent enzyme and is located in the cytoplasm and mitochondria (Lei et al, 2007). GPx-1 is the most abundant selenoperoxidase and is ubiquitously expressed in almost all tissues (Cheng et al, 1997; Cheng et al, 1998). All GPx isoenzymes use GSH to catalyze the reduction of H_2O_2 and lipid hydroperoxides (Lei et al, 2007):

$$H_2O_2 + 2GSH \xrightarrow{GPx} GSSG + 2\ H_2O$$

3) Catalase is a heme-containing enzyme located in peroxisomes which metabolizes H_2O_2 to form water and oxygen, but unlike GPx cannot metabolize lipid peroxides (Singh, 1997).

$$2H_2O_2 \xrightarrow{Catalase} 2H_2O + O_2$$

The body is also equipped with numerous non-enzymatic endogenous antioxidants such as α-tocopherol (vitamin E), β-carotene, ascorbate (vitamin C), and glutathione (GSH). GSH is an endogenous tripeptide (glutamyl-cysteinyl-glycine) that serves as a cofactor for an enzyme called glutathione-S-transferase, which catalyzes the enzymatic conjugation and biotransformation of xenobiotics.

The schematic shown in Figure 1.3 summarizes pathways involved in ROS production and detoxification:

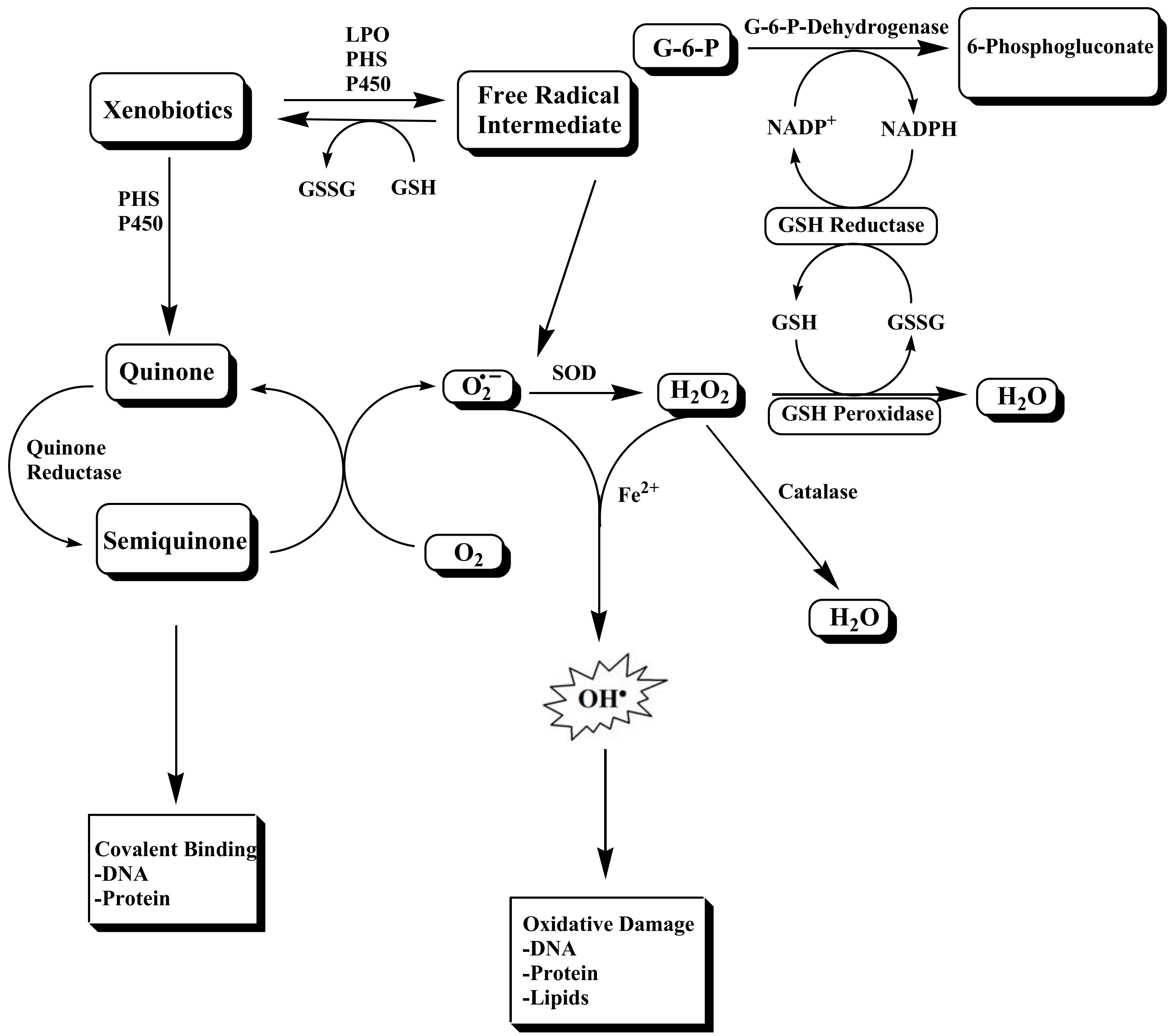

Figure 1.3 Pathways of ROS production and clearance (modified from (Hayes and McLellan, 1999)

LPO: lipoxygenases; PHS: prostaglandin H synthase; G-6-P: glucose-6-phosphate. Under normal conditions, ROS are cleared from the cell by the action of superoxide dismutase (SOD), catalase, or glutathione (GSH) peroxidase. The main damage to cells results from the ROS-induced alteration of macromolecules such as polyunsaturated fatty acids in membrane lipids, essential proteins, and DNA. Additionally, oxidative stress and ROS can originate from xenobiotic bioactivation by prostaglandin H synthases (PHSs) and lipoxygenases (LPOs) or microsomal P450s which can oxidize xenobiotics to free radical intermediates that react directly or indirectly with oxygen to produce reactive oxygen species and oxidative stress.

1.6 ROS-induced injury

1.6.1 Oxidative stress

Oxidative stress occurs when the concentration of ROS generated exceeds the antioxidant capability of the cell. In other words, oxidative stress describes various deleterious processes resulting from an imbalance between the excessive formation of ROS and limited antioxidant defenses. Whilst small fluctuations in the steady-state concentration of these oxidants may actually play a role in intracellular signaling (Droge, 2002), uncontrolled increases in the concentration of these oxidants lead to free radical-mediated chain reactions which indiscriminately target proteins (Stadtman and Levine, 2000), lipid (Rubbo et al, 1994) and DNA (Richter et al, 1988). Oxidative stress plays an important role in many human diseases or complications associated with atherosclerosis (Cook, 2006), diabetes mellitus (Brownlee, 2005), Parkinson's (Gandhi and Wood, 2005) and Alzheimer's disease (Hajieva and Behl, 2006), ischemia-reperfusion injury (Hayashi et al, 2004) and carcinogenesis (Valko et al, 2006).

1.6.2 Lipid peroxidation

Lipid peroxidation in tissues and in tissue fractions represents a degradation process which is the consequence of the production and the propagation of free radical reactions primarily involving membrane polyunsaturated fatty acids (PUFA) (Poli et al, 1987; Slater, 2008). Highly reactive free radicals ($R^{\bullet}$) derived from some chemical agents are capable of abstracting hydrogen atoms from PUFA on phospholipid membranes, resulting in the formation of a lipid radical ($PUFA^{\bullet}$). Reaction with oxygen yields the corresponding peroxy radical ($PUFAOO^{\bullet}$) and chain propagation ensues, leading ultimately to degradation of the lipid to a range of products including aldehydes or gases such as ethane and pentane as shown in Figure 1.4 (Cheeseman, 2008).

The peroxidative breakdown of PUFA has been implicated in the pathogenesis of many types of liver injury in which free radical intermediates are produced in excess of local defense mechanisms. It involves hepatic damage induced by several toxic substances such as carbon tetrachloride (Comporti et al, 1965), trichlorobromomethane (Slater, 2008), chloroform (Ekstrom and Hogberg, 1980) and halothane (Tomasi et al, 1983).

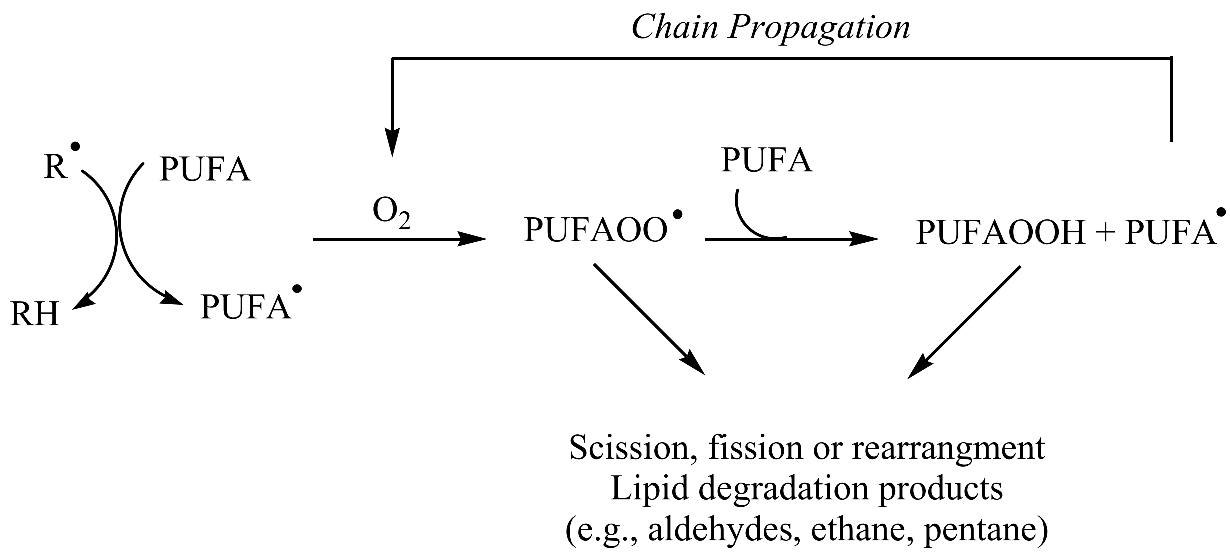

Figure 1.4 Schematic diagram of the process of lipid peroxidation
R•: reactive free radicals; RH: drug/xenobiotics; PUFA: polyunsaturated fatty acids; PUFA•: lipid radical; PUFAOO•: lipid peroxy radical
R• derived form xenobiotics starts a chain reaction by abstracting hydrogen atoms from PUFA, which leads to the formation of PUFA• and its subsequent reaction with oxygen to yield the corresponding PUFAOO• and the chain propagation. This ultimatedly results in the degradation of lipid to a wide variety of products including aldehydes and gases such as ethane and pentane (Cheeseman, 2008).

1.6.3 Role of Kupffer cells and other inflammatory cells in mediating hepatic injury

The liver consists of the hepatic parenchyma and non-parenchymal cells including sinusoidal endothelial cells, Ito cells, and the hepatic macrophages known as the Kupffer cells. The sinusoidal endothelial cells and the sinusoidal space form a barrier, which serves to divide the liver into functional compartments. Kupffer cells are able to traverse this barrier and are able to pass in and out of the hepatic space facilitating their signaling functions (Roberts et al, 2007). Central to this signaling role is the ability of Kupffer cells to respond to local changes by the release of cytokines and other signaling molecules such as ROS. This activation appears to modulate acute hepatocyte injury as well as chronic liver responses (Roberts et al, 2007). Inhibition of Kupffer cell function or depletion of Kupffer cells appears to protect against liver injury from the alkylating agent melphalan (Kresse et al, 2005), the mycotoxin fumonissin B_1 (He et al, 2005), and the industrial chemical thioacetamide (Andres et al, 2003).

1.7 Inflammation and adverse drug reactions (ADRs)

Drugs have been estimated to account for one-third to one-half of acute liver failures. Of these, about 80% of drug toxicities are predictable ADRs resulting from drug–drug interactions, dosages too high for a susceptible patient, and direct toxicity by drug/metabolites or simple pharmacokinetics for the susceptible patient.

Individual susceptibility plays an important role in determining whether or not a person develops an untoward drug reaction. Among the potential determinants of susceptibility are age, gender, co-existing disease, co-exposure to other xenobiotic agents, nutritional status, tissue reserve capacity, and drug metabolism differences. In addition, recent evidence from experimental models suggests that an episode of inflammation during drug treatment predisposes animals to tissue injury (Buchweitz et al, 2002; Luyendyk et al, 2002). This raises the possibility that the presence or absence of inflammation is another susceptibility factor for drug toxicity in humans. This observation presents at least two challenges: The first challenge is to define the role of inflammation in drug toxicity. The second challenge, is to develop models or methods to predict which drugs or drug candidates have the potential to cause toxicity through interaction with inflammation. This knowledge could allow identification of individuals who are susceptible and a better understanding of the confluence of events required for this type of adverse response.

Inflammatory episodes are common in people and animals and are precipitated by numerous stimuli such as bacteria, viruses and exposure to toxins produced by microorganisms. Moreover, episodes of inflammation can be precipitated by the mammalian gastrointestinal (GI) tract. In particular, endotoxin or its lipopolysacharide (LPS) component released from Gram- negative bacteria can translocate across the intestinal mucosa into portal venous circulation (Roth et al, 1997). The cell walls of Gram-negative bacteria contain and release a biologically active component of endotoxin. The rate of LPS translocation and magnitude of exposure can be modulated by disturbance of the gastrointestinal tract or liver, dietary changes (e.g., protein-deficient diets), alcohol consumption, surgical trauma and other conditions (Roth et al, 1997).

Before drug-induced liver injury occurs *in vivo*, an inflammatory response usually occurs and cells other than hepatocytes (e.g., Kupffer cells) become activated. Immune cells (e.g., neutrophils and macrophages) also infiltrate the liver. Numerous studies with animals have shown that a modest inflammatory response enhanced tissue susceptibility to xenobiotics. Therefore, it was hypothesized that commonplace inflammation episodes during drug therapy decreased the threshold for drug toxicity and, thereby, markedly increased the individual's susceptibility to some drugs (Roth et al, 1997). Kupffer cells, and resident liver macrophages normally play a role in protecting hepatocytes from xenobiotics by phagocytozing incoming particles and releasing cytoprotective cytokines (Roberts et al, 2007). Kupffer cell inhibitors, e.g., gadolinium chloride, also prevented hepatotoxicity induced by some hepatotoxic drugs, whereas Kupffer cell activators, e.g., retinol or LPS, markedly enhanced hepatotoxicity induced by acetaminophen, allyl alcohol, diethyldithiocarbamate, halobenzenes, and CCl_4 (Buchweitz et al, 2002; Roth et al, 2003).

It is generally thought that most hepatotoxins are activated by oxidation catalysed by the endoplasmic reticular (ER) mixed function oxidase activity consisting of hepatocyte P450, NADPH, P450 reductase and oxygen. However, peroxidase and H_2O_2 can also oxidatively activate some drugs. Whilst there is little peroxidase activity in hepatocytes, myeloperoxidase was located by immunochemistry in Kupffer cells that are resident macrophages of the human and rodent liver (Brown et al, 2001). Furthermore neutrophil infiltration of the liver in response to inflammation can result in a 50 to 100-fold increase in hepatic myeloperoxidase activity (Kato et al, 2000). Indeed, peroxidase activity is a useful marker for measuring neutrophil/macrophage infiltration as well as the hepatic inflammatory response. Eosinophil infiltration (e.g., following a parasite infection) can also cause a marked increase in liver eosinophil peroxidase activity (Gharib et al, 1999). During the inflammatory response H_2O_2 was also formed by activation of the NADPH oxidase in the infiltrated cells. It is therefore reasonable to suggest that the large increase in drug liver susceptibility could also be attributed to peroxidase catalysed drug oxidation to form reactive pro-oxidant radicals that are toxic to hepatocytes. Drug-induced tissue toxicity is often preceded by infiltration of the tissues by neutrophils, e.g., indomethacin-induced kidney toxicity. This results in a marked increase in hepatic oxygen radicals generated by neutrophils and a sevenfold increase in hepatic myeloperoxidase activity (Basivireddy et al, 2004).

1.8 Idiosyncratic drug reactions (IDRs) and *in vitro* hepatocyte inflammation model

IDRs occur in less than 0.1% of the general population but account for approximately 14,000 deaths in North America annually. More than 75% of cases of IDRs result in liver transplantation or death (Ostapowicz et al, 2002). IDRs appear to be independent of dose, and the onset of injury varies relative to the onset of drug treatment. Each year new drugs have to be withdrawn from the market or their use is severely restricted because they are found to be associated with a risk of idiosyncratic toxicity.

There are two conventional hypotheses to explain IDRs. One is that the reactions occur as a consequence of drug metabolism polymorphisms, which result in different levels of toxic drug metabolites among patients (Williams and Park, 2003). The other one argues that they arise from a specific immune response to a hapten formed by a drug or its metabolites (Pirmohamed et al, 2002). However, convincing evidence for this hypothesis is lacking for the majority of drugs associated with idiosyncratic toxicity. It is equally plausible that other unrecognized events render tissues susceptible to toxicity during drug therapy. Unfortunately, the mechanisms of idiosyncratic reactions are poorly understood despite the large number of drugs associated with these reactions. One of the most common targets of idiosyncratic drug toxicity is the liver.

In order to simulate the marked increase of drug-induced hepatotoxicity caused by inflammation *in vivo,* and assess the potential *in vivo* hepatotoxicity risk of various drugs, we used an *in vitro* hepatocyte screening system. In this system, glucose and glucose oxidase were used for the continuous infusion of H_2O_2, in the absence and presence of horseradish peroxidase

(HRP). HRP was used to effect *in situ* activation of drugs and to simulate myeloperoxidase. Although HRP and myeloperoxidase are not homologous in structure, the catalytically active amino acid residues are positioned in a similar manner (Welinder, 1985) and the metabolites produced are qualitatively similar (Eastmond et al, 1986). HRP belongs to the heme-containing plant analogue peroxidases which contain an iron(III)protoporphyrin prosthetic group at their catalytic site (O'Brien, 2000). The H_2O_2 acts by increasing the oxidation state of the ferric ion which then oxidizes the peroxidase substrates. Furthermore, HRP is a mannose-terminated glycoprotein (Clarke and Shannon, 1976), and is believed to be taken up by fluid-phase endocytosis by hepatocytes (Scharschmidt et al, 1986; Straus, 1981).

Using this model, we were able to mimic the products formed by the inflammatory immune cells and study the mechanism of inflammation-enhanced drug-induced cytotoxicity.

1.9 Hypotheses

Hypothesis 1: *Drugs such as troglitazone, isoniazid, hydralazine and amodiaquine, developed for chronic use, cause oxidative stress when oxidized by H_2O_2 or peroxidase/H_2O_2 to phenoxyl, hydrazyl or semiquinone radicals. In the absence of peroxidase/H_2O_2, these drugs are much less cytotoxic and the cytotoxicity mechanisms do not involve oxidative stress.*

Hypothesis 2: *Drugs or xenobiotic radicals can increase cell vulnerability to inflammation by increasing H_2O_2 formation or by decreasing cellular resistance to H_2O_2.*

1.10 Organization of thesis chapters

As discussed previously, a modest inflammatory response can enhance tissue sensitivity to a variety of chemicals. These observations have led to the hypothesis that inflammation during therapy may decrease the threshold for toxicity and render an individual susceptible to a reaction that might not otherwise occur, or if it occurred might not be serious. To date there are no predictive models to assess the potential of new drug candidates to cause idiosyncratic toxicities.

In the following chapters, the *in vitro* mechanism and toxicity of known idiosyncratic drugs in a hepatocyte inflammation model were investigated, in order to correlate their clinical toxicological profile with their *in vitro* metabolic and toxicological profile. Using this *in vitro* hepatocyte screening method in Chapter 2, the antioxidant and pro-oxidant activities of 6 vitamin E analogues (2,2,5,7,8-pentamethyl-6-hydroxychromane (PMC), Trolox C, α-tocopherol, γ-tocopherol, δ-tocopherol) as well as the idiosyncratic drug, troglitazone were compared. Troglitazone was first introduced to the market in 1997 for the treatment of insulin-resistant diabetes. Shortly after its approval, reports of the liver toxicity were received, resulting in a black box warning which ultimately led to the withdrawal of the drug in March 2000 (Gale, 2001).

In Chapter 3, attention is focused on the anti-tuberculosis drug, isoniazid, which was associated with a high incidence of hepatic injury and received a black box warning in 1969 (Black et al, 1975). In the *in vitro* hepatocyte inflammation model, we assessed the involvement of hydrazine, a major isoniazid metabolite, by studying the molecular mechanism of isoniazid-induced cytotoxicity.

In Chapter 4, the cytotoxic mechanism of hydralazine, an antihypertensive drug, in the hepatocyte inflammation model was investigated. Hydralazine long-term use has also been associated with incidences of hepatitis and an autoimmune syndrome resembling systemic lupus erythematosus (Cameron and Ramsay, 1984; Itoh et al, 1981).

In Chapter 5, the cytotoxic mechanisms of an antimalarial drug, amodiaquine, was investigated. Amodiaquine use had been associated with life-threatening agranulocytosis and hepatotoxicity in about 1 in 2000 patients (Rwagacondo et al, 2003).

Finally, in Chapter 6, a conclusion and summary highlights the findings of this thesis research and identify H_2O_2, a cellular mediator of inflammation, with peroxidase as potential risk factors for the manifestation of adverse drug reactions, especially the reactions associated with IDRs.

Chapter 2

Pro-oxidant and Antioxidant Activity of Vitamin E Analogues and Troglitazone

---

Shahrzad Tafazoli, James S. Wright and Peter J. O'Brien

Reproduced with permission from *Chemical Research in Toxicology* 2005, 18: 1567-1574.

2.1 Abstract

The order of antioxidant effectiveness of low concentrations of vitamin E analogues, in preventing cumene hydroperoxide-induced hepatocyte lipid peroxidation and cytotoxicity, was 2,2,5,7,8-pentamethyl-6-hydroxychromane (PMC) > troglitazone > Trolox C > α-tocopherol > γ-tocopherol > δ-tocopherol. However, vitamin E analogues, including troglitazone at higher concentrations, induced microsomal lipid peroxidation when oxidized to phenoxyl radicals by peroxidase/H_2O_2. Ascorbate or glutathione (GSH) was also co-oxidized, and GSH co-oxidation by vitamin E analogues phenoxyl radicals was also accompanied by extensive oxygen uptake and oxygen activation. When oxidized by non-toxic concentrations of peroxidase/H_2O_2, vitamin E analogues except PMC also caused hepatocyte cytotoxicity, lipid peroxidation, and GSH oxidation. The pro-oxidant order of vitamin E analogues in catalyzing hepatocyte cytotoxicity, lipid peroxidation, and GSH oxidation was troglitazone > Trolox C > δ-tocopherol > γ-tocopherol > α-tocopherol > PMC. A similar order of effectiveness was found for GSH co-oxidation or microsomal lipid peroxidation but not for ascorbate co-oxidation. Except for troglitazone, the toxic pro-oxidant activity of vitamin E analogues was therefore inversely proportional to their antioxidant activity. The high troglitazone pro-oxidant activity could be a contributing factor to its hepatotoxicity. We have also derived equations for three-parameter structure-activity relationships (SARs), which described the correlation between antioxidant and pro-oxidant activity of vitamin E analogues and their lipophilicity (log P), ionization potential (E_{HOMO}), and dipole moment.

2.2 Introduction

Phenolics are one of the major groups of nonessential dietary components that have been associated with the inhibition of atherosclerosis and cancer (Decker, 1997). They are chemical compounds characterized by at least one aromatic ring bearing one or more hydroxyl groups. Tocopherols are a class of lipophilic, phenolic compounds of plant origin. The major tocopherol found in mammalian tissue is α-tocopherol. Vitamin E (α-tocopherol) is the major lipid soluble antioxidant of lipoproteins and biomembranes, and its antioxidant activity relies on its effectiveness at donating hydrogen from the hydroxyl group of the chromanol ring to reactive chain-propagating radicals, to yield a phenoxyl radical ($PhO^{\bullet}$). Electron spin resonance (ESR) studies showed that $PhO^{\bullet}$ oxidized ascorbate ($AscH_2$) and other biomolecules to radicals (Sharma and Buettner, 1993). However, under some specific conditions, the $PhO^{\bullet}$ of vitamin E exerted pro-oxidant activity, e.g., lipoprotein oxidation (Bowry et al, 1995). Furthermore, a recent meta-analysis study of more than 135,000 participants in 19 published randomized, controlled clinical trials has reported increased mortality among adult patients with chronic diseases taking high dose vitamin E supplementation of ≥400 U/day for at least a year. The pooled risk difference for high dosage vitamin E trials reported was 34 per 10,000 patients (Miller et al, 2005).

Trolox C, a phenolic antioxidant originally designed for food preservation, has a chromane structure similar to α-tocopherol but without the polyisoprenoid hydrophobic tail (Figure 2.1). Trolox C is the most hydrophilic vitamin E analogue (Metodiewa et al, 1999) and has been studied chemically for its stabilizing radical-trapping activity (Davies et al, 1988).

PMC (2,2,5,7,8-pentamethyl-6-hydroxy chromane) is a vitamin E analogue in which the phytyl chain is replaced by a methyl group. PMC is less hydrophilic than Trolox C but is more hydrophilic than other α-tocopherol derivatives and has potent radical scavenging activity (Suzuki and Packer, 1993).

Troglitazone, a 2,4-thiazolidinedione with a chromane structure similar to α-tocopherol, was introduced to the market in 1997 for the treatment of type II diabetes. However, approximately 1.9% of patients developed severe hepatic problems with elevated serum transaminase activities. In some severe cases, troglitazone caused fulminant hepatic failures leading to death. Because of numerous reports of liver failure including severe hepatotoxicity and idiosyncratic liver failure, troglitazone was withdrawn from the market in 2002. However, the hepatotoxic mechanisms of troglitazone are unknown (Smith, 2003).

Previously, we showed that phenols and dietary polyphenolics (flavonoids) with a phenolic B ring were metabolized by peroxidase and catalytic amounts of H_2O_2 to form pro-oxidant $PhO^{\bullet}$, which catalyzed the co-oxidation of $AscH_2$, GSH, or reduced nicotinamide adenine dinucleotide (NADH). Reactive oxygen species (ROS) were formed when GSH or NADH was co-oxidized (Galati et al, 2002a; O'Brien, 1988). Electron paramagnetic resonance (EPR) studies were used to show that etoposide, a phenolic anticancer drug, was oxidized by myeloperoxidase/H_2O_2 in HL-60 cells to $PhO^{\bullet}$, which caused oxidative stress toxicity by oxidizing GSH and protein thiols (not phospholipids) and enhancing etoposide-induced topoisomerase II-DNA covalent complex formation (Kagan et al, 2001). The $PhO^{\bullet}$ formed when HL-60 cells were incubated with phenol caused oxidation of intracellular GSH, $AscH_2$, and phospholipids (Ritov et al, 1996). However, although $PhO^{\bullet}$ formed from the vitamin E analogue PMC oxidized $AscH_2$ to semidehydroascorbate ($Asc^{\bullet -}$) radicals, intracellular GSH, protein thiols, and phospholipids were not oxidized (Kagan et al, 2003).

Recently, we have shown that indole-acetic acid derivatives or NSAID drug-induced cytotoxicity towards hepatocytes was markedly increased by non-cytotoxic concentrations of peroxidase/H_2O_2 as a result of GSH oxidation and lipid peroxidation (Galati et al, 2002b; Tafazoli and O'Brien, 2004). In this study, we have shown that in a cell-free system, vitamin E analogues and particularly troglitazone but not PMC, when oxidized to $PhO^{\bullet}$ by peroxidase/H_2O_2, induced microsomal lipid peroxidation as well as GSH and $AscH_2$ oxidation. Furthermore, these vitamin E analogues also caused hepatocyte cytotoxicity and lipid peroxidation and GSH oxidation when oxidized by non-toxic concentrations of peroxidase/H_2O_2. The order of toxic effectiveness was troglitazone > Trolox C > δ-tocopherol > γ-tocopherol > α-tocopherol > PMC. The order of antioxidant and cytoprotective activity of lower concentrations of vitamin E analogues at preventing hepatocyte oxidative stress, however, was inversely related to their pro-oxidant activity with the exception of troglitazone. However, troglitazone had the most pro-oxidant activity, was the most toxic of the tocopherol analogues, but was also an effective antioxidant.

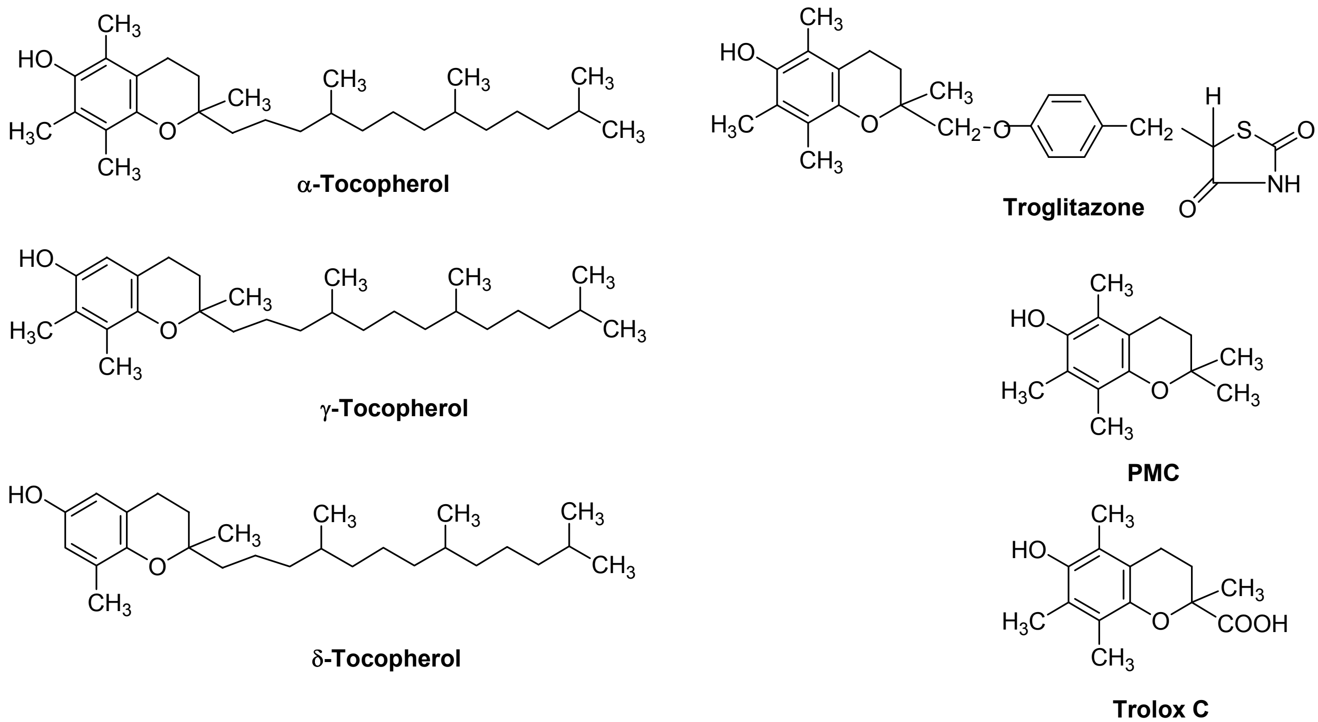

Figure 2.1 Structures of the vitamin E analogues used

2.3 Material and methods

2.3.1 Chemicals

α-Tocopherol, δ-tocopherol, PMC, Trolox C, glucose (G), glucose oxidase (GO), peroxidase from horseradish [EC 1.11.1.7; donor, hydrogen peroxide oxidoreductase, horseradish peroxidase (HRP)], hydrogen peroxide (H_2O_2), butylated hydroxyanisole (BHA), β-nicotinamide adenine dinucleotide (reduced form, β-NADH), L-ascorbic acid, thiobarbituric acid, trichloroacetic acid, 2,4-dinitrofluorobenzene, iodoacetic acid, glutathione (reduced form, GSH), and cumene hydroperoxide were purchased from Sigma-Aldrich Canada (Oakville, Ontario). Collagenase (from Clostridium histoloticum) and 4-(2-Hydroxyethyl)-1-piperazineethanesulfonic acid (HEPES) were purchased from Boehringer-Mannheim (Montreal, Canada). Troglitazone was purchased from Toronto Research Chemicals. γ-Tocopherol was kindly provided by Dr. K. U. Ingold who received the material as a gift from Henkel Corporation (Chicago, U.S.A).

2.3.2 Determination of NADH co-oxidation

To determine the rate of NADH co-oxidation by vitamin E analogue $PhO^{\bullet}$, the reaction mixtures contained 1 mL of 0.1 M Tris-HCl buffer, pH 7.4 [containing 2 mM diethylenetriamine penta-acetic acid (DETAPAC)], 10 μM vitamin E analogue, 100 μM NADH, 100 μM H_2O_2, and 0.01 μM HRP. The rate of NADH oxidation was then measured at 340 nm using a Pharmacia Biotech Ultrospec 1000 (England).

2.3.3 Determination of $AscH_2$ co-oxidation

To determine the rate of $AscH_2$ co-oxidation by vitamin E analogue $PhO^{\bullet}$, the reaction mixture contained 1 mL of 0.1 M Tris-HCl buffer, pH 7.4 (containing 2 mM DETAPAC), 10 μM vitamin E analogue, 50 μM $AscH_2$, 50 μM H_2O_2, and 0.01 μM HRP. The rate of $AscH_2$ oxidation was then measured at 266 nm using a Pharmacia Biotech Ultrospec 1000 (England).

2.3.4 Determination of oxygen uptake and GSH co-oxidation

Oxygen consumption was measured in a 2 mL reaction chamber using a Clarke type electrode (Yellow Springs, U.S.A) at room temperature (20 °C). GSH (400 μM), H_2O_2 (100 μM), and vitamin E analogue (100 μM) were added to the chamber containing 0.1 Tris-HCl buffer, pH 7.4 (containing 2 mM DETAPAC). The reaction was initiated by the addition of 0.1 μM peroxidase.

2.3.5 Microsomal preparation

Adult male Sprague-Dawley rats, 250-300 g, were anesthetized by sodium pentobarbital (60 mg/kg body). Livers were removed under sterile conditions and perfused with KCl solution (1.18% w/v, 4 °C). Hepatic microsomes were prepared by differential centrifugation as previously described (Dallner, 1978). The microsomal pellet was suspended and homogenized in sterile potassium phosphate buffer:KCl solution [50 mM KH_2PO_4 and 0.23% (w/v) KCl, pH 7.4] before storage at -70 °C. Microsomal protein was measured by the method of Joly et al. (Joly et al, 1975). Care and treatment of the rats were in compliance with the guidelines of the Canadian Council on Animal care, and the protocol was approved by the University of Toronto Animal Care Committee.

2.3.6 Isolation of hepatocytes and cytotoxicity determination

Hepatocytes were obtained by collagenase perfusion of the liver of male Sprague-Dawley rats Charles River Laboratories, Montréal, Canada) as described previously (Moldeus et al, 1978). Approximately 85-90% of the hepatocytes excluded trypan blue. Cells were suspended at a density of 10^6 cells/mL in round-bottomed flasks in a water bath maintained at 37 °C in Krebs-Henseleit buffer, pH 7.4, and supplemented with 12.5 mM HEPES under an atmosphere of 95 O_2:5% CO_2. Cell viability was determined by measuring the exclusion of trypan blue (final concentration 0.1% w/v). Hepatocytes were preincubated for 30 min prior to the addition of chemicals. Stock solutions of chemicals were prepared fresh prior to use. Hepatocyte cytotoxicity was determined by the trypan blue exclusion test (Moldeus et al, 1978) as the percentage of cells that take up trypan blue at 2 h following the addition of the vitamin E analogues to the hepatocytes.

2.3.7 Determination of microsomal or hepatocyte lipid peroxidation

Microsomal lipid peroxidation was determined by measuring the amount of thiobarbituric acid reactive substances (TBARS) at 532 nm, formed during the decomposition of lipid hydroperoxides using a Pharmacia Biotech Ultrospec 1000. Briefly, the reaction mixture contained 1 mL of 0.1 M potassium phosphate buffer (containing 2 mM DETAPAC), microsomes (1 mg/mL protein), 100 µM vitamin E derivative, 0.1 µM HRP, 0.5 U/mL glucose oxidase, and 10 mM glucose. Glucose and glucose oxidase were added as a H_2O_2 generator system. The test tubes containing the reaction mixture were then incubated at 37 °C in a water bath with agitation. At different time points, each test tube was treated with 250 µl trichloroacetic acid (70% w/v) and 1 mL thiobarbituric acid (0.8% w/v). The suspension was then boiled for 20 min and read at 532 nm. Alternatively, hepatocyte lipid peroxidation was measured by treating 1 mL aliquots of hepatocyte suspension (10^6 cell/mL) with trichloroacetic acid (70% w/v) and thiobarbituric acid (0.8% w/v) as described (Smith et al, 1982).

2.3.8 HPLC analysis of hepatocyte GSH/glutathione disulfide (GSSG)

Hepatocyte GSH and GSSG contents were measured by HPLC analysis of deproteinized samples (5% metaphosphoric acid), after derivatization with iodoacetic acid and 2,4-dinitrofluorobenzene, by high-performance liquid chromatography (HPLC), using a C18μ Bondapak NH_2 column (Waters Associates, Mildford, MA, U.S.A) (Reed et al, 1980). GSH and GSSG were used as external standards. A Waters 6000A solvent delivery system equipped with a model 600 solvent programmer, a Wisp 710 automatic injector, and a Data Module were used for analysis.

2.3.9 Structure-Activity Relationships (SAR)

SAR equations were derived using Hansch analysis (Hansch et al, 1968), which correlates physicochemical parameters of the vitamin E analogues with their antioxidant and pro-oxidant activities, measured as the amount of lipid peroxidation at 1 h when cells treated with 20 and 100 μM chemicals, respectively (Log lipid peroxidation (LPO) , mM). This type of analysis requires that a congeneric class of compounds (i.e., compounds with a common substructure) be used in derivation of the SAR equation. The analyses were carried out using log P (lipophilicity), representing the octanol/water partition coefficient of the vitamin E analogues, ionization potential (E_{HOMO}), which is comparable to the ease of oxidation or redox potential of the compound, as well as dipole moment. These parameters were derived using MOPAC 2002 in

BioMedCAche 6.1.1 (Fujitsu, U.S.A) after structures were optimized using PM3 Hamiltonian parameters (Table 2.1). The statistical parameters used in the present study validating the SAR equation are as follows: n, the number of observations on which the equation is based; r^2, correlation coefficient; s, standard error of the estimate; and *p*, statistical significance. The most significant SAR equations are those that contained higher r^2, F ratio, and $p < 0.05$.

Table 2.1 Physico-chemical parameters used to derive SAR for vitamin E analogues pro-oxidant and antioxidant activity

Vitamin E Analogues		E_{HOMO} (eV)	Log P	Dipole Moment (D)
1	α-Tocopherol	-8.37	9.60	0.87
2	γ-Tocopherol	-8.42	9.13	1.01
3	δ-Tocopherol	-8.49	8.67	1.31
4	PMC	-8.30	3.78	0.85
5	TroloxC	-8.60	3.23	1.43
6	Troglitazone	-8.49	4.87	1.90

E_{HOMO}: ionization potential; log P: lipophilicity. These parameters were derived using MOPAC 2002 in BioMedCAche 6.1.1 (Fujitsu, U.S.A) after structures were optimized using PM3 Hamiltonian parameters.

2.3.10 Statistical analysis

Statistical significance of difference between control and treatment groups in these studies was determined using one-way analysis of variance (ANOVA). Results represent the means ± standard errors of mean (SEM) of triplicate samples. The minimal level of significance chosen was $p < 0.05$.

2.4 Results

The pro-oxidant activity of the $PhO^{\bullet}$ formed by the peroxidase-catalyzed oxidation of the following vitamin E derivatives, α-tocopherol, γ-tocopherol, δ-tocopherol, PMC, troglitazone, and Trolox C, has been compared. As shown in Table 2.2, vitamin E analogues at concentrations as low as 20 μM inhibited cumene hydroperoxide-induced hepatocyte lipid peroxidation and cytotoxicity. The order of antioxidant activity of vitamin E analogues was PMC > troglitazone > Trolox C > α-tocopherol > γ-tocopherol > δ-tocopherol.

Table 2.2 Antioxidant activity of low concentrations of vitamin E analogues

Addition	**Hepatocyte Lipid peroxidation (μM)**	**Cytotoxicity (%Trypan blue uptake)**
Incubation time (min)	***60***	***120***
Control (only hepatocytes)	0.096 ± 0.005	20 ± 1
+ Cumene hydroperoxide 90 μM	1.89 ± 0.1	85 ± 4
+ δ-Tocopherol 20 μM	1.54 ± 0.08	72 ± 5
+ γ-Tocopherol 20 μM	1.35 ± 0.08*	55 ± 3*
+ α-Tocopherol 20 μM	1.12 ± 0.06*	50 ± 2*
+ Trolox C 20 μM	0.64 ± 0.05*	47 ± 2*
+ Troglitazone 20 μM	0.32 ± 0.02*	45 ± 1*
+ PMC 20 μM	0.21 ± 0.01*	33 ± 2*

The results shown represent the average of three separate experiments ± S.D.
*$p < 0.05$ compared to cumene hydroperoxide-treated hepatocytes.

Vitamin E analogues contain the chromane ring of vitamin E, which can be oxidized to a $PhO^{\bullet}$ in the presence of a peroxidase/H_2O_2 system (Kagan et al, 2003). Previously, our laboratory showed that the $PhO^{\bullet}$ of other phenols co-oxidized GSH and $AscH_2$ (Galati et al, 2002a; O'Brien, 1988). As shown in Table 2.3, addition of catalytic amounts of vitamin E analogues resulted in a marked increase in the oxidation of GSH or $AscH_2$ by peroxidase/H_2O_2 at pH 7.4. At pH 7.4, $AscH_2$ or GSH alone was slowly oxidized by HRP/H_2O_2. GSH oxidation but not $AscH_2$ co-oxidation was accompanied by extensive oxygen uptake (Table 2.3). H_2O_2 formed by GSH co-oxidation contributed to the peroxidase reaction as only catalytic amounts of H_2O_2 were required to oxidize GSH (results not shown). The order of effectiveness of vitamin E analogues in catalyzing GSH or $AscH_2$ co-oxidation was troglitazone > Trolox C > δ-tocopherol > γ-tocopherol > α-tocopherol. PMC was best at catalyzing $AscH_2$ oxidation and poorest at catalyzing GSH oxidation. No NADH oxidation occurred with the vitamin E analogues in the absence or presence of peroxidase/H_2O_2.

To assess whether the pro-oxidant activity of the $PhO^{\bullet}$ of vitamin E analogues could result in lipid peroxidation, rat microsomes were incubated with vitamin E analogues in the presence of peroxidase and H_2O_2 (generated by glucose/glucose oxidase). As shown in Table 2.3, lipid peroxidation was induced by vitamin E analogues at pH 7.4 and little lipid peroxidation occurred in the absence of vitamin E analogues. No malondialdehyde formation was detected when vitamin E derivatives were incubated with microsomes in the absence of glucose/glucose oxidase/HRP system. The order of efficiency of vitamin E analogues in catalyzing microsomal lipid peroxidation was troglitazone > Trolox C > δ-tocopherol > γ-tocopherol > α-tocopherol > PMC.

Table 2.3 Pro-oxidant activity of vitamin E analogues

Addition	Ascorbate oxidation (k x 10^3 min^{-1})	NADH oxidation (k x 10^3 min^{-1})	Microsomal Lipid Peroxidation (μM) *60 min*	$GSH:O_2$ (μM min^{-1})
Control	62 ± 3	23 ± 1	0.16 ± 0.01	<2
+ Troglitazone	713± 38*	24 ± 1	0.91 ± 0.06*	25 ± 1*
+ Trolox C	224± 11*	27 ± 1	0.74 ± 0.05*	23 ± 1*
+ δ-Tocopherol	125 ± 6*	26 ± 1	0.48 ± 0.05*	18 ± 1*
+ γ-Tocopherol	117 ± 5*	24 ± 1	0.39 ± 0.04*	15 ± 1*
+ α-Tocopherol	101 ± 5*	24 ± 1	0.31 ± 0.03*	12 ± 1*
+ PMC	762 ± 35*	26 ± 1	0.18 ± 0.01	7 ± 1*

The results shown represent the average of three separate experiments ± S.D.
* $p < 0.05$ compared to control (buffer only)

As shown in Table 2.4, incubation of Trolox C, α-tocopherol, troglitazone, δ-tocopherol, or γ-tocopherol with isolated rat hepatocytes in the presence of peroxidase/H_2O_2 system resulted in cytotoxicity and lipid peroxidation. The antioxidant, BHA was cytoprotecitve and it also prevented lipid peroxidation. However, PMC in the presence of peroxidase/H_2O_2 did not induce lipid peroxidation and was not cytotoxic. The peroxidase/H_2O_2 system alone was not cytotoxic and did not induce lipid peroxidation at the concentrations used. Trolox C, α-tocopherol, γ-tocopherol, δ-tocopherol, and troglitazone but not PMC caused hepatocyte GSH depletion in the peroxidase/H_2O_2 system, and GSH was oxidized to GSSG.

Table 2.4 Cytotoxic effects of vitamin E analogues pro-oxidant radicals

Addition	Cytotoxicity (% trypan blue uptake)	Hepatocyte Lipid Peroxidation (μM)	Hepatocyte GSH and GSSG (nmol/10^6 cells)	
			GSH	*GSSG*
Incubation time (min)	***120***	***60***	***60***	
Control (only hepatocytes)	21 ± 1	0.18 ± 0.01	52 ± 2	2 ± 1
+ H_2O_2 generating system + HRP	25 ± 1	0.24 ± 0.01	44 ± 2	8 ± 2
+ Troglitazone 100 μM	35 ± 2	0.28 ± 0.01	47 ± 2	2 ± 1
+ H_2O_2 generating system + HRP	63 ± 3*	0.64 ± 0.03*	21 ± 1*	21 ± 2*
+ Trolox C 100 μM	24 ± 1	0.22 ± 0.01	51 ± 3	3 ± 1
+ H_2O_2 generating system + HRP	54 ± 3*	0.50 ± 0.02*	38 ± 2	18 ± 3*
+ BHA 50 μM	23 ± 1**	0.21 ± 0.01**	49 ± 2**	9 ± 1**
+ δ-Tocopherol 100 μM	26 ± 2	0.19 ± 0.01	50 ± 3	3 ± 1
+ H_2O_2 generating system + HRP	59 ± 3*	0.42 ± 0.02*	33 ± 2*	16 ± 3*
+ γ-Tocopherol 100 μM	27 ± 2	0.17 ± 0.01	49 ± 2	3 ± 2
+ H_2O_2 generating system + HRP	58 ± 3*	0.35 ± 0.02*	35 ± 2	15 ± 3*
+ α-Tocopherol 100 μM	24 ± 2	0.16 ± 0.01	50 ± 2	2 ± 1
+ H_2O_2 generating system + HRP	47 ± 2*	0.29 ± 0.01	38 ± 1	12 ± 1
+ PMC 100 μM	23 ± 1	0.19 ± 0.01	49 ± 2	2 ± 1
+ H_2O_2 generating system + HRP	27 ± 2	0.21 ± 0.02	43 ± 1	7 ± 1

The results shown represent the average of three separate experiments ± S.D.

* $p < 0.05$ compared to H_2O_2 generating system/HRP.

** $p < 0.05$ compared to vitamin E analogue + H_2O_2 generating system/HRP.

As shown in Table 2.5, we also derived three-parameter SAR equations (Eqs 1 and 2) to describe the correlation between the antioxidant and the pro-oxidant activity of vitamin E analogues and their lipophilicity (log P), ionization potential (E_{HOMO}), and dipole moment.

Table 2.5 SAR models derived for vitamin E analogues pro-oxidant and antioxidant activity

SAR equation	*n*	r^2	$r^{2adj.}$	*s*	F	*p*
Antioxidant activity (Eq. 1)						
Log LPO (mM) = -22.693 – (2.642 * E_{HOMO}) + (0.103 * Log *P*) – (0.372 * Dipole moment)	6	0.990	0.974	0.056	63.1	0.016
Pro-oxidant activity (Eq. 2)						
Log LPO (mM) = -10.970 - (1.186 * E_{HOMO}) + (0.0162 * Log *P*) + (0.403 * Dipole moment)	6	0.975	0.939	0.063	26.5	0.037

n: number of observations; *s*: standard error of the estimate, which is the sum of squared differecens between observed and calculated values; r^2: correlation coefficient; $r^{2adj.}$: adjusted r^2, which takes into account the number of independent variables used to derive the relationship; F: F-value, an overall indicator of significance; *p*: statistical signifiance

In Figure 2.2a, the experimental values for antioxidant activity of vitamin E analogues (Log lipid peroxidation (Log LPO)) were plotted against the values calculated by Eq 1. Similarly, Figure 2.2b shows the experimental Log LPO values for pro-oxidant activity of vitamin E analogues verses their calculated values using Eq 2.

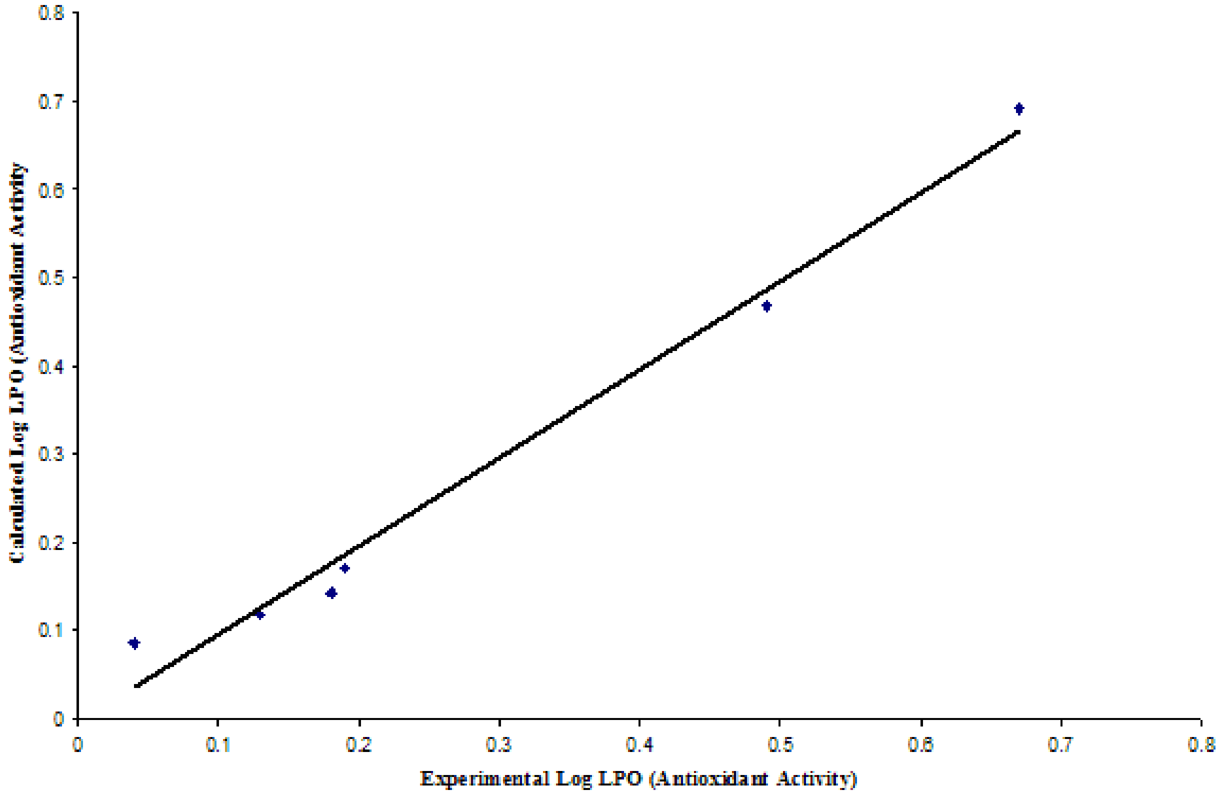

Figure 2.2a Calculated versus experimental log LPO values (antioxidant activity) for hepatocytes treated with vitamin E analogues

The line represents Eq. (1):

Log LPO (mM) = -22.693 – (2.642 * E_{HOMO}) + (0.103 * Log P) – (0.372 * Dipole moment)

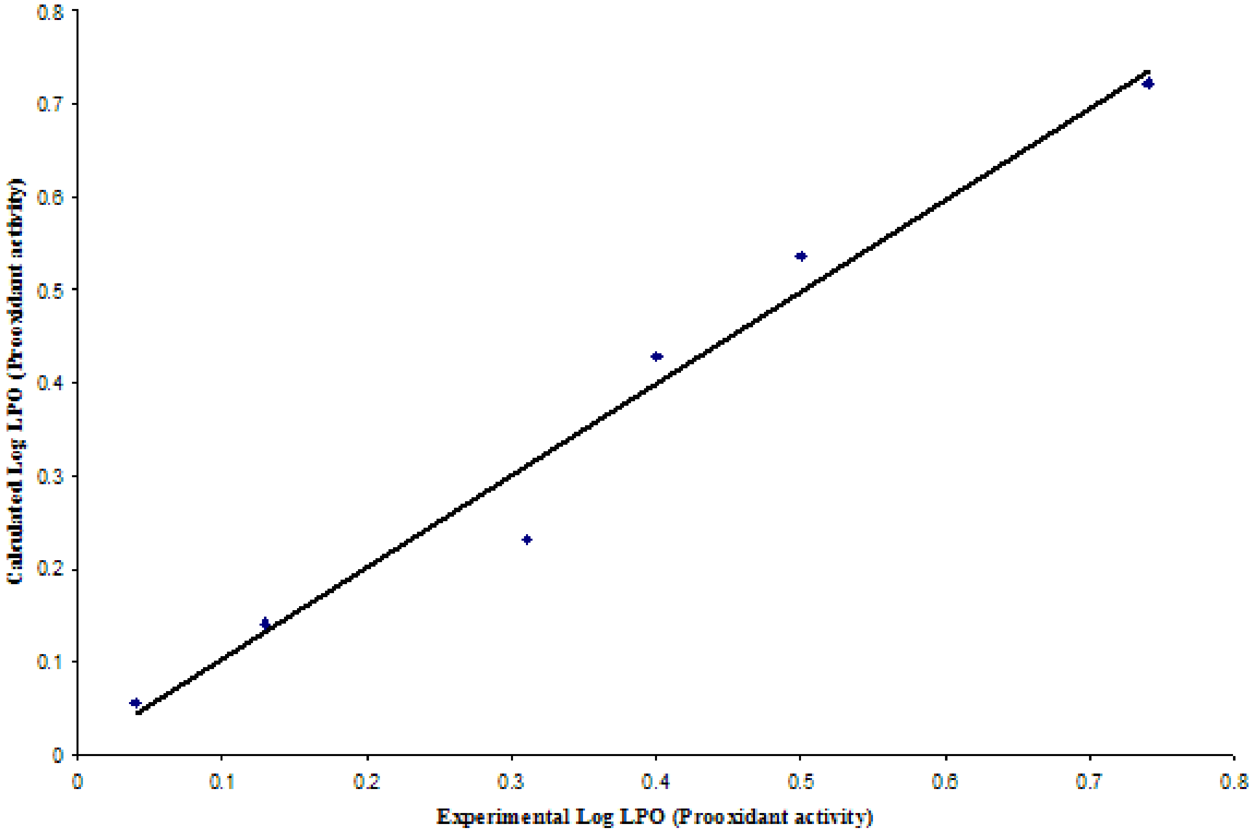

Figure 2.2b Calculated versus experimental log LPO values (pro-oxidant activity) for hepatocytes treated with vitamin E analogues

The line represents Eq. (2):

Log LPO (mM) = -10.970 - (1.186 * E_{HOMO}) + (0.0162 * Log P) + (0.403 * Dipole moment)

2.5 Discussion

While there have been several studies comparing the antioxidant activity of tocopherol analogues towards liposomes or phospholipids (Arai et al, 1995; Fukuzawa et al, 1982; Sheu et al, 1999), this is the first report comparing the antioxidant activity of tocopherol analogues and cytoprotective activity of tocopherol analogues toward freshly isolated intact cells undergoing lipid peroxidation. The order of antioxidant and cytoprotective effectiveness toward isolated hepatocytes found for tocopherol analogues was PMC > troglitazone > Trolox C > α-tocopherol > γ-tocopherol > δ-tocopherol.

Other investigations have reported that the relative antioxidant activities of tocopherols against the phosphatidylcholine liposomal membrane oxidation induced by Fe(II)-$AscH_2$ were $\alpha > \beta > \gamma > \delta$-tocopherols (Fukuzawa et al, 1982). Pretreatment of rats with α-tocopherol for 3 days, decreased hepatic necrosis induced by ischemia reperfusion (Marubayashi et al, 1986).

It was also shown that the α-tocopherol analogue, PMC, in which the phytyl chain is replaced by a methyl group, was more hydrophilic (log P 4.6) than α-tocopherol (log P 12.1) but not Trolox C (log P 3.2) (Kitazawa et al, 1997). PMC was also reported to have more potent radical scavenging activity toward iron-induced lipid peroxidation in rat brain homogenates than α-tocopherol (Sheu et al, 1999). An antioxidant order of effectiveness of PMC > α-tocopherol > Trolox C was also reported for preventing phosphatidylcholine peroxidation catalyzed by iron or lipoxygenase (Arai et al, 1995). However, Trolox C was found to be more effective than α-tocopherol in preventing pro-oxidant cytotoxicity induced by ultraviolet (UV) irradiation, $AscH_2$, or gallic acid (Satoh et al, 1997).

PMC was also shown to be highly effective at preventing carbon tetrachloride-induced hepatotoxicity *in vivo* (Hsiao et al, 2001). PMC, therefore, appears to be a promising therapeutic alternative to α-tocopherol. The high lipophilicity of α-tocopherol and its relatively slow cellular uptake (Ingold et al, 1987) severely limit its clinical usefulness, especially in emergency. Trolox C was also more effective than α-tocopherol in protecting rat hearts *ex vivo* against global ischaemia (Sagach et al, 2002).

Previously, we described evidence indicating that peroxidase enzymes catalyzed the one-electron oxidation of phenolics, aniline compounds, NSAIDs, or indole-acetic acid (IAA) derivatives by H_2O_2 to form highly reactive free radicals, which catalyzed the co-oxidation of NADH, GSH and $AscH_2$ resulting in ROS formation occurring during NADH or GSH co-oxidation but not $AscH_2$ (Galati et al, 2002b; Galati et al, 2002a; O'Brien, 1988; Tafazoli and O'Brien, 2004). The results presented here showed that vitamin E analogues catalyzed the co-oxidation of GSH and $AscH_2$ but not NADH, and also resulted in hepatocyte cytotoxicity and lipid peroxidation.

HRP/H_2O_2 also catalyzed the one-electron oxidation of PMC, Trolox C, and α-tocopherol (Nakamura, 1991), and the rate constants for the rate-determining step, (i.e., peroxidase compound II-catalyzed $PhO^\bullet$ formation) decreased in the following order: PMC > Trolox C >> α-tocopherol (Nakamura, 1991). This was similar to the order of effectiveness of these vitamin E analogues for catalyzing $AscH_2$ co-oxidation when oxidized by HRP/H_2O_2 (Table 2.2) and could partly reflect their redox potential as E_{HOMO} values for PMC, α-tocopherol, δ-tocopherol, and γ-tocopherol have been reported as -8.31, -8.33, -8.35, and -8.39 (eV), respectively (Lien et al, 1999). As we have also shown with the SAR Eq 1, the higher the E_{HOMO}, the better the antioxidant activity (Table 2.5).

The following equations explain the co-oxidation of $AscH_2$ catalyzed by the $PhO^\bullet$ of vitamin E analogues. Peroxidase catalyzed a one-electron oxidation of phenolics (PhOH) to form $PhO^\bullet$ (Eq. (1)), which oxidized ascorbate ($AscH_2$) to semidehydroascorbate radicals (Eq. (2)), which then disproportionate to form dehydroascorbate and ascorbate (Eq.(3)).

$$PhOH + H_2O_2 \xrightarrow{\text{Peroxidase}} PhO^\bullet + H_2O \qquad (1)$$

$$PhO^\bullet + AscH_2 \longrightarrow PhOH + AscH^\bullet \qquad (2)$$

$$AscH^\bullet + AscH^\bullet \longrightarrow AscH_2 + Asc \qquad (3)$$

The lack of NADH co-oxidation with vitamin E analogues, troglitazone, Trolox C, and PMC in the peroxidase/H_2O_2 reaction system may be partly explained by the lower reactivity of the vitamin E $PhO^\bullet$ as a result of their lower one-electron redox potential of 110 mV (Aruoma et al, 1990), as compared to 282 mV for $NAD^\bullet$/NADH (Schafer and Buettner, 2001), whereas the one-electron redox potential of phenolics, e.g., etoposide that catalyzes NADH co-oxidation, was in the range of 250-600 mV (Galati et al, 2002a; O'Brien, 1988). However, in the cell reduced nicotinamide adenine dinucleotide phosphate (NADPH):P450 reductase can catalyze NADPH oxidation by PMC $PhO^\bullet$ radicals (Goldman et al, 1997).

Microsomal lipid peroxidation was also induced by vitamin E analogues but not PMC in the presence of peroxidase/H_2O_2, which can be attributed to the pro-oxidant activity of vitamin E analogues $PhO^\bullet$. Hepatocyte lipid peroxidation was also induced by these vitamin E analogues resulting in cytotoxicity as both cytotoxicity and lipid peroxidation were inhibited by the antioxidant butylated hydroxylanisole (BHA). Other investigators also showed that low-density lipoprotein lipid peroxidation was also induced by α-tocopherol when oxidized by myeloperoxidase/H_2O_2 (Kalyanaraman et al, 1995; Santanam and Parthasarathy, 1995).

GSH was also oxidized to GSSG when vitamin E analogues, Trolox C, α-tocopherol, γ-tocopherol, δ-tocopherol, and troglitazone were incubated with peroxidase/H_2O_2. GSH co-oxidation by the studied vitamin E analogues $PhO^\bullet$ was also accompanied by extensive oxygen uptake. Hepatocyte GSH was also partly oxidized by these analogues.

PMC $PhO^\bullet$ radicals co-oxidized $AscH_2$ but unlike other analogues were poor at co-oxidizing GSH or inducing lipid peroxidation with peroxidase/H_2O_2 and caused little cytotoxicity. Other investigations have also shown that PMC $PhO^\bullet$s did not oxidize intracellular GSH and protein sulfhydryls in HL-60 cells and did not induce lipid peroxidation but did oxidize intracellular $AscH_2$ (Kagan et al, 2000; Kagan et al, 2003). EPR and UV spectroscopy studies showed that PMC (292 nm) was first oxidized to a short-lived $PhO^\bullet$ which subsequently formed an ortho-quinone (274 nm). Ascorbate prevented PMC disappearance and $PhO^\bullet$ appearance indicating that $AscH_2$ co-oxidation to $Asc^\bullet$ involved the $PhO^\bullet$ (Kagan et al, 2003).

Pulse radiolysis research (O'Brien, 1988) suggests the following equations, which could explain how $PhO^\bullet$-catalyzed GSH co-oxidation caused superoxide radical anion and H_2O_2 formation:

$$PhOH + H_2O_2 \xrightarrow{\text{Peroxidase}} PhO^{\bullet} + H_2O$$

$$PhO^{\bullet} + GSH \longrightarrow PhOH + GS^{\bullet}$$

$$GS^{\bullet} + GS^{-} \longrightarrow GSSG^{\bullet -}$$

$$GSSG^{\bullet -} + O_2 \longrightarrow GSSG + O_2^{\bullet -}$$

$$2O_2^{\bullet -} + 2H^{+} \longrightarrow H_2O_2 + O_2$$

In our study, the relative GSH and/or lipid peroxidation activity of the vitamin E analogues oxidized by H_2O_2/peroxidase in a cell-free system seemed to be similar to their relative hepatocyte GSH oxidation and/or lipid peroxidation activity. The order of pro-oxidant activity and cytotoxic effectiveness of the vitamin E analogues when oxidized by H_2O_2/peroxidase was troglitazone > Trolox C > δ-tocopherol > γ-tocopherol > α-tocopherol > PMC.

However, the order of antioxidant and cytoprotective activity at much lower concentrations of vitamin E analogues was inversely proportional to the pro-oxidant order of effectiveness found at higher concentrations with the exception of troglitazone. The antioxidant activity of vitamin E analogues seems to correlate with their estimated bond dissociation energy (BDE) values, which have been calculated as follows: 77 kcal/mol for α-tocopherol, PMC, or troglitazone; 79 kcal/mol for γ-tocopherol; and 81 kcal/mol for δ-tocopherol, respectively (calculated by Wright *et al.,* unpublished data). The higher the BDE values are, the less effective the antioxidant activity is. This suggests that the relative antioxidant and pro-oxidant activities of the vitamin E analogues studied may be associated with their O-H bond dissociation enthalpy (Wright et al, 2001). Other investigators have also shown that the pro-oxidant activity of other $PhO^{\bullet}$ generated by lactoperoxidase/H_2O_2 in oxidizing NAD(P)H or GSH was inversely related to their antioxidant ability for quenching 1,1-diphenyl-2-picrylhydrazyl radicals (Ueda et al, 2001).

We have also derived SAR equations, which revealed that the most cytotoxic vitamin E analogues had the highest dipole moments and the lowest E_{HOMO}. However, for antioxidant activity, it was the opposite where the best antioxidant had the lowest dipole moments and the highest E_{HOMO}. Log P also correlated with cytoprotection and antioxidant activity, as the more hydrophilic analogues were better antioxidants.

In conclusion, our results showed that pro-oxidant radicals of vitamin E analogues caused intracellular lipid peroxidation, GSH oxidation, and cytotoxicity, which were prevented by an antioxidant. The cytotoxic pro-oxidant activity of the vitamin E analogues was inversely proportional to their antioxidant activity. PMC was the most effective antioxidant with the lowest pro-oxidant activity and could have therapeutic advantages over the others. Troglitazone at low concentrations was an effective antioxidant; however, at higher concentrations, troglitazone was the most effective pro-oxidant with the highest pro-oxidant activity and caused the most hepatocyte cytotoxicity suggesting that the troglitazone hepatotoxicity could also involve other mechanisms, which require further research. It is possible that the 2,4-thiazolidione moiety of troglitazone could contribute to its hepatotoxicity, as rosiglitazone and pioglitazone in the clinic were much less hepatotoxic and did not contain the phenolic tocopherol moiety (Tafazoli et al, 2005a). Pro-oxidant $PhO^{\bullet}$ formed by troglitazone could partly explain the life-threatening hepatotoxicity found in some patients, which resulted in the withdrawal of troglitazone from the market place.

Chapter 3

Role of Hydrazine in Isoniazid-Induced Hepatotoxicity in a Hepatocyte Inflammation Model

Shahrzad Tafazoli, Mariam Mashregi and Peter J. O'Brien

Reprinted from Toxicology and Applied Pharmacology 229(1): 94-101., Copyright (2008)

3.1 Abstract

Isoniazid is an anti-tuberculosis drug that can cause hepatotoxicity in 20% of the patients and often is associated with an inflammatory response. Isoniazid toxicity in isolated rat hepatocytes, was prevented by 1-aminobenzotriazole, a non-selective P450 inhibitor or by bis-*p*-nitrophenyl phosphate (BNPP), an esterase inhibitor. Hepatocytes when exposed to non-toxic levels of H_2O_2 (to simulate H_2O_2 formation by inflammatory cells), became twice as sensitive to isoniazid toxicity and cytotoxicity was prevented by P450 and esterase inhibition. Hydrazine, the metabolite formed by the amidase-catalyzed hydrolysis of isoniazid, was 16-fold more cytotoxic with a non-toxic H_2O_2-generating system. The acetylhydrazine metabolite was found to be much less cytotoxic than hydrazine in the presence of the H_2O_2 generating system. Hydrazine, therefore, seems to be the isoniazid reactive metabolite in this inflammation model. The molecular mechanism of hydrazine-induced cytotoxicity was attributed to oxidative stress as reactive oxygen species (ROS) and protein carbonyl formation occurred before the onset of hepatocyte toxicity. Hydrazine toxicity also involved significant endogenous H_2O_2 production which caused lysosomal membrane damage and led to a collapse in the mitochondrial membrane potential. These results implicated H_2O_2, a cellular mediator of inflammation, as a potential risk factor for the manifestation of adverse drug reactions, particularly those caused by hydrazine containing drugs.

3.2 Introduction

Isoniazid (isonicotinic acid hydrazide) introduced in the 1950s, is still the most active agent against *Bacillus tuberculosis* and is used both for the treatment and the prophylaxis of tuberculosis. Currently there are 8 million new patients per year receiving treatment with isoniazid, which is the most cost-effective treatment for tuberculosis. Despite the therapeutic benefits of this drug, daily isoniazid administration is also associated with mild elevations of plasma liver enzyme activities in 20% of patients and severe hepatotoxicity in 1–2% of patients (Garibaldi et al, 1972; Scharer and Smith, 1969). Isoniazid use has also been associated with several cases of systemic lupus erythematosus (Dhand et al, 1987; Zingale et al, 1963). Long-term therapy with hydralazine, another hydrazine containing drug or isoniazid can trigger systemic lupus erythematosus with an incidence during the first year of 5–8% for hydralazine or less than 1% for isoniazid (Rubin, 2005). Hydralazine-induced lupus is an autoimmune disease attributed to hydralazine oxidation by monocytes and neutrophils to form reactive metabolites that bind covalently to proteins, thus making the protein "foreign" and leading to an immune response against this hapten (Uetrecht, 2005).

Isoniazid induced lung tumors in mice (Maru and Bhide, 1982; Toth and Shubik, 1966) , and caused chromosome aberrations and sister chromatid exchanges when incubated with cultured rodent cells (MacRae and Stich, 1979). Isoniazid-induced unscheduled DNA synthesis and chromosome aberrations in these cells were also increased by transition metals (Whiting et al, 1979; Zetterberg and Bostrom, 1981) . Isoniazid received a black box warning in 1969 (Black et al, 1975).

The mechanism of isoniazid-induced hepatotoxicity is unknown. Most of the previous research has focused on a rat model with the hypothesis that acetylhydrazine, a metabolite of isoniazid, is the cause of the hepatotoxicity (Mitchell et al, 1976; Nelson et al, 1976). However, there is more recent evidence in animals and humans suggesting that hydrazine is the metabolite predominately responsible for isoniazid-induced hepatotoxicity (Noda et al, 1983; Woo et al, 1992). A positive correlation between plasma hydrazine levels and severity of isoniazid-induced hepatic necrosis, steatosis and elevated plasma triglycerides was obtained in rabbits (Sarich et al, 1996). Hydrazine was also found in the urine and plasma of patients following treatment with isoniazid or hydralazine (Timbrell and Harland, 1979). Evidence for the role of hydrazine in isoniazid-induced hepatotoxicity in rabbits was that administration of an amidase inhibitor prevented hepatotoxicity and hepatic triglyceride accumulation and markedly decreased plasma hydrazine and triglyceride levels (Sarich et al, 1999). Hydrazine has also been shown to be hepatotoxic when administered to rats (Yard and McKennis, 1955) and sublethal doses of hydrazine induced fatty liver in monkeys and rats (Amenta and Johnston, 1963; Dominguez et al, 1962). Hydrazine can be formed from isoniazid through two different pathways: 1) a direct pathway which involves amidase-catalyzed hydrolysis of isoniazid or 2) an indirect pathway of amidase-catalyzed hydrolysis of acetylhydrazine.

Recent evidence from experimental models suggests that an episode of inflammation during drug treatment predisposes animals to tissue injury (Buchweitz et al, 2002; Luyendyk et al, 2002). The hepatotoxicities of allyl alcohol and aflatoxin B1 in rats were augmented by liver inflammation following co-exposure to LPS (Roth et al, 1997). The hepatocellular necrosis in most of the patients also involved an inflammatory response with a hepatic infiltration of lymphocytes and plasma cells with some eosinophils and neutrophils (Mitchell et al, 1976). However, these infiltrates are more likely the consequence rather than the cause of toxicity. Instead, resident Kupffer cells, stellate cells and hepatocytes, also have NADPH oxidase activity that form H_2O_2 when activated (Bataller et al, 2003; De Minicis and Brenner, 2007; Diaz-Cruz et al, 2007; Reinehr et al, 2005). Furthermore, studies also showed that apocynin, an NADPH oxidase inhibitor, suppressed oxidative stress and inflammatory injuries in rat liver during hypercholesterolaemia (Lu et al, 2007). Hepatocytes were therefore exposed to a low non-toxic continuous infusion of H_2O_2 in the absence and presence of peroxidase. In this way, hepatocyte vulnerability to isoniazid in the presence of activated immune cells could be simulated. We have previously used this H_2O_2 hepatocyte inflammation model, with and without peroxidase, to study the hepatotoxicity of tolcapone (Tafazoli et al, 2005a), troglitazone (Tafazoli et al, 2005b) and carbonyl agents (O'Brien et al, 2007). In this model, troglitazone, tolcapone and some carbonyl agents were shown to be much more cytotoxic, whereas other agents such as 2,2,5,7,8-pentamethyl-6-hydroxychromane (PMC), a vitamin E analogue, tribromoethanol (Avertin®), an anesthetic and acetylsalicylic acid (Aspirin®) toxicities were not affected (O'Brien et al, 2007; Tafazoli et al, 2005a; Tafazoli et al, 2005b).

3.3 Materials and methods

3.3.1 Chemicals

Isoniazid, 1-aminobenzotriazole, glucose, glucose oxidase (Type II, 15,000–25,000 U/g solid), peroxidase from horseradish (EC 1.11.1.7; HRP), 2′,7′-dichlorofluorescein diacetate (DCFD-DA), rhodamine 123, deferoxamine mesylate, leupeptin hydrochloride, chloroquine diphosphate salt, methylamine, 4-Hydroxy-2,2,6,6-tetramethylpiperidene-1-oxyl (TEMPOL), dinitrophenylhydrazine (DNPH), bis-*p*-nitrophenylphosphate (BNPP), hydrazine hydrate, and acetylhydrazine were purchased from Sigma-Aldrich Corp. (Oakville, Ontario, Canada).

3.3.2 Animal treatment and hepatocyte preparation

Male Sprague-Dawley rats weighing 275–300 g (Charles River Laboratories, Montréal, Canada) were housed in ventilated plastic cages over PWI 8-16 hardwood bedding. There were 12 air changes per hour, 12-h light photoperiod (lights on at 0800 h) and an environmental temperature of 21–23 °C with a 50–60% relative humidity. The animals were fed with a normal standard chow diet and water *ad libitum*. Care and treatment of the rats were in compliance with the guidelines of the Canadian Council on Animal care, and the protocol was approved by the University of Toronto Animal Care Committee. Hepatocytes were isolated from rats by collagenase perfusion of the liver as described by (Moldeus et al, 1978). Isolated hepatocytes (10 mL, 10^6 cells/mL) were suspended in Krebs–Henseleit buffer (pH 7.4) containing 12.5 mM HEPES in continually rotating 50 mL round bottom flasks, under an atmosphere of 95% O_2 and 5% CO_2 in a 37 °C water bath for 30 min. Glucose (10 mM)/glucose oxidase (0.5 U/mL; H_2O_2 generating system) was used to generate H_2O_2.

3.3.3 Cell viability

Hepatocyte viability was assessed microscopically by plasma membrane disruption as determined by the trypan blue (0.1%, w/v) exclusion test (Moldeus et al, 1978). Hepatocyte viability was determined every 30 min during the first hour and then at 2 and 3 h incubation. The hepatocytes used were at least 85–95% viable before their use.

3.3.4 H_2O_2 generating system

When H_2O_2 was added to hepatocytes, most of the H_2O_2 was metabolized by catalase within seconds (Ou and Wolff, 1996). Therefore, a H_2O_2 generating system was employed by adding glucose 10 mM to the hepatocyte suspension followed by glucose oxidase (0.5 U/mL). This glucose/glucose oxidase system continuously supplied H_2O_2 to the hepatocytes over the experimental period without affecting GSH levels.

3.3.5 H_2O_2 measurement

H_2O_2 was measured in hepatocytes by taking aliquots at 30, 90 and 180 min using the FOX 1 reagent (ferrous oxidation of xylenol orange). The FOX 1 reagent consisted of 25 mM sulfuric acid, 250 µM ferrous ammonium sulfate, 100 µM xylenol orange and 0.1 M sorbitol. At the given time intervals 50 µL of hepatocytes (1.0×10^6 cells/mL) were added to 950 µL FOX1 reagent and incubated for 30 min at room temperature. The absorbance of the samples was read at 560 nm and the concentration of H_2O_2 was determined using the extinction coefficient of $2.67 \times 10^5\ M^{-1}\ cm^{-1}$ (Ou and Wolff, 1996).

3.3.6 Protein carbonylation assay

Total protein-bound carbonyl content was measured by derivatizing the carbonyl adducts with DNPH at 30, 90 and 180 min. Briefly an aliquot of the suspension of cells (0.5 mL, 0.5×10^6 cells) was added to an equivalent volume (0.5 mL) of 0.1% DNPH (w/v) in 2.0 N HCl and allowed to incubate for 1 h at room temperature. This reaction was terminated and total cellular protein precipitated by the addition of an equivalent 1.0 mL volume of 20% TCA (w/v). Cellular protein was rapidly pelleted by centrifugation at $50 \times g$, and the supernatant was discarded. Excess unincorporated DNPH was extracted three times using an excess volume (0.5 mL) of ethanol:ethyl acetate (1:1) solution. Following the extraction, the recovered cellular protein was dried under a stream of nitrogen and solubilized in 1 mL of Tris-buffered 8.0 M guanidine–HCl, pH 7.2. The resulting solubilized hydrazones were measured at 366–370 nm. The concentration of 2,4-DNPH derivatized protein carbonyls was determined using the extinction coefficient of 22,000 M^{-1} cm^{-1} (Hartley et al, 1997).

3.3.7 ROS formation

The rate of hepatocyte ROS generation was determined by adding dichlorofluorescein-diacetate (DCFH-DA) to the hepatocyte incubation. DCFH-DA penetrates hepatocytes and becomes hydrolyzed to form non-fluorescent dichlorofluorescein. Dichlorofluorescein then reacts with ROS to form the highly fluorescent dichlorofluorescein that effluxes the cell (LeBel et al, 1992). Aliquots (1 mL) were withdrawn at 30, 90 and 180 min after incubation. These samples were then centrifuged for 1 min at $50 \times g$. The cells were resuspended in 1 mL of Krebs–Henseleit media containing 1.6 μM DCFD-DA. The cells were incubated at 37 °C for 10 min. The fluorescence intensity of dichlorofluorescein was measured using a Shimadzu

RF5000U fluorescence spectrophotometer (U.S.A.). Excitation and emission wavelengths were 500 and 520 nm, respectively (LeBel et al, 1992).

3.3.8 Mitochondrial membrane potential assay

The uptake and retention of the cationic fluorescent dye, rhodamine 123, has been used for the estimation of mitochondrial membrane potential. This assay is based on the fact that rhodamine 123 accumulates selectively in the mitochondria by facilitated diffusion. However, when the mitochondrial potential is decreased, the amount of rhodamine 123 that enters the mitochondria is decreased as there is no facilitated diffusion. Thus the amount of rhodamine 123 in the supernatant is increased and the amount in the pellet is decreased. Samples (500 μL) were taken from the cell suspension incubated at 37 °C at 30, 90 and 180 min, and centrifuged at $50 \times g$ for 1 min. The cell pellet was then resuspended in 2 mL of fresh incubation medium containing 1.5 μM rhodamine 123 and incubated at 37 °C in a thermostatic bath for 10 min with gentle shaking. Hepatocytes were separated by centrifugation and the amount of rhodamine 123 appearing in the incubation medium was measured fluorimetrically using Shimadzu RF5000U fluorescence spectrophotometer set at 490 nm excitation and 520 nm emission wavelengths. The capacity of mitochondria to take up the rhodamine 123 was calculated as the difference in fluorescence intensity between control and treated cells (Andersson et al, 1987).

3.3.9 Statistical analysis

Statistical analysis was preformed by a one-way ANOVA (analysis of variance) test and significance was assessed by employing Tukey's post hoc test.

3.4 Results

As shown in Figure 3.1, incubation of isolated hepatocytes with 10 mM isoniazid induced a 50% loss in hepatocyte viability in 2 h as measured by the trypan blue exclusion assay (LC_{50}). To determine the molecular mechanism for the toxicity, different compounds were added to the incubation medium to determine their ability to modulate the toxic response. For this purpose the LC_{50} of isoniazid (10 mM) was selected.

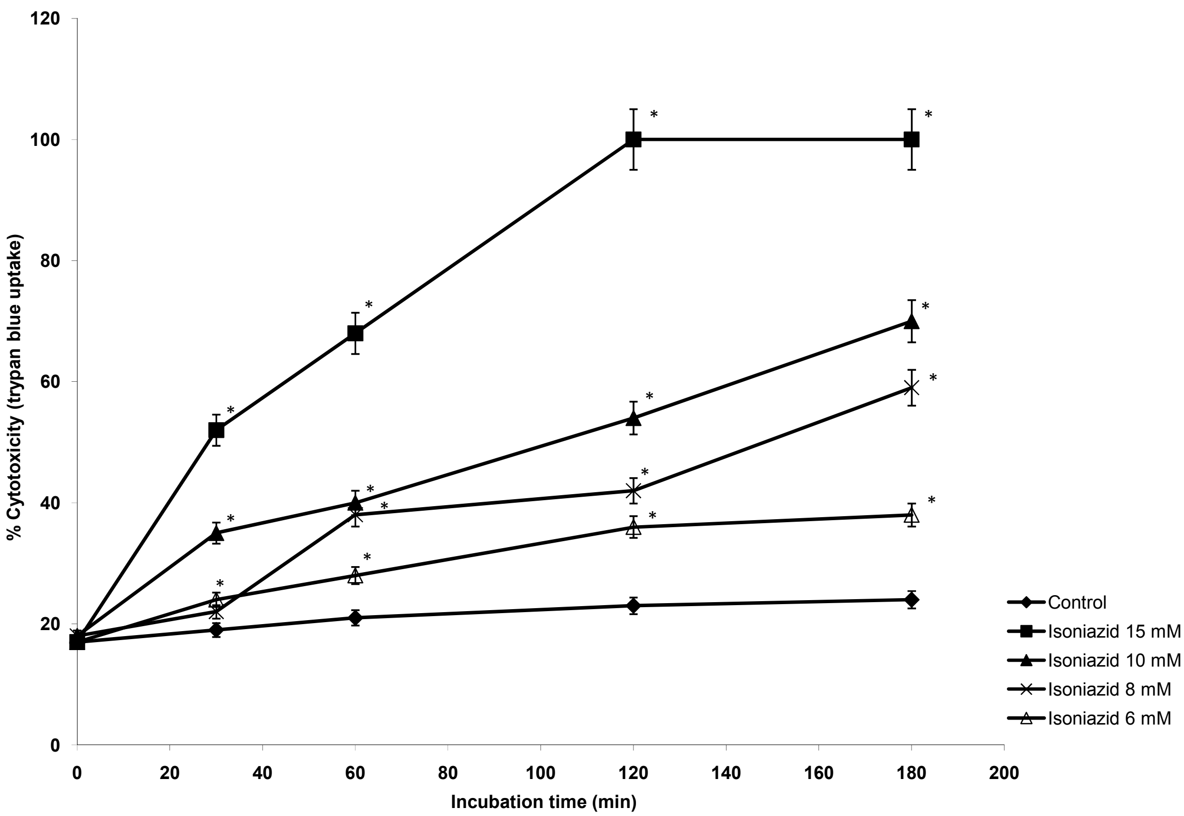

Figure 3. 1 Isoniazid-induced cytotoxicity towards isolated rat hepatocytes
Refer to Materials and Methods for a description of experiments performed.
Means ± SE for three separate experiments are given.
* Significant as compared to control ($p < 0.05$).

As shown in Table 3.1, the presence of BNPP, an amidase inhibitor (Buch et al, 1969), markedly decreased isoniazid cytotoxicity suggesting that hydrazine formed by the amidase-catalyzed hydrolysis of isoniazid contributed to cytotoxicity. Furthermore, 1-aminobenzotriazole, a non-selective P450 inhibitor was also cytoprotective, indicating a role for P450 in isoniazid toxicity. On the other hand, there was about a 2-fold increase in isoniazid toxicity if a non-toxic (did not affect cell viability or GSH levels significantly) H_2O_2 generating system, to simulate inflammation, was added at 1 h (to allow for isoniazid bioactivation), i.e., 6 mM isoniazid now caused the same degree of cytotoxicity as 10 mM isoniazid without the H_2O_2 generating system. Addition of 1-aminobenzotriazole, before the H_2O_2 generating system, also prevented toxicity suggesting a role for P450/H_2O_2 in the increased isoniazid hepatotoxicity. Addition of BNPP to the hepatocytes prior to the H_2O_2 generating system, also decreased isoniazid toxicity indicating that metabolism of isoniazid to hydrazine was necessary for toxicity. In the absence of isoniazid, none of the modulators at the doses used, affected hepatocyte viability.

A marked increase in isoniazid-induced protein carbonyl formation occurred with the addition of a H_2O_2 generating system, whereas isoniazid in the absence of the H_2O_2 generating system did not enhance protein carbonylation. P450 inhibition and BNPP both resulted in a marked decrease in protein carbonylation induced by isoniazid and H_2O_2 generating system. Endogenous H_2O_2 levels, as measured using the FOX 1 reagent, was also markedly increased by isoniazid and the non-toxic H_2O_2 generating system, but did not increase in the absence of isoniazid or the H_2O_2 generating system. Inhibition of amidase with BNPP or inhibition of P450 by 1-aminobenzotriazole prevented the increase in isoniazid toxicity by the H_2O_2 generating system.

Table 3.1 Bioactivation of isoniazid in the hepatocyte inflammation model

Addition	Cytotoxicity (%Trypan blue uptake)			Protein carbonylation (nmoles/10^6 cells)	Endogenous H_2O_2 formation (nmoles/10^6 cells)
Incubation time (min)	***60***	***120***	***180***	***90***	***90***
Control (only hepatocytes)	18 ± 2	21 ±1	26 ± 3	8.45 ± 0.42	6.96 ± 0.32
+ H_2O_2 generating system	24 ± 2	29 ± 2	34 ± 2	9.36 ± 0.45	8.26 ± 0.41
+ HRP 0.1 µM	23 ± 3	33 ± 3	38 ± 2	9.84 ± 0.51	8.47 ± 0.37
+ Isoniazid 10 mM	42 ± 3^a	57 ± 4^a	78 ± 5^a	10.3 ± 0.35	8.91 ± 0.43^a
+ BNPP* 1 mM	27 ± 2^b	34 ± 3^b	49 ± 5^b	9.06 ± 0.32	8.86 ± 0.39
+ 1-Aminobenzotriazole* 100 µM	26 ± 3^b	31 ± 2^b	44 ± 3^b	8.86 ± 0.41	8.66 ± 0.32
+ H_2O_2 generating system	47 ± 3	66 ± 7	83 ± 6	11.29 ± 0.49	9.83 ± 0.57
+ HRP 0.1 µM	49 ± 4	63 ± 5	88 ± 4	11.85 ± 0.56	10.01 ± 0.61
+ Isoniazid* 10 mM + H_2O_2 generating system	88 ± 7^b	100^b	100^b	33.4 ± 1.2^b	22.09 ± 1.1^b
+ BNPP** 1 mM	51 ± 4^c	62 ± 4^c	74 ± 6^c	16.28 ± 0.8^c	13.47 ± 0.57^c
+ Isoniazid 6 mM	29 ± 3	33 ± 2	39 ± 2	9.13 ± 0.41	8.43 ± 0.4
+ H_2O_2 generating system	36 ± 2	46 ± 4	51 ± $3^{c,e}$	10.71 ± 0.34	9.63 ± 0.48
+ Isoniazid* 6 mM + H_2O_2 generating system	42 ± 3	58 ± 4^d	72 ± 6^d	24.56 ± 1^d	16.74 ± 0.75^d
+ 1-Aminobenzotriazole** 100 µM	29 ± 2	36 ± 3^e	49 ± 5^e	14.16 ± 0.7^e	11.4 ± 0.59^e
+ BNPP** 1 mM	31 ± 3	39 ± 2^e	53 ± 3^e	12.04 ± 0.8^e	10.52 ± 0.4^e

H_2O_2 generating system: Glucose 10 mM and glucose oxidase 0.5 U/mL; BNPP: Bis-*p*-nitrophenyl phosphate (esterase inhibitor); 1-Aminobenzotriazole: non-selective P450 inhibitor; HRP: Horseradish peroxidase
* Hepatocytes were pre-incubated with BNPP or aminobenzotriazole or isoniazid for 60 min prior to the addition of other agents.
** Hepatocytes were pre-incubated with BNPP or aminobenzotriazole along with isoniazid for 60 min prior to the addition of H_2O_2 generating system.
Refer to Materials and Methods for a description of experiments performed.
Means ± SE for three separate experiments are given.
[a] Significant as compared to control ($p < 0.05$).
[b] Significant as compared to isoniazid 10 mM alone ($p < 0.05$).
[c] Significant as compared to isoniazid*10 mM + H_2O_2 generating system ($p < 0.05$).
[d] Significant as compared to isoniazid 6 mM alone ($p < 0.05$).
[e] Significant as compared to isoniazid* 6 mM + H_2O_2 generating system ($p < 0.05$).

As shown in Figure 3.2, hydrazine toxicity towards isolated rat hepatocytes was concentration-dependent and about 8 mM hydrazine was required to cause 50% hepatocyte cytotoxicity in 2 h (LC_{50}).

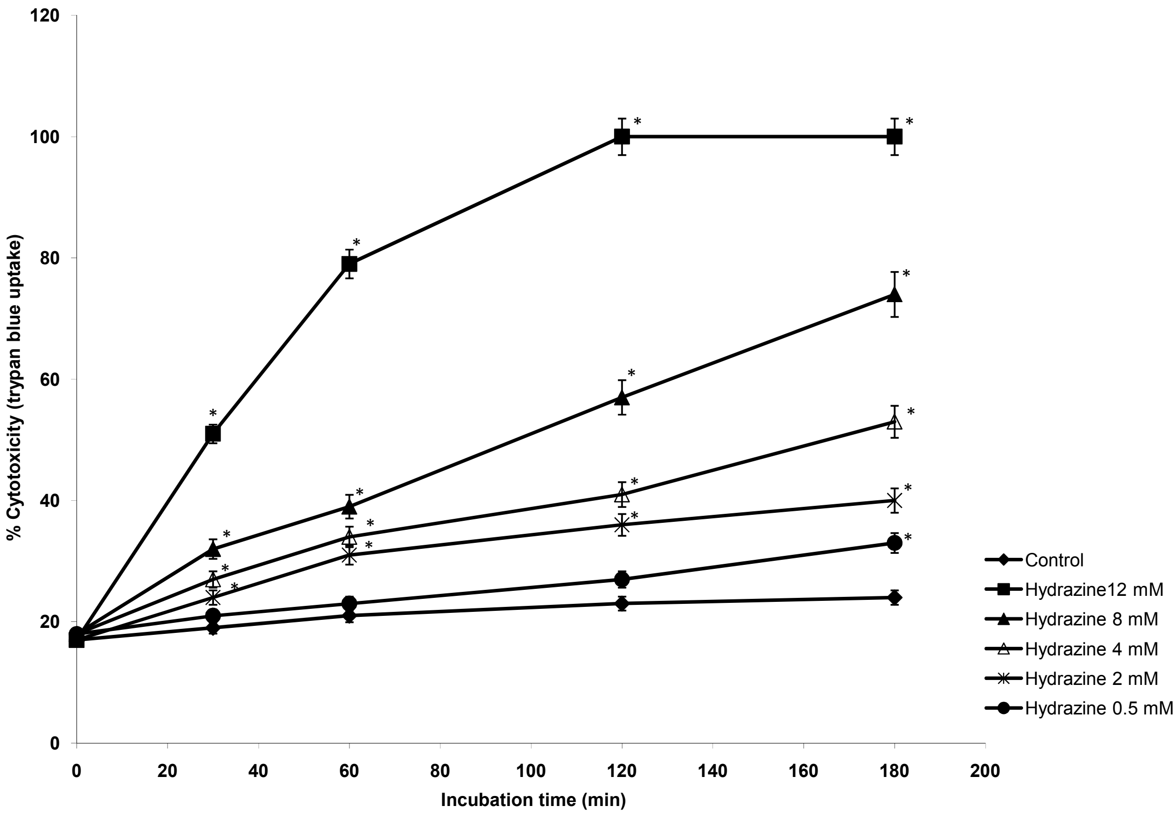

Figure 3.2 Hydrazine-induced cytotoxicity towards isolated rat hepatocytes
Refer to Materials and Methods for a description of experiments performed.
Means ± SE for three separate experiments are given.
* Significant as compared to control ($p < 0.05$).

Summarized in Table 3.2, two of the major isoniazid metabolites, hydrazine and acetylhydrazine, were next tested in the hepatocyte inflammation model. Hydrazine toxicity in the presence of a non-toxic H_2O_2 generating system was markedly increased and cytotoxicity was also concentration-dependent. Hydrazine LC_{50} in the absence of the H_2O_2 generating system was 8 mM, and in the presence of the H_2O_2 generating system it was 0.5 mM, a 16-fold increase. Hepatocyte oxidative stress was also markedly increased and was accompanied by significant endogenous ROS and H_2O_2 formation as well as protein carbonylation. P450 inhibition by 1-aminobenzotriazole and the ROS scavenger, TEMPOL both prevented hydrazine toxicity, and ROS formation as well as protein carbonylation. Hepatocyte viability in the absence of hydrazine was not affected by any of the modulators at the doses shown.

Table 3.2 Contribution of hydrazine to isoniazid-induced toxicity in the hepatocyte inflammation model

Addition	Cytotoxicity (%Trypan blue uptake)			Protein carbonylation (nmoles/10^6 cells)	Endogenous H_2O_2 formation (nmoles/10^6 cells)	ROS formation (Fluorescent Intensity)
Incubation time (min)	***60***	***120***	***180***	***90***	***90***	***90***
Control (only hepatocytes)	17 ± 1	22 ± 1	27 ± 2	8.34 ± 0.46	7.01 ± 0.23	102 ± 9
+ H_2O_2 generating system	23 ± 2	29 ± 2	33 ± 1	8.86 ± 0.53	8.13 ± 0.32	123 ± 11
+ HRP 0.1 μM	25 ± 1	32 ± 2	36 ± 2	9.07 ± 0.58	8.53 ± 0.39	Interference†
+ Hydrazine 8 mM	36 ± 3[a]	57 ± 4[a]	68 ± 5[a]	12.4 ± 0.53[a]	14.6 ± 0.68[a]	167 ± 14[a]
+ H_2O_2 generating system	100[b]	100[b]	100[b]	46.37 ± 2.1[b]	37.02 ± 1.8[b]	391 ± 16[b]
+ Hydrazine 2 mM	29 ± 2	33 ± 1	37 ± 2	8.45 ± 0.42	7.67 ± 0.31	108 ± 7
+ H_2O_2 generating system	58 ± 4[c]	78 ± 6[c]	100[c]	36.9 ± 1.5[c]	30.71 ± 1.5[c]	352 ± 9[c]
+ Hydrazine 0.5 mM	22 ± 1	27 ± 3	32 ± 1	8.37 ± 0.36	7.41 ± 0.4	113 ± 7
+ H_2O_2 generating system	39 ± 5[d]	56 ± 5[d]	76 ± 5[d]	28.31 ± 1.4[d]	21.64 ± 0.9[d]	321 ± 15[d]
+ 1-Aminobenzotriazole*100 μM	25 ± 2[e]	34 ± 4[e]	46 ± 3[e]	11.07 ± 0.5[e]	16.45 ± 0.7[e]	257 ± 18[e]
+ TEMPOL 200 μM	27 ± 3[f]	37 ± 6[f]	51 ± 4[f]	12.3 ± 0.4[f]	14.7 ± 0.6[f]	216 ± 13[f]
+ HRP 0.1 μM	41 ± 3	59 ± 7	79 ± 7	27.09 ± 1.7	22.42 ± 1.1	Interference†
+ Acetylhydrazine 5 mM	36 ± 2[a]	54 ± 5[a]	71 ± 6[a]	11.97 ± 0.58[a]	10.59 ± 0.5	121 ± 14
+ H_2O_2 generating system	37 ± 4	57 ± 3	74 ± 5	12.09 ± 0.54	10.71 ± 0.7	129 ± 8

† Due to oxidation of 2',7'-dichlorofluorescin by peroxidase
* Hepatocytes were pre-incubated with aminobenzotriazole, for 60 min prior to the addition of other agents
H_2O_2 generating system: Glucose 10 mM and glucose oxidase 0.5 U/mL; 1-Aminobenzotriazole: non-selective P450 inhibitor; TEMPOL: 4-Hydroxy-2,2,6,6-tetramethylpiperidene-1-oxyl (ROS scavenger)
Refer to Materials and Methods for a description of experiments performed.
Means ± SE for three separate experiments are given.
[a] Significant as compared to control ($P < 0.05$).
[b] Significant as compared to hydrazine 8 mM alone ($P < 0.05$).
[c] Significant as compared to hydrazine 2 mM alone ($P < 0.05$).
[d] Significant as compared to hydrazine 0.5 mM alone ($P < 0.05$).
[f] Significant as compared to hydrazine 0.5 mM + H_2O_2 generating system ($P < 0.05$).

Acetylhydrazine cytotoxicity was not increased by the H_2O_2 generating system, even if hepatocytes were pre-incubated with acetylhydrazine for 60 min prior to the addition of H_2O_2 generating system (results not shown). Furthermore, inhibition of amidase by BNPP did not affect acetylhydrazine cytotoxicity in the presence of H_2O_2 generating system, indicating that acetylhydrazine did not undergo deacetylation to form hydrazine (results not shown).

As shown in Figure 3.3, hydrazine toxicity in the inflammation model involved lysosomal membrane damage as deferoxamine, an iron chelator was cytoprotective as well as methylamine and chloroquine, lysosomotropic agents. The hepatocyte lysosomal protease inhibitor leupeptin also prevented hydrazine-induced cytotoxicity in the inflammation model.

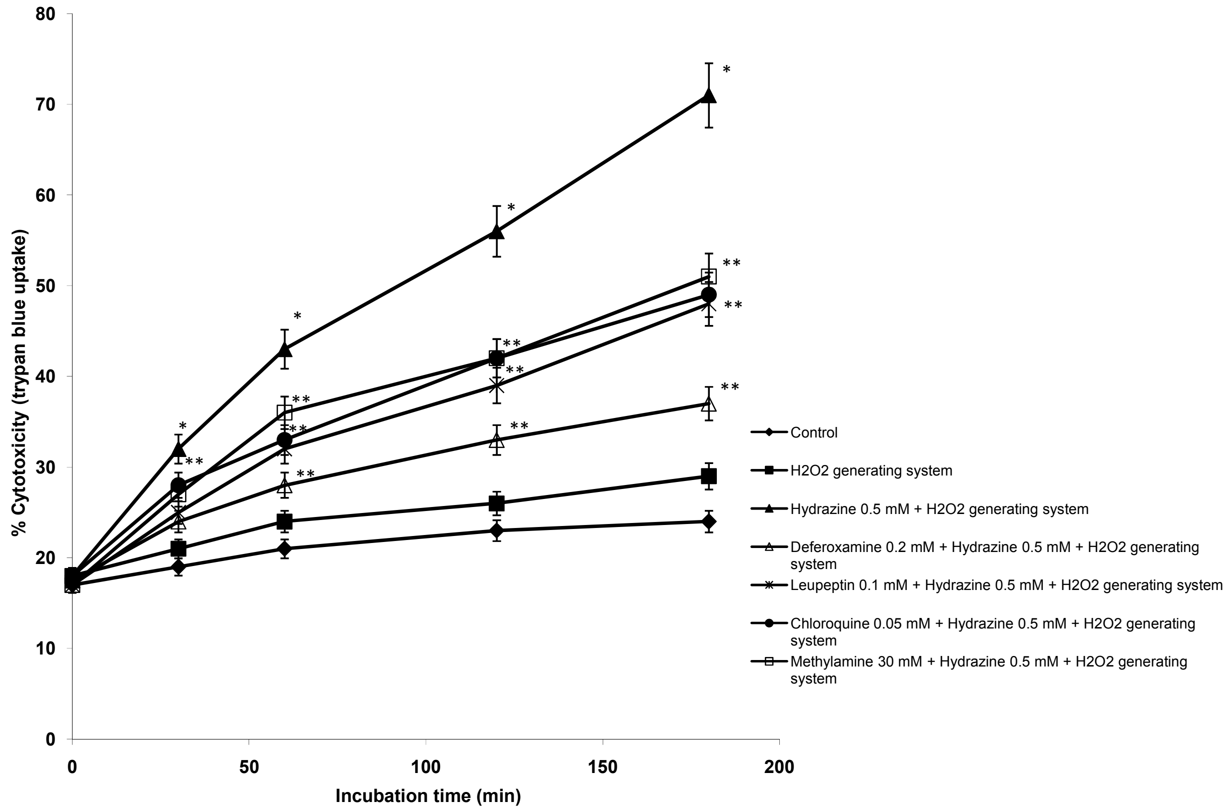

Figure 3.3 Hydrazine-induced toxicity in the hepatocyte inflammation model involves lysosomal labilization and mitochondrial toxicity

H_2O_2 generating system: Glucose 10 mM and glucose oxidase 0.5 U/mL; Deferoxamine: iron chelator; Leupeptin: protease inhibitor; Chloroquine and methylamine: lysosomotropic agents

Refer to Materials and Methods for a description of experiments performed.

Means ± SE for three separate experiments are given.

* Significant as compared to H_2O_2 generating system ($p < 0.05$).

**Significant as compared to hydrazine 0.5 mM + H_2O_2 generating system ($p < 0.05$).

Furthermore, hydrazine induced a rapid decline of mitochondrial membrane potential which was prevented by deferoxamine, methylamine, chloroquine and leupeptin indicating that hydrazine-induced collapse in mitochondrial membrane potential was a consequence of lysosomal damage (Figure 3.4).

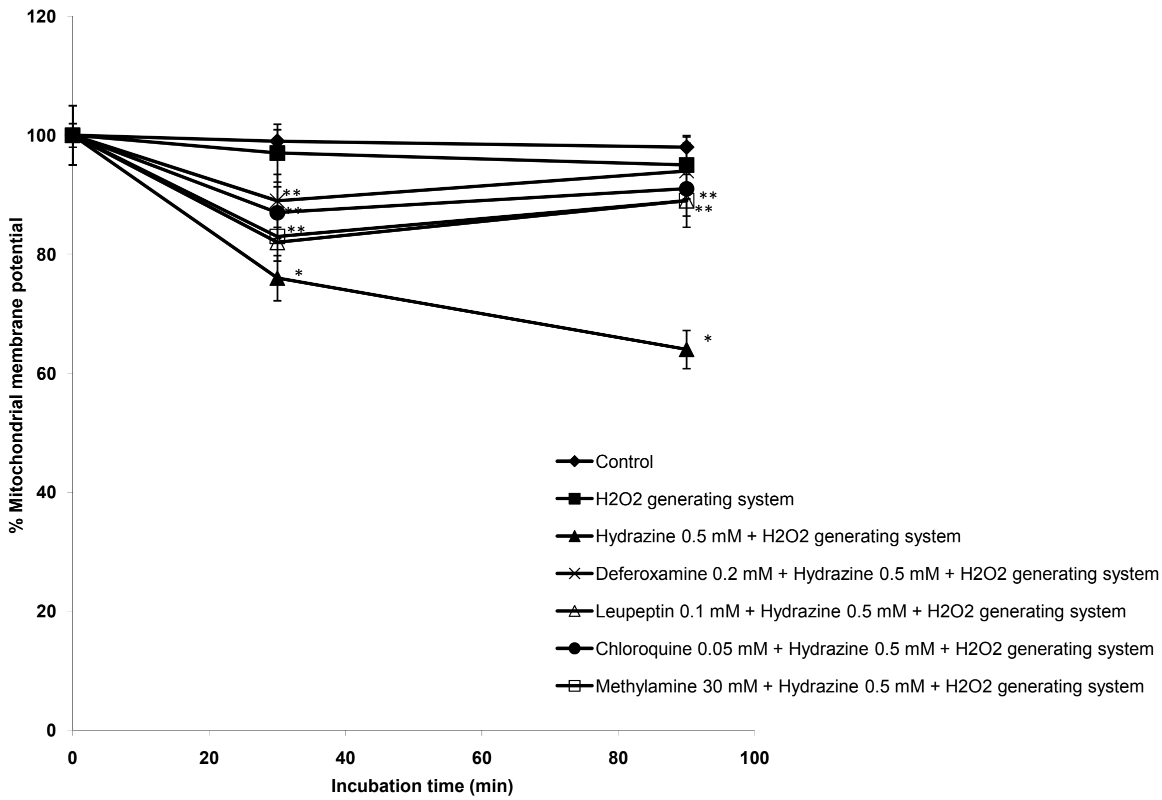

Figure 3.4 Prevention of hydrazine-induced mitochondrial membrane collapse by lysosomotropic agents, iron chelators and protease inhibitors

H_2O_2 generating system: Glucose 10 mM and glucose oxidase 0.5 U/mL; Deferoxamine: iron chelator; Leupeptin: protease inhibitor; Chloroquine and methylamine: lysosomotropic agents Refer to Materials and Methods for a description of experiments performed.

Means ± SE for three separate experiments are given.

* Significant as compared to H_2O_2 generating system ($P < 0.05$).

**Significant as compared to hydrazine 0.5 mM + H_2O_2 generating system ($P < 0.05$).

3.5 Discussion

Previously we introduced an inflammation hepatocyte model for screening candidate drugs for idiosyncratic drug reaction hepatotoxicity potential (Tafazoli et al, 2005a; Tafazoli and O'Brien, 2005). Instead of co-culturing the hepatocytes with Kupffer cells and activating the Kupffer cells with LPS (Tukov et al, 2006), we have selected to use a slow H_2O_2 generating system (glucose/glucose oxidase) that simulates ROS generation by immune cells in the liver that are activated during inflammation. Hepatocyte GSH levels, protein carbonylation and cell viability were not affected by the H_2O_2 generating system. However, it was found that the hepatotoxicity of several drugs e.g., tolcapone or troglitazone that caused idiosyncratic drug reaction hepatotoxicity and were withdrawn or received a black box warning, were markedly increased by this non-toxic slow infusion of H_2O_2 (Tafazoli et al, 2005a; Tafazoli et al, 2005b).

In this study, we showed that isoniazid cytotoxicity increased by a 2-fold factor in the hepatocyte inflammation model only when isoniazid was pre-incubated with hepatocytes for 1 h prior to the H_2O_2 addition. This pre-incubation time allowed for the metabolism of isoniazid to its toxic metabolites. BNPP, an amidase inhibitor, prevented isoniazid toxicity both in the absence and presence of the H_2O_2 generating system, indicating the role of amidase in isoniazid toxicity by catalyzing isoniazid hydrolysis to the more toxic hydrazine. Furthermore, toxicity was preceded by a significant increase in endogenous H_2O_2 production and protein carbonyl formation. The isoniazid metabolites hydrazine and acetylhydrazine were then tested using the hepatocyte inflammation model. Hydrazine toxicity was found to be increased 16-fold in the presence of H_2O_2. BNPP administration also prevented *in vivo* acetylisoniazid-induced hepatotoxicity which was attributed to the prevention of acetylisoniazid hydrolysis to acetylhydrazine, the suspected isoniazid-derived hepatotoxin at that time (Mitchell et al, 1975).

However, in our hepatocyte inflammation model, acetylhydrazine toxicity was not increased in the presence of the H_2O_2 generating system. Previously it was reported that BNPP acts as a potent amidase inhibitor *in vitro*, inhibiting the conversion of isoniazid to hydrazine catalyzed by rat hepatic microsomes (Sendo et al, 1984). Therefore, the prevention of isoniazid-induced toxicity in our hepatocyte model with BNPP would provide evidence that the mechanism for the protection is likely due to inhibition of hydrazine formation.

The increased hepatocyte susceptibility to hydrazine by the H_2O_2 generating system could result from catalase and superoxide dismutase inactivation by hydrazine (Hussain and Frazier, 2002), as there was a significant increase in endogenous H_2O_2 levels as measured by FOX 1 reagent. Previously, it was shown that in red blood cells, catalase was inactivated by phenylhydrazine, another hydrazine with a similar structure, but only if H_2O_2 was present (Cohen and Hochstein, 1964). *In vitro* catalase experiments showed that the inactivation mechanism involved the catalase-catalyzed oxidation of phenylhydrazine by H_2O_2 to a radical cation, phenyl radical and other oxidation products which resulted in a σ-coordination of a phenyl residue to the catalase prosthetic heme iron (Ortiz de Montellano and Kerr, 1983).

Furthermore, previous evidence also showed that in rabbits, isoniazid-induced hepatocellular damage correlated with plasma hydrazine levels but not with isoniazid or acetylhydrazine levels (Sarich et al, 1996). Administration of BNPP, 30 min before the administration of isoniazid, to rabbits also prevented the elevation of plasma liver enzymes as well as hepatic and plasma triglyceride levels but decreased plasma hydrazine levels (Sarich et al, 1999).

1-Aminobenzotriazole, a non-selective P450 inhibitor, prevented isoniazid and hydrazine-induced cytotoxicities in the presence of H_2O_2, suggesting a role for P450/H_2O_2 or oxidative activation of P450 metabolites by H_2O_2 for isoniazid and hydrazine hepatotoxicities. The microsomal P450/H_2O_2 system has been shown to catalyze the oxidative metabolism of other oxidisable substrates such as catechols and phenylenediamines (Anari et al, 1997). Isoniazid oxidation was catalyzed by a microsomal cytochrome P450 system to form reactive free radical metabolites that were trapped by spin-trapping agents (Albano and Tomasi, 1987). Hydrazine metabolism by rat hepatocytes was also increased in P450-induced hepatocytes (phenobarbital) and hydrazine metabolism was decreased by P450 inhibitors, e.g., metyrapone and piperonyl butoxide (Timbrell et al, 1982).

An abnormal endogenous production of H_2O_2, has been shown to result in a rapid decrease in cell viability preceded by the loss of lysosomal integrity, as judged by the relocalization of acridine orange, a lysosomotropic weak base (Zdolsek et al, 1993). Influx of H_2O_2 into the lysosomal apparatus initiates processes through a primary interaction with lysosomal ferrous iron resulting in the formation of hydroxyl radicals which lead to disruption of lysosomal normal stability and leakage of hydrolytic enzymes (Starke et al, 1985; Zdolsek et al, 1993). A marked increase in endogenous H_2O_2 formation by hydrazine also caused lysosomal labilization as the lysosomotropic agents, chloroquine and methylamine, the iron chelator, deferoxamine, as well as leupeptin, a protease inhibitor, all prevented hydrazine toxicity in the inflammation model. There was also a significant collapse in mitochondrial membrane potential which was inhibited by the lysosomotropic agents, methylamine and chloroquine as well as leupeptin and deferoxamine. This suggests that the lysosomal damage contributed to mitochondrial toxicity.

In summary our results showed that hydrazine is the likely metabolite involved in the cytotoxic mechanism of isoniazid since inhibition of the amidase that catalyzes the hydrolysis of isoniazid to hydrazine prevented isoniazid-induced hepatocyte cytotoxicity. Furthermore, a non-toxic H_2O_2 generating system to simulate the ROS formation by immune cells increased isoniazid cytotoxicity by two fold whereas hydrazine cytotoxicity was increased 16-fold whilst acetylhydrazine cytotoxicity was not affected. The molecular cytotoxic mechanism likely involved lysosomal permeabilization and mitochondrial membrane collapse. The cytotoxic mechanism also involved extensive oxidative stress as endogenous ROS and H_2O_2 as well as protein carbonylation were markedly increased and ROS scavengers that prevented ROS formation also prevented the ensuing cytotoxicity. ROS formation may also arise from the reduction of oxygen by hydrazinyl radicals formed by hydrazine oxidation.

Chapter 4

Accelerated Cytotoxic Mechanism Screening of Hydralazine Using an *In vitro* Hepatocyte Inflammatory Cell Peroxidase Model

---

Shahrzad Tafazoli, and Peter J. O'Brien

Reproduced with permission from *Chemical Research in Toxicology* 2008, 21: 904-910.

4.1 Abstract

Long-term treatment of hypertensive disorders with hydralazine has resulted in some patients developing hepatitis and lupus erythematosus, an autoimmune syndrome. The concentration of hydralazine required to cause 50% cytotoxicity in 2 h (LC_{50}) toward isolated rat hepatocytes was found to be 8 mM. Cytotoxicity was delayed by the P450 inhibitor, 1-aminobenzotriazole, suggesting that P450 catalyzed the formation of toxic metabolites from hydralazine. No hydralazine-induced oxidative stress was apparent as there was little effect on hepatocyte lipid peroxidation, protein carbonyl formation, intracellular H_2O_2, or hepatocyte GSH levels and no effect of butylated hydroxyanisole (BHA) on cytotoxicity. Drug-induced hepatotoxicity *in vivo* has often been attributed to infiltrating inflammatory cells, for example, neutrophils or resident Kupffer cells whose NADPH oxidase generates H_2O_2, when activated. The effect of a non-toxic continuous infusion of H_2O_2 on hydralazine cytotoxicity was investigated. It was found that H_2O_2 increased hepatocyte susceptibility to hydralazine 4-fold (LC_{50}, 2 mM). Cytotoxicity was still prevented by the P450 inhibitor but now involved some oxidative stress as shown by increased protein carbonyls, endogenous H_2O_2, and GSH oxidation. Lipid peroxidation was not increased, and cytotoxicity was not inhibited by BHA. Cytotoxicity, however, was inhibited by 4-hydroxy-2,2,6,6-tetramethylpiperidene-1-oxyl (TEMPOL), a ROS scavenger. Because neutrophils or Kupffer cells release myeloperoxidase on activation, the effect of adding peroxidase to the hepatocytes exposed to H_2O_2 on hydralazine cytotoxicity was also investigated. It was found that peroxidase/H_2O_2 increased hepatocyte susceptibility to hydralazine 80-fold (LC_{50}, 0.1 mM). Furthermore, cytotoxicity occurred following extensive oxidative stress that included lipid peroxidation, and cytotoxicity that was now prevented by the antioxidant BHA. These results indicate that three cytotoxic pathways exist for hydralazine: a P450-catalyzed

pathway not involving oxidative stress, a P450/H_2O_2-catalyzed oxidative stress-mediated cytotoxic pathway not involving lipid peroxidation, and a peroxidase/H_2O_2-catalyzed lipid peroxidation-mediated cytotoxic pathway.

4.2 Introduction

Hydralazine, an aromatic hydrazine derivative, has been in clinical use since 1950 for the long-term treatment of hypertensive disorders. Associated with hydralazine exposure is the development of hepatitis with confluent centrilobular necrosis (Itoh et al, 1981; Murata et al, 2007). Circulating autoantibodies reacting with liver CYP1A2 have been found in patients with dihydralazine-induced hepatitis (Bourdi et al, 1992). An autoimmune syndrome resembling systemic lupus erythematosus occurred between 2 and 40 months after the start of hydralazine administration and was dose-related (Cameron and Ramsay, 1984). The reactive metabolites causing hydralazine side effects are not known, and various reactive metabolites have been proposed by different investigators (Hofstra et al, 1991; Hofstra and Uetrecht, 1993; Sinha, 1983; Wong et al, 1988; Yamamoto and Kawanishi, 1991).

Hydralazine has also been shown to induce DNA fragmentation and DNA repair in isolated rat hepatocytes (Martelli et al, 1995), but no other cytotoxic molecular mechanism studies have been carried out. There have also been reports of hydralazine mutagenicity found in bacterial test systems (Parodi et al, 1981) and a modest increase in lung tumors in mice (Toth, 1978). Hydralazine has also been shown to undergo autoxidation at an alkaline pH catalyzed by the transition metals Cu(II) or Fe(III), to form phthalazine and nitrogen-centered hydralazyl radical intermediates, which caused site-specific DNA damage (Sinha, 1983; Yamamoto and Kawanishi, 1991). Leukocyte myeloperoxidase (MPO), H_2O_2, and chloride ion catalyzed hypochlorite formation, which oxidized hydralazine to phthlazine (Hofstra and Uetrecht, 1993). A reactive intermediate was trapped with *N*-acetyl cysteine, and the adduct was identified as 1-phthalazylmercapturic acid. The reactive intermediate proposed was the diazonium salt formed from the diazene intermediate in the phthalazine product pathway (Hofstra and Uetrecht, 1993).

Electron spin resonance studies were also used to show that liver microsomes/NADPH catalyzed hydralazine to phthalazine via a radical pathway catalyzed by P450 (LaCagnin et al, 1986). Mitochondrial pyruvate dehydrogenase also catalyzed oxidation of the pyruvate hydralazine hydrazone to form a $CO_2^{\bullet-}$ radical (Wong et al, 1988).

Idiosyncratic adverse drug reactions, although rare, can be a cause for removal of the drug from the market. Liver injury has been induced in rats if the rats were cotreated with lipopolysaccharide (LPS) when the drug for example, ranitidine or trovafloxacin, was administered (Deng et al, 2007; Shaw et al, 2007). An immune cell-mediated cytotoxic mechanism has been proposed in which cytokines, for example, tumor necrosis factor-α and cytotoxic proteases, were released by the drug and/or LPS(Deng et al, 2007; Shaw et al, 2007). Liver gene expression in rats showed that the hemostatic system, hypoxia, as well as infiltrated neutrophils could also be critical mediators of LPS/ranitidine-induced liver injury(Luyendyk et al, 2006). Neutrophil activation by cytokines, chemokines, and microbial products results in a massive increase in superoxide radicals and H_2O_2 formation, probably for host defense against invading microorganisms (Quinn et al, 2006). LPS also increased cellular NADPH oxidase transcription, resulting in superoxide radical and H_2O_2 formation (Kawahara et al, 2005). Kupffer cells resident in the liver contain high NADPH oxidase activity (Quinn et al, 2006), and Kupffer cells contribute to drug hepatotoxicity (Tafazoli and O'Brien, 2005).

To find a more robust *in vitro* screening method for assessing the potential hepatotoxicity risk of hydralazine, hepatocyte susceptibility to hydralazine was also investigated when hepatocytes were exposed to a low non-toxic continuous infusion of H_2O_2 in the absence or presence of peroxidase such as could be released by activated immune cells. In this way, hepatocyte vulnerability to hydralazine in the presence of H_2O_2 generated by oxidative stress or NADPH oxidase of activated immune cells could be simulated. We have previously used this H_2O_2-enhanced hepatocyte cytotoxicity model, with or without peroxidase, to study the hepatotoxcity of tolcapone (Tafazoli et al, 2005a), troglitazone (Tafazoli et al, 2005b), and carbonyl agents (O'Brien et al, 2007). In this model, troglitazone, tolcapone, and some carbonyl agents were shown to be much more cytotoxic, whereas other agents such as 2,2,5,7,8-pentamethyl-6-hydroxychromane (PMC), a vitamin E analogue, tribromoethanol (avertin), an anesthetic, and acetylsalicylic acid (aspirin) were not affected (O'Brien et al, 2007; Tafazoli et al, 2005a; Tafazoli et al, 2005b; Tafazoli and O'Brien, 2005).

4.3 Material and methods

4.3.1 Chemicals

Hydralazine hydrochloride, catalase, sodium azide, 1-aminobenzotriazole, 6-*n*-propyl-thiouracil (PTU), horseradish peroxidase (EC 1.11.1.7; HRP), myeloperoxidase (MPO), 4-hydroxy-2,2,6,6-tetramethylpiperidene-1-oxyl (TEMPOL), gallic acid, butylated hydroxyanisole (BHA), 2′,4′-dinitrofluorobenzene (DNFB), thiobarbituric acid, trichloroacetic acid (TCA), iodoacetic acid, glucose, glucose oxidase, 2′,7′-dichlorofluorescein diacetate (DCFD-DA), and dinitrophenylhydrazine (DNPH) were purchased from Sigma Aldrich Corp. (Oakville, Ont., Canada).

4.3.2 Animal treatment and hepatocyte preparation

Male Sprague–Dawley rats weighing 275–300 g (Charles River Laboratories, Montréal, Canada) were housed in ventilated plastic cages over PWI 8–16 hardwood bedding. There were 12 air changes per hour, 12 h light photoperiod (lights on at 0800 h), and an environmental temperature of 21–23 °C with 50–60% relative humidity. The animals were fed a normal standard chow diet and water ad libitum. Care and treatment of the rats were in compliance with the guidelines of the Canadian Council on Animal care, and the protocol was approved by the University of Toronto Animal Care Committee. Hepatocytes were isolated from rats by collagenase perfusion of the liver as described by Moldeus et al. (Moldeus et al, 1978). Isolated hepatocytes (10 mL, 10^6 cells/mL) were suspended in Krebs–Henseleit buffer (pH 7.4) containing 12.5 mM HEPES in continually rotating 50 mL round-bottom flasks, under an atmosphere of 95% O_2 and 5% CO_2 in a 37 °C water bath for 30 min. Stock solutions of chemicals were made in double-distilled water or dimethylsulfoxide (DMSO).

4.3.3 Cell viability

Hepatocyte viability was assessed microscopically by plasma membrane disruption as determined by the Trypan blue (0.1%, w/v) exclusion test (Moldeus et al, 1978). Hepatocyte viability was determined every 30 min during the first hour and then at 2 and 3 h of incubation. Only cell preparations with viabilities of 85–95% were used.

4.3.4 H_2O_2 generating system

When H_2O_2 was added to hepatocytes, most of the H_2O_2 was metabolized by catalase within seconds (Ou and Wolff, 1996). Therefore, a H_2O_2 generating system (Antunes and Cadenas, 2001) was employed by adding 10 mM glucose to the hepatocyte suspension followed by glucose oxidase (0.5 U/mL). The rate of oxygen uptake and hydrogen peroxide formation was verified using an oxygen electrode to monitor the release of oxygen with catalase. This glucose/glucose oxidase system continuously supplied H_2O_2 to the hepatocytes over the experimental period, without affecting GSH levels.

4.3.5 Hepatocyte lipid peroxidation

Lipid peroxidation was determined by measuring the amount of thiobarbituric acid reactive substances (TBARS) at 532 nm, formed during the decomposition of lipid hydroperoxides using a Pharmacia Biotech Ultrospec 1000. At different time points, each test tube containing 1 mL aliquots of hepatocyte suspension (10^6 cell/mL) was treated with 250 µL of TCA (70% w/v) and

1 mL of thiobarbituric acid (0.8% w/v). The suspension was then boiled for 20 min and read at 532 nm as previously described (Smith et al, 1982). An extinction coefficient of 156 mM^{-1} cm^{-1} was used to determine the concentration of malondialdehyde produced.

4.3.6 Cellular GSH and oxidized glutathione (GSSG) content

GSH and GSSG were measured by HPLC analysis of deproteinized samples (25% *meta*-phosphoric acid) after derivatization with iodoacetic acid and DNFB as per the method outlined (Reed et al, 1980). A Waters HPLC system (model 150 pumps, WISP 710B autoinjector, and model 410 UV–vis detector) equipped with a Waters μBondapak NH_2 (10 μm) 3.9 mm × 300 mm column was used. Detection was carried out using UV absorption at 364 nm.

4.3.7 H_2O_2 measurement

H_2O_2 levels in hepatocytes were measured by taking samples at 15, 30, 60, and 120 min using the FOX 1 reagent (ferrous oxidation of xylenol orange). The FOX 1 reagent consisted of 25 mM sulfuric acid, 250 μM ferrous ammonium sulfate, 100 μM xylenol orange, and 0.1 M sorbitol. At the given time intervals, 50 μL of hepatocytes (1.0×10^6 cells/mL) was added to 950 μL of FOX 1 reagent and incubated for 30 min at room temperature. The absorbance of the samples was read at 560 nm, and the concentration of H_2O_2 was determined using the extinction coefficient of 2.67×10^5 M^{-1} cm^{-1} (Ou and Wolff, 1996).

4.3.8 Protein carbonylation assay

The total protein-bound carbonyl content was measured by derivatizing the protein carbonyl adducts with DNPH. Briefly, an aliquot of the suspension of cells (0.5 mL, 0.5×10^6 cells) at 30, 60, and 120 min was added to an equivalent volume (0.5 mL) of 0.1% DNPH (w/v) in 2.0 N HCl and allowed to incubate for 1 h at room temperature. This reaction was terminated and the total cellular protein precipitated by the addition of an equivalent of 1.0 mL volume of 20% TCA (w/v). Cellular protein was pelleted by centrifugation at 50 × *g*, and the supernatant was discarded. Excess unincorporated DNPH was extracted three times using an excess volume (0.5 mL) of ethanol:ethyl acetate (1:1) solution. Following extraction, the recovered cellular protein was dried under a stream of nitrogen and dissolved in 1 mL of Tris-buffered 8.0 M guanidine–HCl, pH 7.2. The resulting solubilized hydrazones were measured at 366–370 nm. The concentration of 2,4-DNPH derivatized protein carbonyls was determined using an extinction coefficient of 22000 M^{-1} cm^{-1}(Hartley et al, 1997).

4.3.9 Statistical analysis

Statistical analysis was preformed by a one-way ANOVA (analysis of variance) test, and significance was assessed by employing Tukey’s posthoc test.

4.4 Results

As shown in Table 4.1, incubation of isolated hepatocytes with 8 mM hydralazine induced a 50% loss in hepatocyte viability in 2 h (LC_{50}) as measured by the trypan blue exclusion assay. Hepatocyte susceptibility to hydralazine was also concentration-dependent and increased as the concentration of hydralazine increased. 1-Aminobenzotriazole, a P450 inhibitor, delayed hydralazine cytotoxicity; however, BHA, an antioxidant, did not affect hydralazine-induced cytotoxicity. Furthermore, H_2O_2 markedly increased hepatocyte cytotoxicity induced by 4 or 1 mM hydralazine. The H_2O_2 was generated at a rate that caused little cytotoxicity toward control hepatocytes. Hepatocyte susceptibility to hydralazine in the presence of H_2O_2 was enhanced as the dose of hydralazine increased. Hydralazine cytotoxicity was also increased a further 2-fold when hepatocytes were preincubated with hydralazine for 60 min prior to addition of the H_2O_2 generating system to allow for hydralazine bioactivation. Moreover, P450 inhibition by 1-aminobenzotriazole delayed toxicity, suggesting a role for P450 in H_2O_2-enhanced hydralazine cytotoxicity. The superoxide scavenger, TEMPOL, delayed cytotoxicity, but the antioxidant BHA was not cytoprotective.

Table 4.1 Hydralazine-induced toxicity in the presence and absence of hepatocyte H_2O_2 oxidative stress model

Addition	**Cytotoxicity (%Trypan blue uptake)**		
Incubation time (min)	***60***	***120***	***180***
Control (only hepatocytes)	18 ± 2	21 ± 1	26 ± 1
+ Hydralazine 8 mM	42 ± 2[a]	51 ± 3[a]	68 ± 5[a]
+ 1-Aminobenzotriazole* 100 μM	28 ± 1[b]	37 ± 2[b]	48 ± 3[b]
+ BHA 50 μM	43 ± 3	53 ± 2	70 ± 4
+ Hydralazine 4 mM	30 ± 2[a]	38 ± 2[a]	44 ± 2[a]
+ H_2O_2 generating system	36 ± 1	59 ± 4[c]	74 ± 5[c]
+ 1-Aminobenzotriazole* 100 μM	25 ± 1[d]	39 ± 3[d]	53 ± 3[d]
+ BHA 50 μM	37 ± 2	57 ± 2	78 ± 4
+ TEMPOL 200 μM	27 ± 2[d]	36 ± 2[d]	53 ± 4[d]
+ Hydralazine* 4 mM + H_2O_2 generating system	86 ± 6[c]	100[c]	100[c]
+ Hydralazine 1 mM	28 ± 1[a]	33 ± 2[a]	37 ± 1[a]
+ H_2O_2 generating system	39 ± 2[e]	48 ± 3[e]	64 ± 4[e]
+ Hydralazine* 1 mM + H_2O_2 generating system	57 ± 5[e]	78 ± 7[e]	100[e]
+ H_2O_2 generating system	24 ± 2	29 ± 2	34 ± 2

H_2O_2 generating system: Glucose 10 mM and glucose oxidase 0.5 U/mL; BHA (butylated hydroxyanisole): antioxidant; 1-Aminobenzotriazole: P450 inhibitor; TEMPOL: 4-Hydroxy-2,2,6, 6-tetramethylpiperidene-1-oxyl (ROS scavenger)
Refer to Materials and Methods for a description of experiments performed.
* Hepatocytes were pre-incubated with aminobenzotriazole or hydralazine for 60 min prior to the addition of other agents.
Means ± SE for three separate experiments are given.
[a] Significant as compared to control ($P < 0.05$).
[b] Significant as compared to Hydralazine 8 mM alone ($P < 0.05$).
[c] Significant as compared to Hydralazine 4 mM alone ($P < 0.05$).
[d] Significant as compared to Hydralazine 4 mM + H_2O_2 generating system ($P < 0.05$).
[e] Significant as compared to Hydralazine 1 mM alone ($P < 0.05$).

As shown in Table 4.2, hydralazine cytotoxicity was not accompanied by oxidative stress as measured by lipid peroxidation, protein carbonylation, or increased H_2O_2 levels. Moreover, hydralazine cytotoxicity in the presence of a H_2O_2 generating system increased protein carbonylation and intracellular H_2O_2 levels, which were partly prevented by TEMPOL but not BHA. Cytotoxicity did not result in lipid peroxidation. Pre-incubation of hepatocytes with hydralazine for 60 min prior to addition of the H_2O_2 generating system further increased protein carbonyl formation and endogenous H_2O_2 levels.

Table 4.2 Oxidative stress induced by P450/H_2O_2-catalyzed hydralazine oxidation in the hepatocyte H_2O_2 oxidative stress model

Addition	**Lipid peroxidation (μM)**	**Protein carbonylation (nmoles/10^6 hepatocytes)**	**Endogenous H_2O_2 measurement (nmoles/10^6 cells)**
Incubation time (min)	***90***	***90***	***120***
Control (only hepatocytes)	0.16 ± 0.05	8.16 ± 0.39	7.4 ± 0.31
+ Hydralazine 8 mM	0.19 ± 0.07	9.56 ± 0.34	7.6 ± 0.29
+ Hydralazine 4 mM	0.15 ± 0.05	8.28 ± 0.43	7.8 ± 0.28
+ H_2O_2 generating system	0.20 ± 0.07	12.6 ± 0.6[a]	14.1± 0.5[a]
+ 1-Aminobenzotriazole* 100 μM	0.18 ± 0.06	8.17 ± 0.49[b]	9.98 ± 0.22[b]
+ BHA 50 μM	0.21 ± 0.06	12.47 ± 0.41	13.76 ± 0.34
+ TEMPOL 200 μM	0.23 ± 0.05	9.31 ± 0.36[b]	10.42 ± 0.3[b]
+ Hydralazine*4 mM + H_2O_2 generating system	0.21 ± 0.08	19.7 ± 0.82[a]	18.3 ± 0.65[a]
+ H_2O_2 generating system	0.26 ± 0.06	8.54 ± 0.42	8.1 ± 0.32

H_2O_2 generating system: Glucose 10 mM and glucose oxidase 0.5 U/mL; 1-Aminobenzotriazole: P450 inhibitor; BHA (butylated hydroxyanisole): antioxidant; TEMPOL: 4-Hydroxy-2,2,6, 6-tetramethylpiperidene-1-oxyl (ROS scavenger)

* Hepatocytes were pre-incubated with aminobenzotriazole or hydralazine for 60 min prior to the addition of other agents.

Refer to Materials and Methods for a description of experiments performed.

1-Aminobenzotriazole: P450 inhibitor

Means ± SE for three separate experiments are given.

[a] Significant as compared to Hydralazine 4 mM alone ($P < 0.05$).

[b]Significant as compared to Hydralazine 4 mM + H_2O_2 generating system ($P < 0.05$).

As shown in Figure 4.1a, only a small amount of hepatocyte GSH was depleted by hydralazine at this concentration. H_2O_2, however, increased hepatocyte GSH depletion by hydralazine. This effect was greater, and hydralazine caused about 50% GSH depletion within 30 min if the hepatocytes were preincubated with hydralazine 60 min before the addition of H_2O_2 generating system. Furthermore, the P450 inhibitor 1-aminobenzotriazole inhibited the GSH depletion (Figure 4.1a).

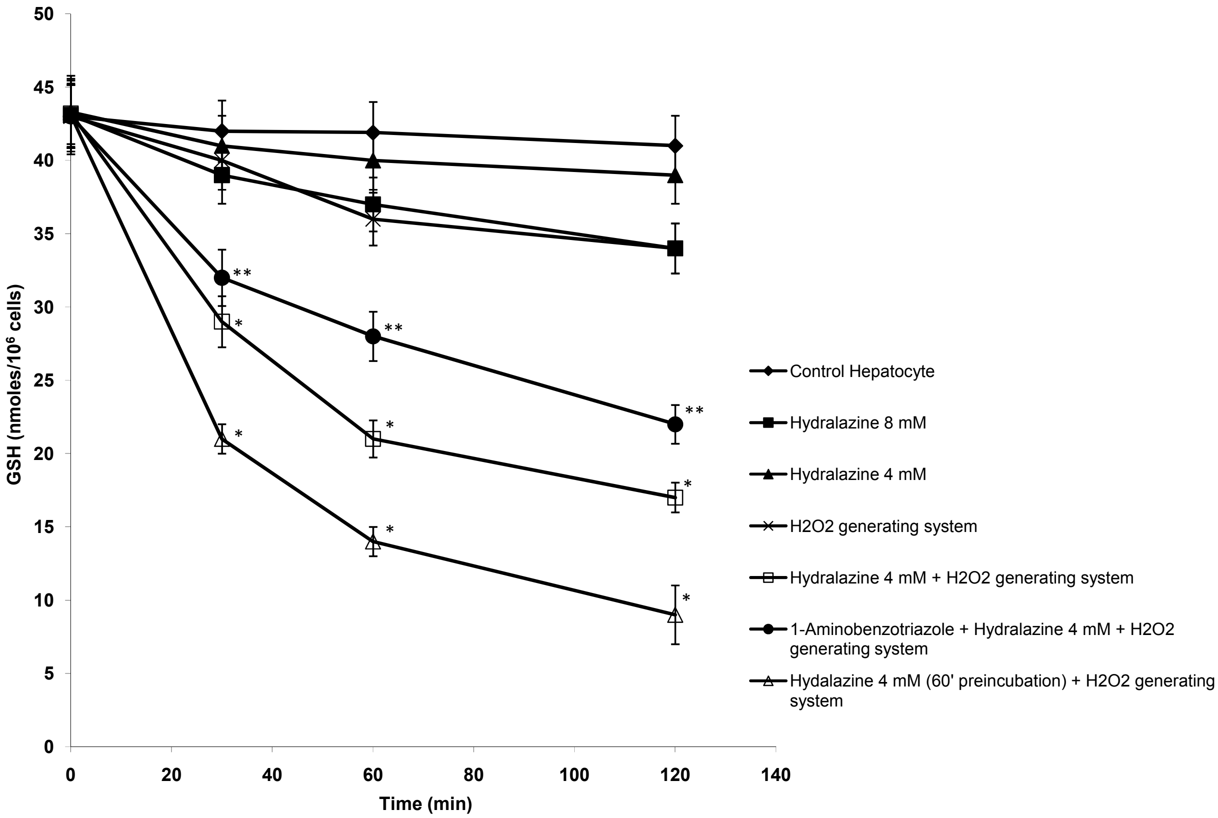

Figure 4.1a Hepatocyte GSH depletion by hydralazine/H_2O_2 generating system

H_2O_2 generating system consisted of glucose 10 mM and glucose oxidase 0.5 U/mL. The concentration of other chemicals used was as follows: 1-aminobenzotriazole 100 μM (P450 inhibitor). Refer to Materials and Methods for a description of experiments performed.

Means ± SE for three separate experiments are given.

[*] Significant as compared to H_2O_2 generating system ($P < 0.05$).

[**] Significant as compared to hydralazine 4 mM + H_2O_2 generating system ($P < 0.05$).

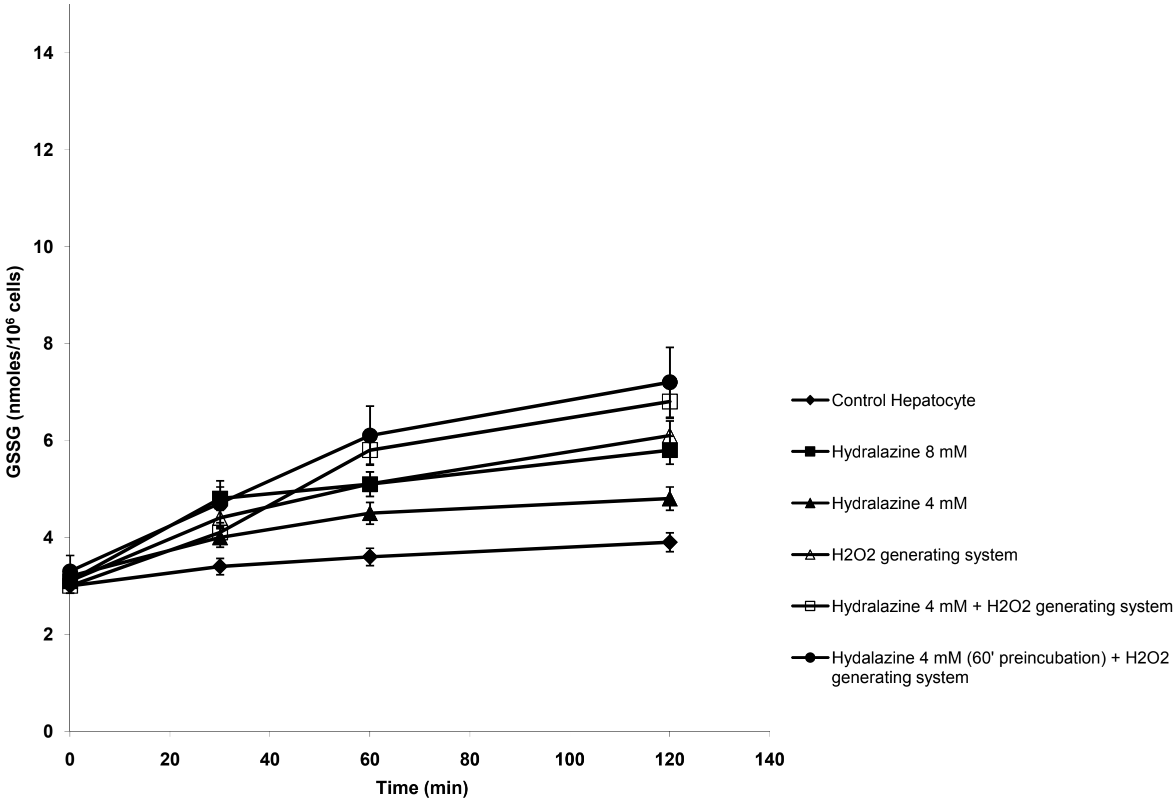

Figure 4.1b Hepatocyte GSSG formation by hydralazine/H_2O_2 generating system
H_2O_2 generating system consisted of glucose 10 mM and glucose oxidase 0.5 U/mL.
Refer to Materials and Methods for a description of experiments performed.
Means ± SE for three separate experiments are given.

As shown in Table 4.3, if hepatocytes were incubated with hydralazine in the presence of a non-toxic amount of H_2O_2 and MPO or HRP, only 100 μM hydralazine was required to cause 50% cytotoxicity in 2 h (LC_{50}). Furthermore, this cytotoxicity was delayed by PTU, a peroxidase inhibitor, the antioxidant BHA, as well as the ROS scavengers, TEMPOL and gallic acid. In the absence of hydralazine, none of the modulators at the doses used affected hepatocyte viability.

Table 4.3 Hydralazine-induced toxicity in the peroxidase oxidative stress-enhanced model

Addition	Cytotoxicity (%Trypan blue uptake)		
Incubation time (min)	*60*	*120*	*180*
Control (only hepatocytes)	17 ± 1	21 ± 2	25 ± 2
+ H_2O_2 generating system + HRP 0.1 μM	23 ± 2	26 ± 2	31 ± 2
+ H_2O_2 generating system + MPO 0.05 μM	26 ± 1	29 ± 1	32 ± 1
+ Hydralazine 1 mM	31 ± 1[a]	34 ± 2[a]	44 ± 2[a]
+ H_2O_2 generating system + MPO 0.05 μM	100[b]	100[b]	100[b]
+ H_2O_2 generating system + HRP 0.1 μM	100[b]	100[b]	100[b]
+ Hydralazine 500 μM	26 ± 1[a]	30 ± 1[a]	34 ± 1[a]
+ H_2O_2 generating system + HRP 0.1 μM	57 ± 5[c]	81 ± 6[c]	100[c]
+ Hydralazine 100 μM	23 ± 1	27 ± 1	30 ± 1
+ H_2O_2 generating system + MPO 0.05 μM	41 ± 3[d]	53 ± 6[d]	81 ± 5[d]
+ H_2O_2 generating system + HRP 0.1 μM	38 ± 2[d]	58 ± 4[d]	74 ± 4[d]
+ 1-Aminobenzotriazole* 100 μM	32 ± 1	41 ± 2[e]	59 ± 3[e]
+ PTU 5 μM	27 ± 1[e]	47 ± 3[e]	58 ± 3[e]
+ Gallic Acid 150 μM	25 ± 2[e]	39 ± 1[e]	53 ± 3[e]
+ BHA 50 μM	30 ± 1	43 ± 4[e]	52 ± 2[e]
+ TEMPOL 200 μM	31 ± 2	44 ± 2[e]	49 ± 2[e]

H_2O_2 generating system: Glucose 10 mM and glucose oxidase 0.5 U/mL; MPO: Myeloperoxidase; HRP: Horseradish peroxidase; PTU: 6-n-Propyl-thiouracil (peroxidase inhibitor); BHA (butylated hydroxyanisole): Antioxidants; Gallic acid and TEMPOL: 4-Hydroxy-2,2,6, 6-tetramethylpiperidene-1-oxyl (ROS scavenger); 1-Aminobenzotriazole: P450 inhibitor

* Hepatocytes were pre-incubated with aminobenzotriazole or hydralazine for 60 min prior to the addition of other agents.

Refer to Materials and Methods for a description of experiments performed.

Means ± SE for three separate experiments are given.

[a] Significant as compared to control ($P < 0.05$).

[b] Significant as compared to Hydralazine 1 mM alone ($P < 0.05$).

[c] Significant as compared to Hydralazine 500 μM alone ($P < 0.05$).

[d] Significant as compared to Hydralazine 100 μM alone ($P < 0.05$).

[e] Significant as compared to Hydralazine 100 μM + H_2O_2 generating system + HRP 0.1 μM ($P < 0.05$).

With peroxidase present, there was a marked increase in lipid peroxidation, protein carbonyl formation, and endogenous H_2O_2 levels before cytotoxicity ensued (Table 4.4). These oxidative stress biomarkers were also delayed by the peroxidase inhibitor PTU and antioxidant BHA or ROS scavengers TEMPOL and gallic acid.

Table 4.4 Oxidative stress induced by peroxidase/H_2O_2-catalyzed hydralazine oxidation in the hepatocyte peroxidase oxidative stress model

Addition	Lipid peroxidation (μM)	Protein carbonylation (nmoles/10^6 cells)	EndogenousH_2O_2 measurement (nmoles/10^6 cells)
Incubation time (min)	***90***	***90***	***120***
Control (only hepatocytes)	0.16 ± 0.05	8.16 ± 0.39	7.4 ± 0.31
+ H_2O_2 generating system + HRP 0.1 μM	0.37 ± 0.06	8.67 ± 0.47	8.4 ± 0.31
+ H_2O_2 generating system + MPO 0.05 μM	0.23 ± 0.03	8.58 ± 0.43	8.7 ± 0.30
+ Hydralazine 100 μM	0.14 ± 0.06	8.09 ± 0.47	7.5 ± 0.30
+ H_2O_2 generating system + MPO 0.05 μM	1.31 ± 0.07^a	32.7 ± 1.4^a	29.4 ± 0.1^a
+ H_2O_2 generating system + HRP 0.1 μM	1.87 ± 0.12^a	38.5 ± 1.3^a	23.2 ± 0.1^a
+ PTU 5 μM	0.74 ± 0.04^b	12.7 ± 0.53^b	11.3 ± 0.7^b
+ Gallic Acid 150 μM	0.57 ± 0.06^b	14.8 ± 0.75^b	14.3 ± 0.8^b
+ BHA 50 μM	0.54 ± 0.05^b	13.6 ± 0.66^b	12.7 ± 0.6^b
+ TEMPOL 200 μM	0.74 ± 0.03^b	14.1 ± 0.79^b	13.9 ± 0.7^b

H_2O_2 generating system: Glucose 10 mM and glucose oxidase 0.5 U/mL; MPO: Myeloperoxidase; HRP: Horseradish peroxidase; PTU: 6-n-Propyl-thiouracil (peroxidase inhibitor); BHA (butylated hydroxyanisole): Antioxidants; Gallic acid and TEMPOL: 4-Hydroxy-2,2,6, 6-tetramethylpiperidene-1-oxyl (ROS scavenger)
Refer to Materials and Methods for a description of experiments performed.
Means ± SE for three separate experiments are given.
^{a} Significant as compared to Hydralazine 100 μM alone (P < 0.05).
^{c} Significant as compared to Hydralazine 100 μM + H_2O_2 generating system + HRP 0.1 μM

As shown in Figure 4.2a, the hepatocyte GSH depletion that occurred with hydralazine and the H_2O_2 generating system/peroxidase was extensive and was accompanied by GSSG formation even though hydralazine concentration was only 100 μM (Figure 4.2b). Furthermore, PTU and BHA delayed both GSH depletion and GSSG formation. In the absence of hydralazine, the peroxidase and H_2O_2 generating system did not affect hepatocyte viability or GSH levels.

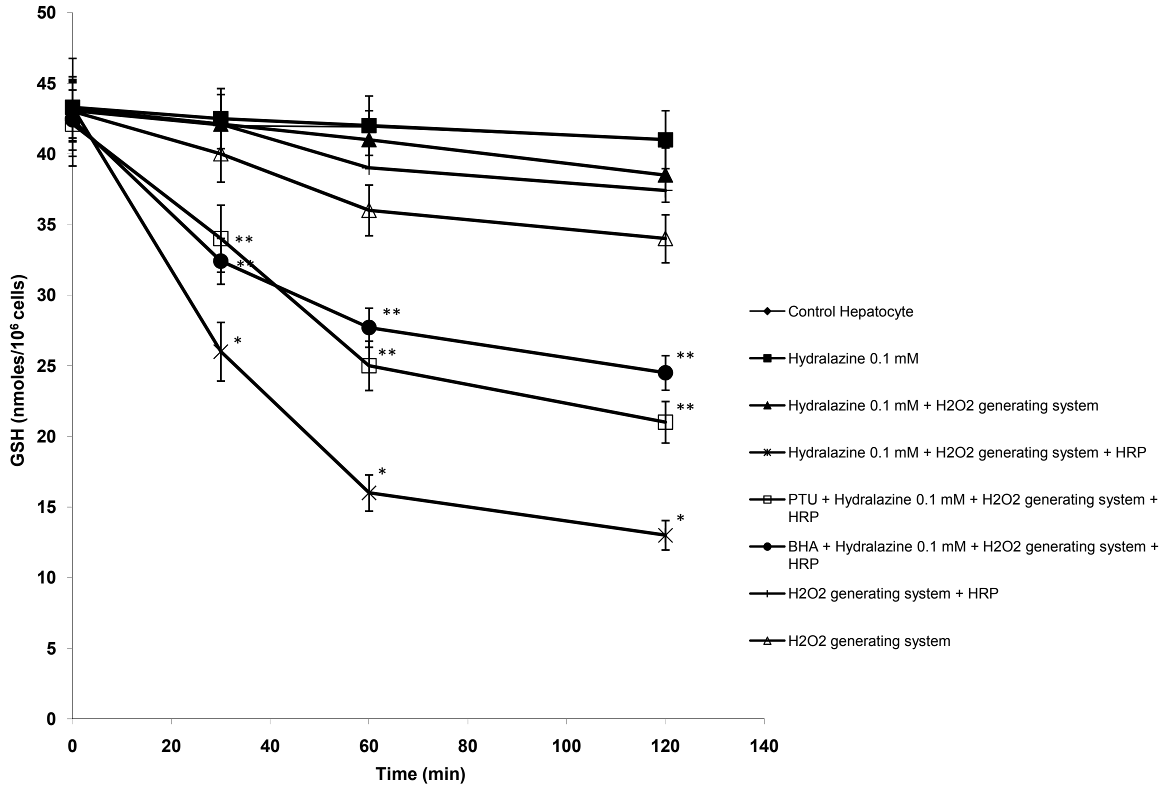

Figure 4.2a Hepatocyte GSH oxidation by hydralazine/H_2O_2 generating system + peroxidase

H_2O_2 generating system consisted of glucose 10 mM and glucose oxidase 0.5 U/mL. The concentration of other chemicals used was as follows: PTU 10 μM (peroxidase inhibitor) and BHA 50 μM (antioxidant).

Refer to Materials and Methods for a description of experiments performed.

Means ± SE for three separate experiments are given.

* Significant as compared to H_2O_2 generating system + HRP 0.1 μM ($P < 0.05$).

** Significant as compared to hydralazine 100 μM + H_2O_2 generating system + HRP 0.1 μM ($P < 0.05$).

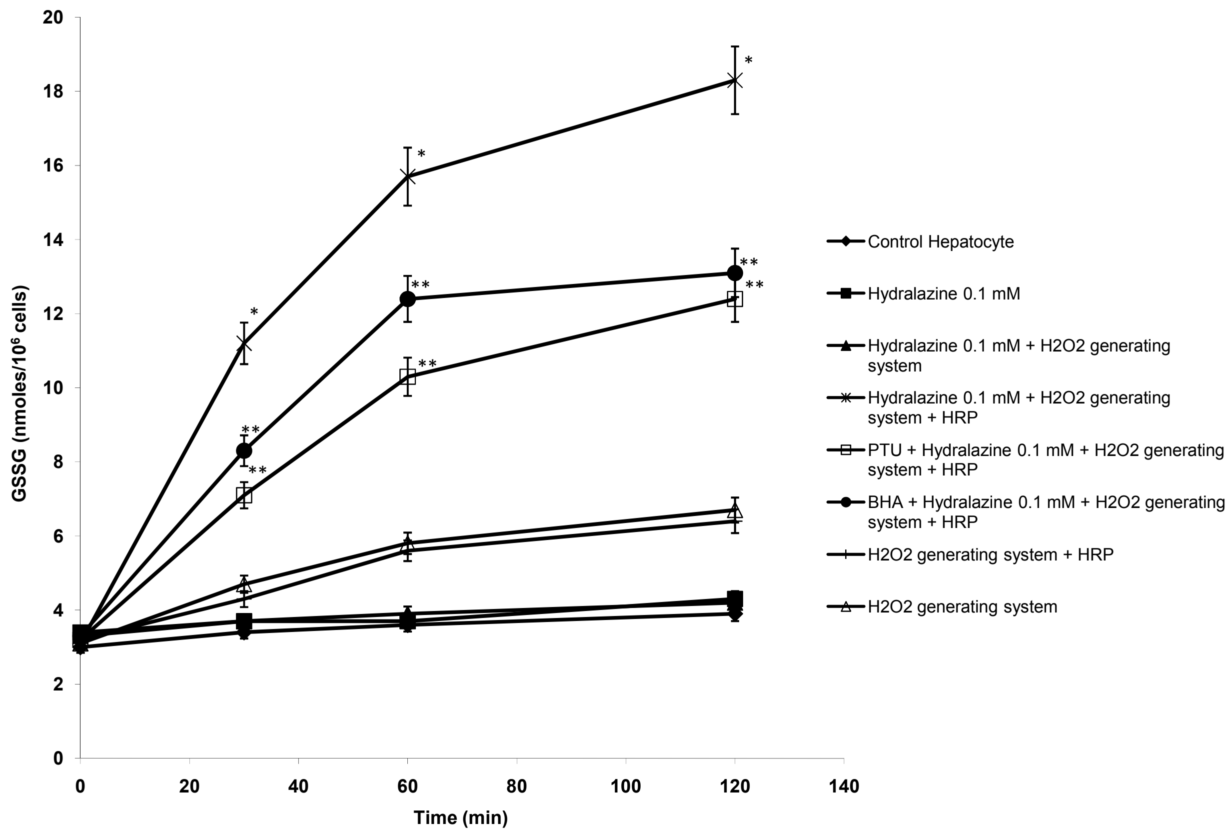

Figure 4.2b Hepatocyte GSSG formation by peroxidase catalyzed hydralazine oxidation
H_2O_2 generating system consisted of glucose 10 mM and glucose oxidase 0.5 U/mL. The concentration of other chemicals used was as follows: PTU 10 μM (peroxidase inhibitor) and BHA 50 μM (antioxidant)
Refer to Materials and Methods for a description of experiments performed.
Means ± SE for three separate experiments are given.
[*] Significant as compared to H_2O_2 generating system + HRP 0.1 μM ($P < 0.05$).
[**] Significant as compared to hydralazine 100 μM + H_2O_2 generating system + HRP 0.1 μM ($P < 0.05$).

4.5 Discussion

Hydralazine cytotoxicity toward isolated rat hepatocytes was delayed by the P450 inhibitor, 1-aminobenzotriazole, but oxidative stress was not induced and cytotoxicity was not prevented by the antioxidant BHA. However, hydralazine was 2-fold more cytotoxic toward hepatocytes exposed to non-toxic levels of H_2O_2 and was 4-fold more toxic if the hepatocytes were preincubated with hydralazine prior to the addition of the H_2O_2 generating system. This suggests that a reactive metabolite compromised the hepatocytes resistance to H_2O_2 or that H_2O_2 oxidatively activated the hydralazine P450-catalyzed metabolites formed or that P450/H_2O_2 catalyzed hydralazine oxidation to reactive metabolites (Anari et al, 1997). Furthermore, 1-aminobenzotriazole, a nonselective P450 inhibitor (Ortiz de Montellano and Mathews, 1981), prevented hydralazine-induced toxicity and suggested a role for P450 in the H_2O_2-enhanced bioactivation of hydralazine. Furthermore, hydralazine toxicity in the presence of H_2O_2 was accompanied by some protein carbonylation, GSH depletion with GSSG formation, and an increase in intracellular H_2O_2 levels. There was also no lipid peroxidation, and BHA did not prevent cytotoxicity. Cytotoxicity was, however, prevented by TEMPOL, a superoxide scavenger and superoxide dismutase mimic, suggesting that reactive oxygen species (ROS) caused the cytotoxicity.

When hydralazine was incubated with hepatocytes and peroxidase/H_2O_2, toxicity was increased up to 80-fold and extensive lipid peroxidation and GSH oxidation occurred. Lipid peroxidation was likely induced by hydralazyl radicals or diimines that were formed when hydralazine underwent a one-electron oxidation catalyzed by H_2O_2/peroxidase (Sinha, 1983; Yamamoto and Kawanishi, 1991). Moreover, the antioxidant BHA inhibited both lipid peroxidation and hydralazine cytotoxicity, suggesting that lipid peroxidation was a major contributor to hydralazine-induced cytotoxicity. Cytotoxicity was also prevented by ROS scavengers or a peroxidase inhibitor.

The lipid peroxidation induced by the peroxidase/H_2O_2 can be readily explained as we previously showed that peroxidase enzymes and H_2O_2 caused the one-electron oxidation of phenolics, aniline compounds, nonsteroidal anti-inflammatory drugs, indoleacetic acid derivatives, or vitamin E analogues to form highly reactive free radicals, which co-oxidized ascorbate, NADH, or GSH or unsaturated fatty acids. When hepatocytes were present, hepatocyte lipid peroxidation, ROS formation, and GSH oxidation to GSSG ensued (Galati et al, 2002a; O'Brien, 1988; Tafazoli et al, 2005a; Tafazoli et al, 2005b; Tafazoli and O'Brien, 2005).

It is not likely that the large increase in hydralazine cytotoxicity by peroxidase/H_2O_2 was due to catalase inactivation as high concentrations of hydralazine (about 2.5 M) were required to inhibit catalase activity by 50% in cultured fibroblasts (Weglarz et al, 1989). It was also shown that 1 mM phenylhydrazine caused a 20% catalase inactivation in red blood cells, as long as H_2O_2 was present (Cohen and Hochstein, 1964). Liver catalase experiments also showed that the inactivation mechanism involved a catalase-catalyzed oxidation of phenylhydrazine by H_2O_2 to a phenyl radical, which forms an iron−phenyl complex with catalase (Ortiz de Montellano and Kerr, 1983).

Hydralazine markedly increased hepatocyte endogenous H_2O_2 levels in the presence of H_2O_2/peroxidase. Other investigators showed that hydralazine or phenelzine added to human red blood cells increased endogenous H_2O_2 levels (Runge-Morris and Novak, 1993). While oxyhemoglobin or reduced transition metals could be a source of the H_2O_2 (Cohen and Hochstein, 1964; Yamamoto and Kawanishi, 1991), it is more likely that the hydralazyl radicals and diimine oxidation products reacted with oxygen to form H_2O_2 as was shown for the peroxidase-catalyzed oxidation of hydralazine or phenylhydralazine (Misra and Fridovich, 1976; Yamamoto and Kawanishi, 1991).

MPO was more effective than HRP at increasing hydralazine toxicity as only 0.05 μM MPO (half-of HRP required) was required to cause about 50% hepatocyte death in 2 h and toxicity was also accompanied by protein carbonylation and significant H_2O_2 formation. MPO/H_2O_2/chloride unlike HRP forms hypochlorite, which could also contribute to MPO-catalyzed hydralazine cytotoxicity. The lupus erythematosus side effect of hydralazine could involve activation by hypochlorite generated by neutrophils MPO/H_2O_2/chloride (Hofstra et al, 1991; Hofstra and Uetrecht, 1993).

Our results demonstrate that a non-toxic exposure to H_2O_2 markedly increased hepatocyte susceptibility to hydralazine, much like the conditions by which asymptomatic inflammation increases drug-induced hepatotoxicity. These results implicate H_2O_2, a cellular mediator of inflammation, as a potential risk factor for the manifestation of adverse drug reactions, particularly those caused by oxidizable hydrazine-containing drugs. In summary, H_2O_2-enhanced hepatocyte system in the presence and absence of peroxidase may prove useful for a more robust screening of drugs for assessing toxicity risk potential associated with inflammation. The cytotoxic molecular mechanism involved was dependent on the hydralazine metabolic activation mechanism and involved oxidative stress if H_2O_2 was present. The presence of MPO markedly increased both oxidative stress and cytotoxicity.

Chapter 5

Amodiaquine-Induced Oxidative Stress in a Hepatocyte Inflammation Model

---

Shahrzad Tafazoli, and Peter J. O'Brien

Submitted to *Toxicology*

5.1 Abstract

Amodiaquine is an antimalarial drug, however associated with its use are life-threatening agranulocytosis and hepatotoxicity in about 1 in 2000 patients, which is usually associated with an inflammatory response. It was found that the LC_{50} (2h) of amodiaquine towards isolated rat hepatocytes was 1 mM. The cytotoxic mechanism involved protein carbonylation as well as P450 activation to a reactive metabolite. The cytotoxicity, however, was not reactive oxygen species (ROS)-mediated, as ROS scavengers did not prevent cytotoxicity or protein carbonylation, and it was not accompanied by glutathione (GSH) oxidation or intracellular H_2O_2 formation. On the other hand, the cytotoxicity could be attributed to quinoneimine metabolite formation which formed GSH conjugates as GSH depleted hepatocytes were much more susceptible to amodiaquine. Furthermore, when a non-toxic H_2O_2 generating system and peroxidase was used to mimic the products formed by inflammatory immune cells, only 15 μM amodiaquine was required to cause 50% cell death. In the absence of amodiaquine, hepatocyte viability and glutathione (GSH) levels were not affected by the H_2O_2 generating system with or without peroxidase. The toxic mechanism of amodiaquine in this hepatocyte H_2O_2/peroxidase model involved oxidative stress, as cytotoxicity was accompanied by GSH oxidation, decreased mitochondrial membrane potential and protein carbonyl formation which were inhibited by ROS scavengers, 4-hydroxy-2,2,6,6-tetramethylpiperidene-1-oxyl (TEMPOL) or mannitol suggesting a role for a semiquinoneimine radical and ROS in the amodiaquine-H_2O_2-mediated cytotoxic mechanism.

5.2 Introduction

Malaria kills between 1 and 2 million people every year especially in Africa. There are few effective antimalarial drugs and most of Africa still relies on chloroquine because of its low cost, wide spread availability, and good oral tolerance. Chloroquine however, can no longer be relied upon for the treatment of *Plasmodium falciparum* malaria because of the development of resistance (Wernsdorfer, 1983). Amodiaquine, a chloroquine derivative and a 4-aminoquinoline, was synthesized in the late 1940s and is used in the prophylaxis and treatment of malaria, especially against chloroquine-resistant isolates of *Plasmodium falciparum* (Bepler et al, 1959). However, amodiaquine use has been associated with hepatotoxicity (Larrey et al, 1986; Neftel et al, 1986), agranulocytosis (Rhodes et al, 1986) and aplastic anemia (Hatton et al, 1986; Rwagacondo et al, 2003). Adverse drug reactions are more common with prophylaxis compared with treatment; so much so, that the drug has now been withdrawn from prophylactic use (Olliaro et al, 1996). The risk of each of these adverse effects is estimated to be 1:15,500 for hepatotoxicity, 1:2100 for agranulocytosis and 1:30,000 for aplastic anemia (Hatton et al, 1986; Rwagacondo et al, 2003). A liver biopsy of patients with amodiaquine-induced hepatitis showed mild hepatocyte necrosis, inflammatory infiltration, cholestasis and portal fibrosis (Larrey et al, 1986).

Amodiaquine is rapidly absorbed and extensively metabolized upon oral administration. The main metabolite of amodiaquine is *N*-desethylamodiaquine with other minor metabolites being 2-hydroxydesethylamodiaquine and *N*-bisdesethylamodiquine (Churchill et al, 1985; Mount et al, 1986). CYP2C8 was the main hepatic isoform that was involved in the clearance of amodiaquine and its hepatic metabolism to *N*-desethylamodiaquine (Li et al, 2002). Amodiaquine is readily oxidized to a quinoneimine that reacts rapidly and directly with proteins, forming thio-ether conjugates (Maggs et al, 1987). This facile oxidation is a consequence of the presence of a *p*-hydroxyaniline moiety adjacent to an aromatic nucleus in the amodiaquine molecule (Maggs et al, 1987).

Studies showed a high incidence of anti-amodiaquine antibodies in patients suffering adverse reactions from amodiaquine (Maggs et al, 1988). Specific IgG anti-amodiaquine antibodies were detected in the serum from five patients who exhibited serious adverse reaction after amodiaquine administration at a weekly dose of 400 mg, for several weeks, but not in volunteers who had not received the drug (Christie et al, 1989).

In order to find a more robust *in vitro* screening method for assessing the potential hepatotoxicity risk of amodiaquine, hepatocyte susceptibility to amodiaquine was investigated where hepatocytes were exposed to a low non-toxic continuous infusion of H_2O_2 in the absence or presence of peroxidase such as could be released by activated immune cells. In this way, hepatocyte vulnerability to amodiaquine in the presence of H_2O_2 formed during NADPH oxidase activation of immune cells could be simulated. Hepatocyte injury in the liver induced by a variety of hepatotoxins *in vivo,* has been partly attributed to cytokines released from resident macrophages or infiltrating neutrophils activated by inflammation. The NADPH oxidase of these cells produced large amounts of ROS during an inflammatory response. Recent evidence from experimental models suggests that an episode of inflammation during drug treatment predisposes animals to tissue injury (Buchweitz et al, 2002; Luyendyk et al, 2006). The hepatotoxicities of allyl alcohol and aflatoxin B1 in rats were augmented by liver inflammation following co-exposure to LPS (Buchweitz et al, 2002; Roth et al, 1997). We have previously used this H_2O_2-enhanced hepatocyte cytotoxicity model, with and without peroxidase, to study the hepatotoxicity of tolcapone (Tafazoli et al, 2005a), troglitazone (Tafazoli et al, 2005b), isoniazid

(Tafazoli et al, 2008), hydralazine (Tafazoli and O'Brien, 2008) and some carbonyl agents (O'Brien et al, 2007) which were shown to be much more cytotoxic. Other agents such as 2,2,5,7,8-pentamethyl-6-hydroxychromane (PMC, a vitamin E analogue), tribromoethanol (Avertin®), an anesthetic and acetylsalicylic acid (Aspirin®), though were not affected (O'Brien et al, 2007; Tafazoli et al, 2005a; Tafazoli et al, 2005b).

5.3 Material and methods

5.3.1 Chemicals

Amodiaquine dihydrochloride dihydrate, 1-aminobenzotriazole, 6-n-propyl-thiouracil (PTU), peroxidase from horseradish (EC 1.11.1.7; HRP), 4-hydroxy-2,2,6,6-tetramethylpiperidene-1-oxyl (TEMPOL), butylated hydroxyanisole (BHA), mannitol, 3-amino-1,2,4-triazole, 3,3′-Methylenebis(4-hydroxycoumarin) (dicumarol), 1-bromoheptane, borneol, 2′,4′-dinitrofluorobenzene (DNFB), thiobarbituric acid, trichloroacetic acid (TCA), iodoacetic acid, glucose, glucose oxidase, dinitrophenylhydrazine (DNPH), were purchased from Sigma–Aldrich Corp. (Oakville, Ont., Canada).

5.3.2 Animal treatment and hepatocyte preparation

Male Sprague–Dawley rats weighing 275–300 g (Charles River Laboratories, Montréal, Canada) were housed in ventilated plastic cages over PWI 8-16 hardwood bedding. There were 12 air changes per hour, 12-h light photoperiod (lights on at 0800 h) and an environmental temperature of 21–23 °C with a 50–60% relative humidity. The animals were fed a normal standard chow diet and water *ad libitum*. Care and treatment of the rats were in compliance with the guidelines of the Canadian Council on Animal care, and the protocol was approved by the University of Toronto Animal Care Committee. Hepatocytes were isolated from rats by collagenase perfusion of the liver as described by Moldeus *et al*. (Moldeus et al, 1978). Isolated hepatocytes (10 mL, 10^6 cells/mL) were suspended in Krebs–Henseleit buffer (pH 7.4) containing 12.5 mM HEPES in continually rotating 50 mL round bottom flasks, under an atmosphere of 95% O_2 and 5% CO_2 in a 37 °C water bath for 30 min.

5.3.3 Cell viability

Hepatocyte viability was assessed microscopically by plasma membrane intactness as determined by the trypan blue (0.1%, w/v) exclusion test (Moldeus et al, 1978). Hepatocyte viability was determined every 30 min during the first hour and then at 2 and 3 h incubation. Only cell preparations with viability of 85–95% were used.

5.3.4 Preparation of the enzyme-inhibited hepatocytes

P450-inhibited hepatocytes were prepared by adding the nonspecific suicide inhibitor of CYP450s, 1-aminobenzotriazole (Balani et al, 2002) to hepatocytes 1 hr prior to the other agents.

GSH-depleted hepatocytes were obtained by preincubating hepatocytes with 1-bromoheptane (200 μM), 30 min before the start of the experiment as previously described (Khan and O'Brien, 1991).

For NAD(P)H/quinone oxidoreductase (NQO)-inhibited hepatocytes, cells were preincubated with 20 μM dicumarol for 15 min prior to the addition of other agents (Preusch et al, 1991).

Glucuronidation-inhibited hepatocytes were obtained by incubating cell with 500 μM borneol for 15 min prior to the addition of other agents (Gregus et al, 1983; Kretz-Rommel and Boelsterli, 1993).

Peroxidase activity was inhibited by 6-n-propyl-thiouracil (PTU) (Lee et al, 1990) by incubating it with hepatocytes for 15 min along with HRP, prior to the start of the experiment.

Catalase activity was inhibited by preincubating hepatocytes with 500 μM 3-Amino-1,2,4-triazole 30 min prior to the addition of other agents (Boutin et al, 1989).

Stock solutions of all chemicals were made in water, dimethylsulfoxide (DMSO), or methanol.

5.3.5 H_2O_2 generating system

When H_2O_2 was added as a bolus dose to hepatocytes, most of the H_2O_2 was metabolized by catalase within seconds (Ou and Wolff, 1996). Therefore, a H_2O_2 generating system (Antunes and Cadenas, 2001) was employed by adding glucose 10 mM to the hepatocyte suspension followed by glucose oxidase (0.5 U/mL). The rate of oxygen uptake and H_2O_2 formation was verified using an oxygen electrode to monitor the release of oxygen with catalase (Tafazoli and O'Brien, 2004). This glucose/glucose oxidase system continuously supplied H_2O_2 during the experimental period, without affecting GSH levels or cell viability.

5.3.6 Cellular GSH and oxidized glutathione (GSSG) content

GSH and GSSG were measured by HPLC analysis of deproteinized samples (25% *meta*-phosphoric acid) after derivatization with iodoacetic acid and DNFB as per the method outlined by Reed *et al*. (Reed et al, 1980). A Waters HPLC system (Model 150 pumps, WISP 710B auto injector and model 410 UV–vis detector) equipped with waters µBondapak® NH_2 (10 µm) 3.9 × 300 mm column was used and detection was followed at 364 nm.

5.3.7 H_2O_2 measurement

H_2O_2 was measured in hepatocytes by taking samples at 15, 30 and 60 and 120 min and adding the FOX 1 reagent (ferrous oxidation of xylenol orange). The FOX 1 reagent consisted of 25 mM sulfuric acid, 250 µM ferrous ammonium sulfate, 100 µM xylenol orange and 0.1 M sorbitol. At the given time intervals 50 μL of hepatocytes (1.0×10^6 cells/mL) were added to 950 μL FOX 1 reagent and incubated for 30 min at room temperature. The absorbance of the samples were read at 560 nm and the concentration of H_2O_2 was determined using the extinction coefficient of 2.67×10^5 $M^{-1}.cm^{-1}$ (Ou and Wolff, 1996).

5.3.8 Protein carbonylation assay

Total protein-bound carbonyl content was measured by derivatizing the carbonyl adducts with dinitrophenylhydrazine (DNPH). Briefly an aliquot of the suspension of cells (0.5 mL, 0.5×10^6 cells) was added to an equivalent volume (0.5 mL) of 0.1% DNPH (w/v) in 2.0N HCl and allowed to incubate for an hour at room temperature with vortexing every 15 min. This reaction was terminated and total cellular protein precipitated by the addition of an equivalent 1.0 mL volume of 20% TCA (w/v). Cellular protein was rapidly pelleted by centrifugation at 10,000 rpm, and the supernatant was discarded. Excess unincorporated DNPH was extracted three times using an excess volume (0.5 mL) of ethanol:ethyl acetate (1:1) solution. Following the extraction, the recovered cellular protein was dried under a stream of nitrogen and solubilized in 1 mL of Tris-buffered 8.0 M guanidine–HCl, pH 7.2. The resulting solubilized hydrazones were measured at 366–370 nm. The concentration of 2,4-DNPH derivatized protein carbonyls was determined using an extinction coefficient of 22000 $M^{-1}.cm^{-1}$ (Hartley et al, 1997).

5.3.9 Mitochondrial membrane potential assay

The uptake and retention of the cationic fluorescent dye, rhodamine 123, has been used for the estimation of mitochondrial membrane potential. This assay is based on the fact that rhodamine 123 accumulates selectively in the mitochondria by facilitated diffusion. However, when the mitochondrial potential is decreased, the amount of rhodamine 123 that enters the mitochondria is decreased as there is no facilitated diffusion. Thus the amount of rhodamine 123 in the supernatant is increased and the amount in the pellet is decreased. Samples (500 μL) were taken from the cell suspension incubated at 37 °C, and centrifuged at 1000 rpm for 1 min. The cell pellet was then resuspended in 2 mL of fresh incubation medium containing 1.5 μM rhodamine 123 and incubated at 37 °C in a thermostatic bath for 10 min with gentle shaking. Hepatocytes were separated by centrifugation and the amount of rhodamine 123 appearing in the incubation medium was measured fluorimeterically using a Shimadzu RF5000U fluorescence spectrophotometer set at 490 nm excitation and 520 nm emission wavelengths. The capacity of mitochondria to take up the rhodamine 123 was calculated as the difference in fluorescence intensity between control and treated cells (Andersson et al, 1987).

5.3.10 Statistical analysis

Statistical analysis was preformed by a one-way ANOVA (analysis of variance) test and significance was assessed by employing Tukey's post hoc test.

5.4 Results

As shown in Figure 5.1, amodiaquine toxicity towards isolated rat hepatocytes was concentration-dependent with 1 mM amodiaquine causing about 50% death in two hours (LC_{50}) as measured by the trypan blue exclusion assay To determine the molecular cytotoxic mechanism, different compounds were added to the incubation medium to determine their ability to modulate the toxic response. For this purpose the LC_{50} of amodiaquine (1 mM) was selected.

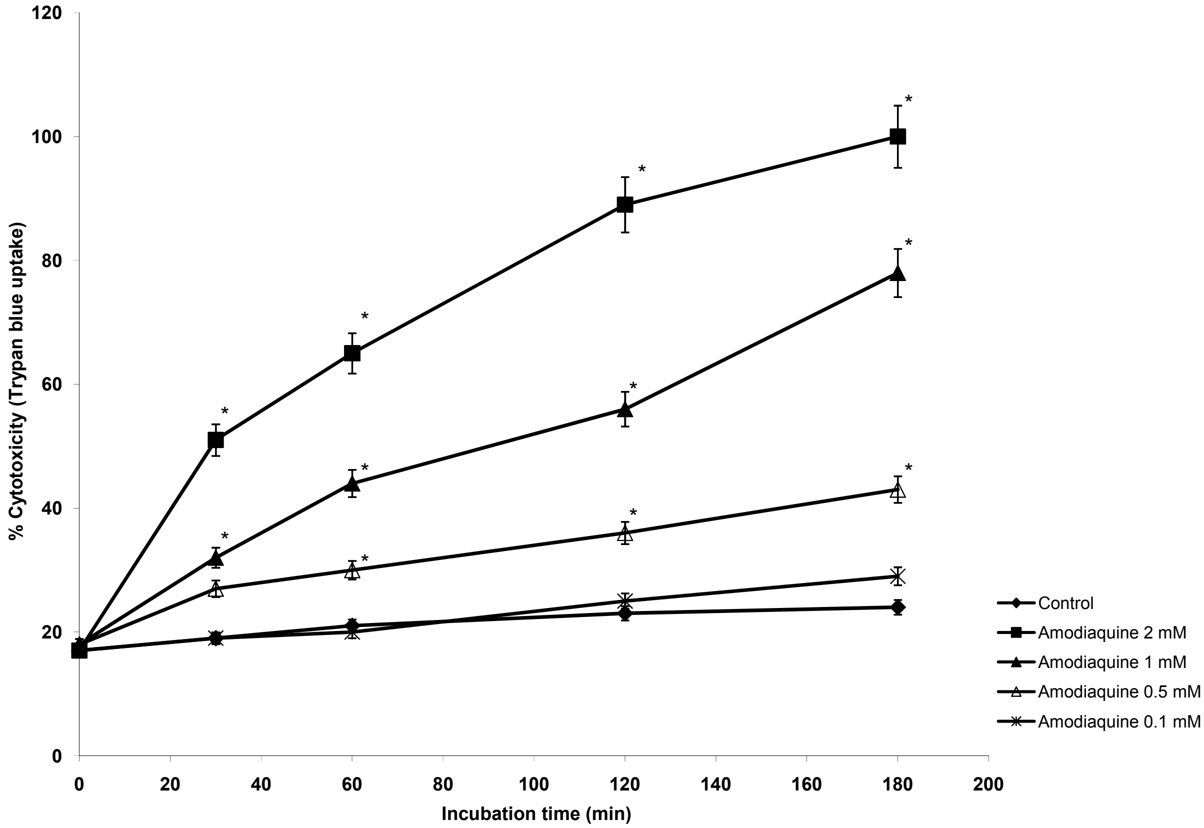

Figure 5.1 Dose response of amodiaquine-induced cytotoxicity towards isolated rat hepatocytes

Refer to Materials and Methods for a description of experiments performed.

Means ± SE for three separate experiments are given.

* Significant as compared to control ($P < 0.05$).

As shown in Figure 5.2, the non-selective P450 inhibitor (Balani et al, 2002) , 1-aminobenzotriazole delayed amodiaquine toxicity suggesting a role for P450 in activating amodiaquine to a toxic metabolite. On the other hand, dicumarol, a NAD(P)H/quinone oxidoreductase (NQO) inhibitor (Preusch et al, 1991), borneol, a glucuronidation inhibitor (Gregus et al, 1983; Kretz-Rommel and Boelsterli, 1993) and GSH depletion by bromoheptane (Gregus et al, 1983; Kaderlik et al, 1994; Khan and O'Brien, 1991) all resulted in a significant increase in amodiaquine-induced cytotoxicity. ROS scavengers, TEMPOL and mannitol, and antioxidants BHA and quercetin, however, did not affect cytotoxicity (results not shown).

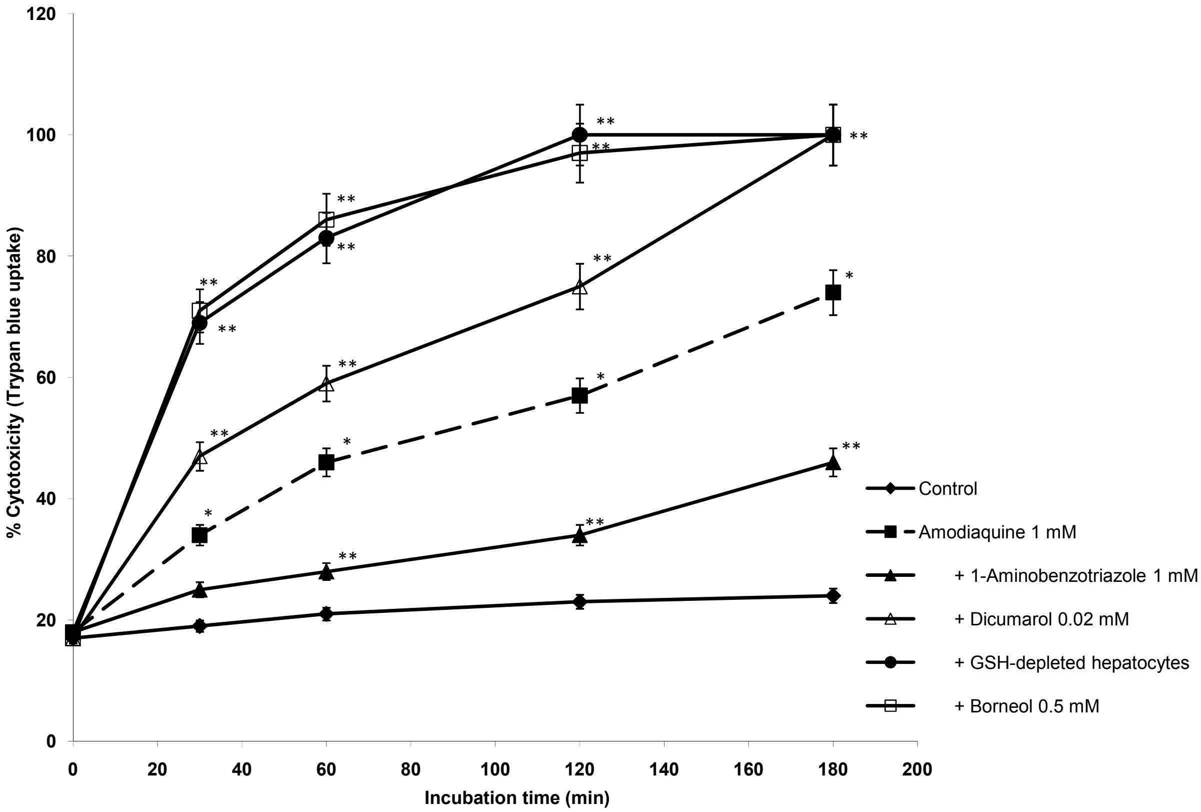

Figure 5.2 Modulating amodiaquine-induced cytotoxicity by chelators, NQO, P450 or glucuronidation inhibitors and GSH depletion

Refer to Materials and Methods for a description of experiments performed.

Dicumarol: a NAD(P)H/quinone oxidoreductase (NQO) inhibitor; 1-Aminobenzotriazole: P450 inhibitor; GSH-depleted hepatocytes were prepared by pre-incubation of hepatocytes for 30 min with 200 μM bromoheptane before the addition of other agents.

Means ± SE for three separate experiments are given.

* Significant as compared to control ($P < 0.05$).

** Significant as compared to amodiaquine-treated hepatocytes ($P < 0.05$).

As summarized in Figure 5.3, amodiaquine cytotoxicity was accompanied by a decrease in the mitochondrial membrane potential which was partly prevented by the P450 inhibitor, 1-aminobenzotriazole. NQO, GSH depletion and glucuronidation inhibition all increased amodiaquine toxicity. ROS scavengers did not have an effect in preventing the decrease in the mitochondrial membrane potential (results not shown).

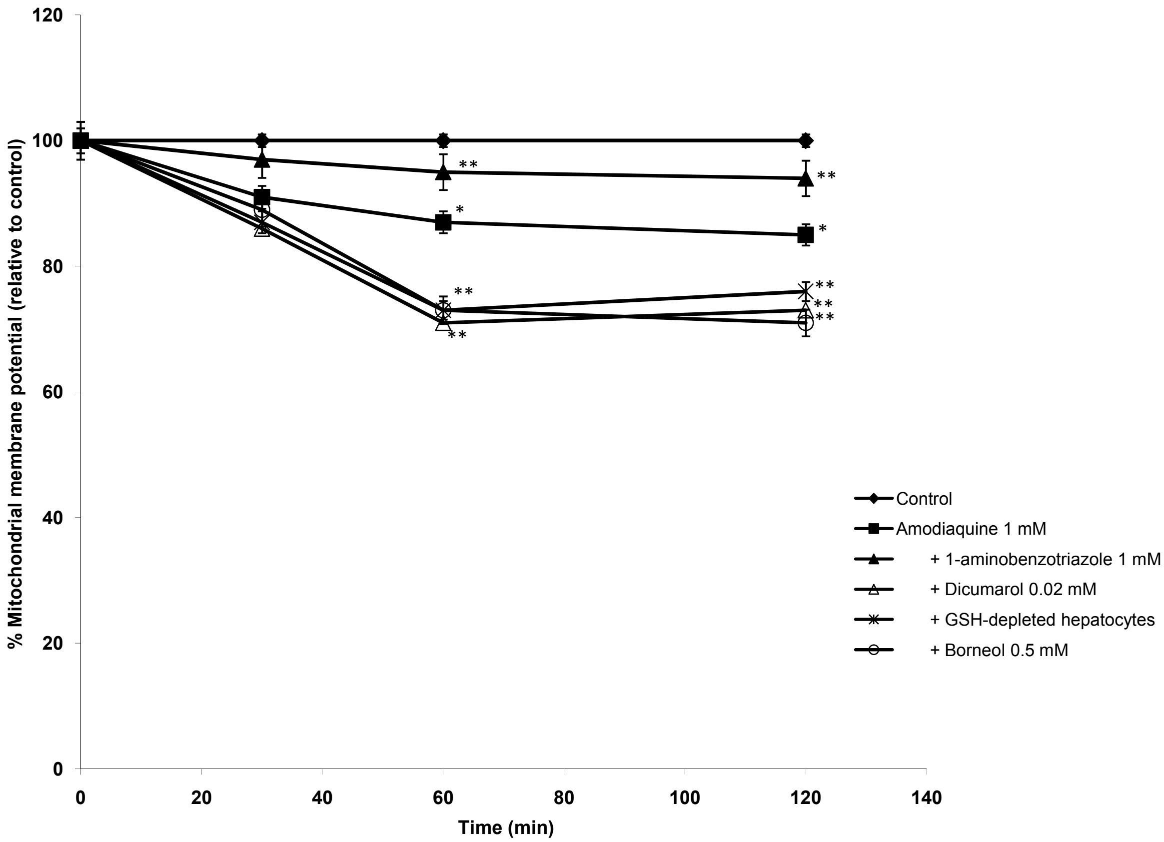

Figure 5.3 Modulating amodiaquine-induced mitochondrial membrane potential collapse by NQO, P450 or glucuronidation inhibitors and GSH depletion

Refer to Materials and Methods for a description of experiments performed.

Dicumarol: a NAD(P)H/quinone oxidoreductase (NQO) inhibitor; GSH-depleted hepatocytes were prepared by pre-incubation of hepatocytes for 30 min with 200 μM bromoheptane before the addition of other agents; 1-Aminobenzotriazole: P450 inhibitor

Means ± SE for three separate experiments are given.

[*] Significant as compared to control ($P < 0.05$).

[**] Significant as compared to amodiaquine-treated hepatocytes ($P < 0.05$).

As shown in Figure 5.4, protein carbonylation was markedly increased by the glucuronidation inhibitor, GSH depletion or NQO inhibition. Protein carbonylation by amodiaquine, however, was not delayed by the ROS scavengers TEMPOL and mannitol (results not shown).

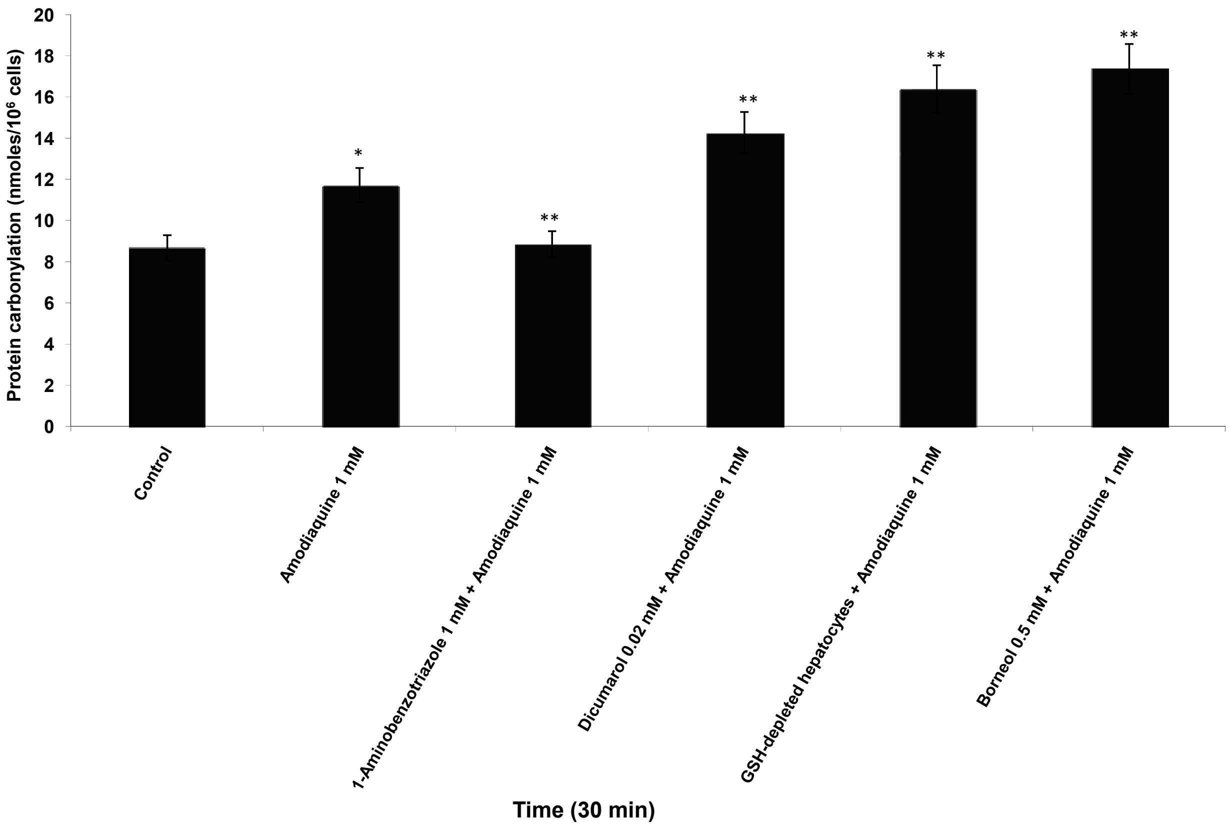

Figure 5.4 Modulating amodiaquine-induced protein carbonylation by NQO, P450 or glucuronidation inhibitors and GSH depletion

Refer to Materials and Methods for a description of experiments performed.

Dicumarol: a NAD(P)H/quinone oxidoreductase (NQO) inhibitor; GSH-depleted hepatocytes were prepared by pre-incubation of hepatocytes for 30 min with 200 μM bromoheptane before the addition of other agents; 1-Aminobenzotriazole: P450 inhibitor

Means ± SE for three separate experiments are given.

* Significant as compared to control ($P < 0.05$).

** Significant as compared to amodiaquine-treated hepatocytes ($P < 0.05$).

As shown in Table 5.1, the H_2O_2-enhanced hepatocyte model in the absence of peroxidase did not affect amodiaquine cytotoxicity. However, when peroxidase was added, only 15 μM amodiaquine was required to cause about 50% cell death in two hours (LC_{50}) representing a 66-fold increase in toxicity. Amodiaquine toxicity in the presence of the H_2O_2 generating system and peroxidase was also dependent on the amodiaquine concentration. Hepatocyte viability in the absence of amodiaquine was not affected by H_2O_2 generating system in the presence or absence of peroxidase. Amodiaquine cytotoxicity was delayed by PTU, a peroxidase inhibitor, suggesting that peroxidase was required for the oxidative stress-induced amodiaquine toxicity. The ROS scavengers TEMPOL and mannitol both delayed amodiaquine-induced cytotoxicity with peroxidase and the H_2O_2 generating system. Furthermore, catalase inactivation with 3-amino-1,2,4-triazole resulted in a significant increase in hepatocyte susceptibility to amodiaquine. The antioxidants BHA and quercetin or P450 inhibition by 1-aminobenzotriazole, however, did not affect amodiaquine-induced toxicity in this hepatocyte cytotoxicity model (results not shown). In the absence of amodiaquine, none of the modulators at the doses used, affected hepatocyte viability.

Table 5.1 Amodiaquine-induced cytotoxicity in the hepatocyte inflammation model

Addition	Cytotoxicity (%Trypan blue uptake)		
Incubation time (min)	***60***	***120***	***180***
Control (only hepatocytes)	17 ± 2	21 ±1	26 ± 3
+ H_2O_2 generating system	24 ± 2	27 ± 2	31 ± 1
+ HRP 0.1 μM	23 ± 3	29 ± 1	33 ± 2
HRP 0.1 μM* + H_2O_2 generating system	25 ± 2	31 ± 2	35 ± 1
+ Amodiaquine 1 mM	44 ± 5[a]	56 ± 3[a]	75 ± 5[a]
+ H_2O_2 generating system	46 ± 4	51 ± 3	79 ± 6
+ HRP 0.1 μM	100[b]	100[b]	100[b]
+ Amodiaquine 100 μM	20 ± 1	25 ± 2	29 ± 1
+ H_2O_2 generating system	22 ± 2	25 ± 3	32 ± 2
+ HRP 0.1 μM	68 ± 7[c]	100[c]	100[c]
+ Amodiaquine 15 μM	20 ± 2	23 ± 1	25 ± 1
+ H_2O_2 generating system + HRP 0.1 μM	38 ± 2[d]	57 ± 6[d]	78 ± 5[d]
+ PTU 10 μM	29 ± 2	34 ± 2[e]	48 ± 4[e]
+ TEMPOL 200 μM	27 ± 2[e]	37 ± 2[e]	56 ± 4[e]
+ Mannitol 50 mM	25 ± 1[e]	33 ± 2[e]	47 ± 3[e]
+ Dicumarol 20 μM	37 ± 3	56 ± 4	77 ± 6
+ Borneol 500 μM	36 ± 2	54 ± 5	81 ± 4
+ 3-Amino-1,2,4-triazole 500 μM	66 ± 5[e]	83 ± 5[e]	100[e]
+1-Bromoheptane 200 μM	79 ± 7[e]	92 ± 7[e]	100[e]
HRP 0.1 μM* + H_2O_2 generating system + Amodiaquine 15 μM	65 ± 5[d]	81 ± 6[d]	100[d]

* Hepatocytes were preincubated with HRP for 30 min prior to the addition of other agents.

H_2O_2 generating system: Glucose 10 mM and glucose oxidase 0.5 U/mL; HRP: Horseradish peroxidase; PTU: 6-n-Propyl-thiouracil (peroxidase inhibitor); TEMPOL: 4-hydroxy-2,2,6,6-tetramethylpiperidene-1-oxyl (ROS scavenger). Dicumarol: a NAD(P)H/quinone oxidoreductase (NQO) inhibitor; 1-Bromoheptane: GSH depletor

Refer to Materials and Methods for a description of experiments performed.

Means ± SE for three separate experiments are given.

[a] Significant as compared to control ($P < 0.05$).

[b] Significant as compared to amodiaquine 1 mM ($P < 0.05$).

[c] Significant as compared to amodiaquine 100 μM .

[d] Significant as compared to amodiaquine 15 μM .

[e] Significant as compared to amodiaquine 15 μM + H_2O_2 generating system + HRP 0.1 μM ($P < 0.05$).

As shown in Table 5.2, 15 μM amodiaquine in the presence of the H_2O_2 generating system and peroxidase, induced mitochondrial toxicity as shown by a marked decrease in mitochondrial membrane potential within the first 30 min which was restored by the peroxidase inhibitor PTU (Lee et al, 1990) and the ROS scavenger mannitol. GSH depletion and catalase inhibition by 3-amino-1,2,4-triazole both further increased the collapse in mitochondrial potential. Furthermore, amodiaquine-induced protein carbonylation was significantly increased in the presence of the H_2O_2 generating system and peroxidase before cytotoxicity ensued. Peroxidase inhibition was effective at inhibiting protein carbonyl formation by amodiaquine in the presence of peroxidase and H_2O_2 generating system. Protein carbonylation was significantly increased when GSH depleted hepatocytes were used. The ROS scavenger mannitol or the catalase inactivator 3-amino-benzo-1,2,4-triazole, however, did not delay amodiaquine-induced protein carbonylation (Table 5.2).

Moreover, as shown in Table 5.2, amodiaquine toxicity with H_2O_2 generating system and peroxidase, resulted in a marked increase in the intracellular H_2O_2 levels which was delayed by PTU or mannitol and was increased in GSH depleted or catalase inhibited hepatocytes. Furthermore, pre-incubation of hepatocytes with HRP for 30 min prior to addition of the H_2O_2 generating system and amodiaquine, further increased cytotoxicity.

Table 5.2 Oxidative stress induced by peroxidase/H_2O_2-catalyzed amodiaquine oxidation in a hepatocyte inflammation model

Addition	%Mitochondrial membrane potential	Protein carbonylation (nmoles/10^6 cells)	Cellular H_2O_2 measurement (nmoles/10^6 cells)
Incubation time (min)	***30***	***30***	***60***
Control (only hepatocytes)	100	8.23 ± 0.31	7.6 ± 0.36
+ H_2O_2 generating system + HRP 0.1 μM	97 ± 3	8.69 ± 0.41	8.4 ± 0.31
+ Amodiaquine 1 mM	89 ± 4	11.74 ± 0.53^a	7.7 ± 0.29
+ H_2O_2 generating system + HRP 0.1 μM	63 ± 5^b	38.1 ± 1.6^b	28.3 ± 0.1^b
+ Amodiaquine 100 μM	96 ± 2	8.18 ± 0.41	7.5 ± 0.30
+ H_2O_2 generating system + HRP 0.1 μM	79 ± 4^c	33.2 ± 1.3^c	21.2 ± 0.1^c
+ Amodiaquine 15 μM	98 ± 2	8.07 ± 0.44	7.4 ± 0.33
+ H_2O_2 generating system + HRP 0.1 μM	84 ± 3^d	26.7 ± 1.4^d	18.7 ± 0.96^d
+ PTU 10 μM	94 ± 2^e	12.6 ± 0.63^e	10.3 ± 0.7^e
+ Mannitol 50 mM	93 ± 3^e	27.2 ± 0.9	13.6 ± 0.47^e
+ Dicumarol 20 μM	86 ± 3	27.1 ± 0.37^e	18.2 ± 0.5
+ Bromoheptane 200 μM	74 ± 2^e	36.3. ± 0.31^e	24.6 ± 0.42^e
+ 3-Amino-1,2,4-triazole 500 μM	91 ± 3^e	28.7 ± 0.26	87.4 ± 5.1^e
+ Borneol 500 μM	84 ± 3	26.3 ± 0.27	19.4 ± 0.82

H_2O_2 generating system: Glucose 10 mM and glucose oxidase 0.5 U/mL; HRP: Horseradish peroxidase; PTU: 6-n-Propyl-thiouracil (peroxidase inhibitor); TEMPOL: 4-hydroxy-2,2,6,6-tetramethylpiperidene-1-oxyl (ROS scavenger). Dicumarol: a NAD(P)H/quinone oxidoreductase (NQO) inhibitor
Refer to Materials and Methods for a description of experiments performed.
Means ± SE for three separate experiments are given.
^{a} Significant as compared to control ($P < 0.05$).
^{b} Significant as compared to amodiaquine 1 mM + H_2O_2 generating system ($P < 0.05$).
^{c} Significant as compared to amodiaquine 100 μM + H_2O_2 generating system ($P < 0.05$).
^{d} Significant as compared to amodiaquine 15 μM ($P < 0.05$).
^{e} Significant as compared to amodiaquine 15 μM + H_2O_2 generating system + HRP 0.1 μM ($P < 0.05$).

As shown in Figure 5.5a, incubation of hepatocytes with amodiaquine and the H_2O_2 generating system/peroxidase caused a time-dependent decrease in hepatocyte GSH levels, with about 65% GSH depletion occurring after 30 min of incubation that was further inhibited by the peroxidase inhibitor PTU. Moreover, GSH depletion was accompanied by significant GSSG formation (Figure 5.5b) indicating that GSH depletion was mainly due to its oxidation to GSSG. The peroxidase inhibitor, PTU also diminished GSSG formation. In the absence of amodiaquine, the peroxidase and H_2O_2 generating system did not affect hepatocyte GSH levels.

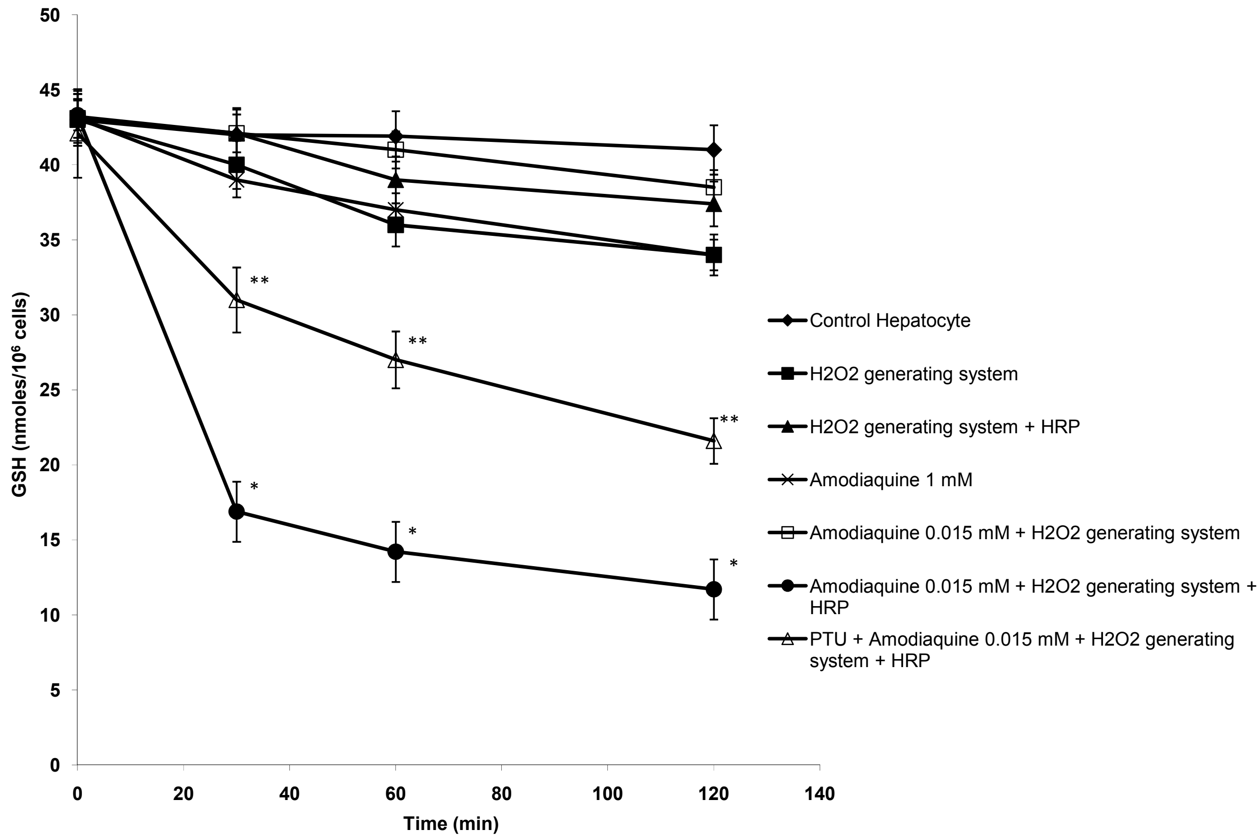

Figure 5.5a Hepatocyte GSH oxidation by amodiaquine catalyzed by H_2O_2 generating system/peroxidase

H_2O_2 generating system consisted of glucose 10 mM and glucose oxidase 0.5 U/mL. The concentration of other chemicals used was as follows: PTU 10 μM (peroxidase inhibitor)

Refer to Materials and Methods for a description of experiments performed.

Means ± SE for three separate experiments are given.

* Significant as compared to H_2O_2 generating system + HRP 0.1 μM ($P < 0.05$).

** Significant as compared to amodiaquine 15 μM + H_2O_2 generating system + HRP 0.1 μM ($P < 0.05$).

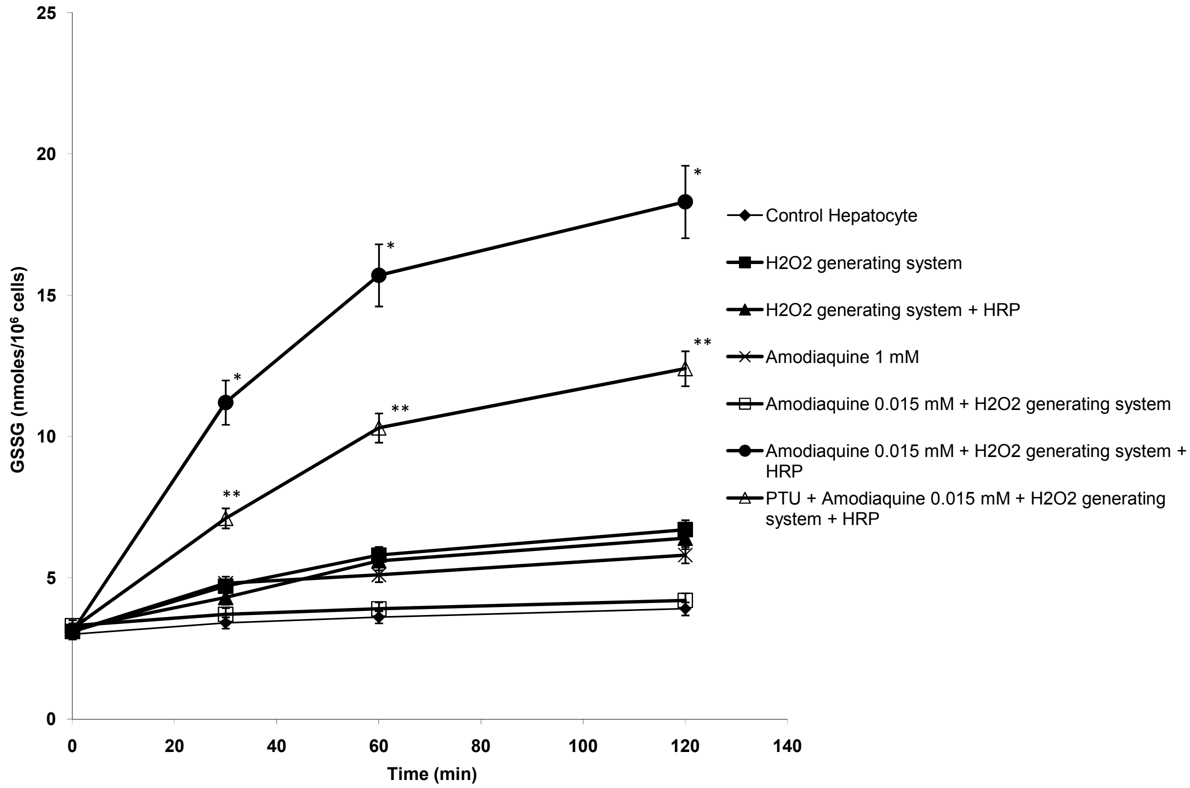

Figure 5.5b Hepatocyte GSSG formation by peroxidase catalyzed hydralazine oxidation
H_2O_2 generating system consisted of glucose 10 mM and glucose oxidase 0.5 U/mL. The concentration of other chemicals used was as follows: PTU 10 μM (peroxidase inhibitor)
Refer to Materials and Methods for a description of experiments performed.
Means ± SE for three separate experiments are given.
* Significant as compared to H_2O_2 generating system + HRP 0.1 μM ($P < 0.05$).
** Significant as compared to amodiaquine 15 μM + H_2O_2 generating system + HRP 0.1 μM ($P < 0.05$).

5.5 Discussion

In this study, amodiaquine cytotoxicity towards isolated rat hepatocytes was found to be concentration-dependent and a cytotoxic amodiaquine metabolite was generated by P450-catalyzed amodiaquine oxidation. The amodiaquine oxidation product also formed GSH conjugates as amodiaquine caused a decrease in GSH levels without GSSG formation (Figure 5.5 a,b) and GSH depleted hepatocytes were more susceptible to toxicity. This was attributed to the formation of the electrophilic metabolite quinoneimine which was detoxified by the reaction with GSH.

In rats, amodiaquine is excreted in the bile exclusively as the $5'$-thioether conjugates which suggest that amodiaquine undergoes extensive bioactivation *in vivo* to form amodiaquine quinoneimine or semiquinoneimine with subsequent conjugate addition of glutathione resulting in glutathione depletion (Harrison et al, 1992; Maggs et al, 1988). Covalent binding to tissue proteins and glutathione conjugates of amodiaquine have been detected in rat bile as well (Harrison et al, 1992). Enzyme inhibition studies using ketoconazole, a P450 inhibitor, resulted in a significant decrease in the excretion of thioether metabolites in rat bile (Harrison et al, 1992).

Toxicity, however, was not oxidative stress-mediated as it was not prevented by the antioxidants BHA and quercetin or the ROS scavenger mannitol, and was accompanied by little GSH depletion, intracellular H_2O_2 increase and low mitochondrial toxicity. This can be partly due to amodiaquine acting as an antioxidant, as only 30 μM amodiaquine was required to cause a 50% inhibition in *tert*-butylhydroperoxide-induced lipid peroxidation in isolated rat hepatocytes (results not shown).

The two electron reduction pathway catalyzed by DT-diaphorase was considered to be non-toxic as DT-diaphorase inactivated hepatocytes were much more susceptible to amodiaquine cytotoxicity indicating that a quinoneimine was involved in amodiaquine-mediated cytotoxic mechanism. If the DT-diaphorase was inhibited, the ability of the cells to reduce quinoneimine to amodiaquine was prevented. NQO inhibition by dicumarol also increased amodiaquine-induced protein carbonylation and further increased the collapse in mitochondrial membrane potential. ROS scavengers however, were not protective against protein carbonylation and mitochondrial toxicity, suggesting that the quinoneimine was responsible for protein oxidation and caused mitochondrial toxicity.

Furthermore, hepatocyte glucuronidation has been shown to be readily inhibited by borneol (Kretz-Rommel and Boelsterli, 1993). When hepatocytes were pretreated with borneol, amodiaquine toxicity significantly increased, which suggests that glucuronidation is involved in the detoxification pathway. Furthermore, the reactive metabolite likely conjugated GSH since GSH depleted hepatocytes were more susceptible to amodiaquine toxicity. Amodiaquine metabolism by glucuronidation has not yet been demonstrated.

In previous studies, peroxidase enzymes and H_2O_2 were shown to catalyze a one-electron oxidation of phenolics, aniline compounds, non-steroidal anti-inflammatory drugs (NSAIDs), indole-acetic acid derivatives, troglitazone and other vitamin E analogues to form highly reactive free radicals which co-oxidized ascorbate, NADH, GSH or unsaturated fatty acids. A continuous H_2O_2 generating system and peroxidase was used which was not cytotoxic and did not cause GSH depletion or oxidation at the concentrations used but became markedly cytotoxic towards hepatocytes in the presence of a low non-toxic dose of NSAIDs, troglitazone and phenolics. Furthermore, hepatocyte lipid peroxidation, ROS formation and GSH oxidation to GSSG ensued

(Galati et al, 2002b; Galati et al, 2002a; Tafazoli et al, 2005a; Tafazoli and O'Brien, 2004; Tafazoli and O'Brien, 2005).

Amodiaquine also showed a concentration-dependent toxicity towards hepatocytes in the presence of a H_2O_2 generating system and peroxidase. Hepatocyte susceptibility to amodiaquine was increased by a factor of 66 when peroxidase and a non-toxic H_2O_2 generating system were added to the isolated hepatocytes compared to control hepatocytes without H_2O_2 and peroxidase. The cytotoxicity further increased once hepatocytes were pre-incubated with HRP for 30 min, prior to the addition of amodiaquine and the H_2O_2 generating system. This pre-incubation likely allowed HRP to be internalized by hepatocytes via endocytosis as previously shown (Scharschmidt et al, 1986; Straus, 1981). The hepatocyte cytotoxic mechanism involved oxidative stress as cytotoxicity was preceded by a significant collapse in mitochondrial membrane potential, GSH oxidation, and protein carbonyl formation which were prevented by the ROS scavenger, mannitol and the peroxidase inhibitor, PTU. BHA, completely prevents lipid peroxidation but is poor at scavenging ROS (Robak and Gryglewski, 1988). However, BHA was not cytoprotective and no malondialdehyde formation was observed (results not shown), which suggests that lipid peroxidaton was not involved in amodiaquine-induced cytotoxicity and that membrane phospholipids were not significant cytotoxic targets for the cytotoxic semiquinoneimine radical.

Moreover, amodiaquine in the presence of peroxidase/H_2O_2 generating system markedly increased endogenous H_2O_2 formation suggesting that peroxidase catalyzed amodiaquine oxidation to semiquinoneimine radicals which reacted with oxygen to form H_2O_2. When hepatocyte catalase was inactivated with 3-amino-1,2,4-triazole, cytotoxicity and intracellular H_2O_2 formation markedly increased which suggests that cytotoxicity was due to ROS formation.

Primaquine, another antimalarial drug, has been shown to cause oxidative stress in erythrocytes following its reduction and subsequent autooxidation to from H_2O_2, which led to hemolysis in glucose-6-phosphate deficient individuals (Agarwal et al, 1988). The increased hepatocyte susceptibility to amodiaquine by the H_2O_2 generating system could also partly result from catalase inactivation by amodiaquine as there was a significant increase in endogenous H_2O_2 levels. Following single and multiple dose amodiaquine treatment, activities of superoxide dismutase and glutathione peroxidase were increased 30% and 133% respectively, while catalase activity was decreased by 45% (Farombi, 2000).

Hepatocyte NQO inhibition with dicumarol did not affect amodiaquine toxicity in the presence of H_2O_2 and peroxidase indicating that the hepatocyte GSH oxidation was more likely due to semiquinoneimine radical formation which caused GSH oxidation. Protein carbonylation, also could be associated with protein oxidation by semiquinoneimine radicals and not ROS, as the ROS scavenger, mannitol and catalase inhibitor 3-amino-1,2,4-triazole did not affect protein carbonylation. Mannitol, however, restored mitochondrial membrane potential, suggesting that the collapse in mitochondrial membrane potential was ROS-mediated.

In summary, our results showed that amodiaquine toxicity towards isolated rat hepatocytes involved two distinct pathways: a non-oxidative stress pathway involving P450-catalyzed amodiaquine oxidation to a quinoneimine metabolite which caused protein carbonylation, mitochondrial membrane potential collapse and formed conjugates with GSH. The second pathway, however, was oxidative stress-mediated and involved peroxidase-catalyzed oxidation of amodiaquine to semiquinoneimine radicals which caused GSH oxidation, protein carbonylation and mitochondrial toxicity.

In conclusion, a non-toxic exposure to H_2O_2/peroxidase markedly increased hepatocyte susceptibility to amodiaquine, much like the conditions of asymptomatic inflammation which enhanced drug-induced cytotoxicity (Buchweitz et al, 2002; Roth et al, 1997). Therefore, the peroxidase/H_2O_2 hepatocyte system seems to be useful for screening drugs for any hepatotoxicity potential that may be associated with inflammation.

Chapter 6

General Conclusions and Summary

6.1 Hypotheses revisited

6.1.1 Hypothesis 1: *Drugs such as troglitazone, isoniazid, hydralazine and amodiaquine developed for chronic use, cause oxidative stress when oxidized by H_2O_2 or peroxidase/H_2O_2 to phenoxyl, hydrazyl or semiquinone radicals. In the absence of peroxidase/H_2O_2, these drugs are much less cytotoxic and the cytotoxicity mechanisms do not involve oxidative stress.*

As described in the Introduction section, a modest inflammatory response can enhance tissue sensitivity to a variety of chemicals. Using immunohistochemistry, myeloperoxidase and its oxidation products were located in Kupffer cells of the human liver (Brown et al, 2001). H_2O_2 is also formed by the activation of NADPH oxidase in the infiltrating cells during the inflammatory response. Furtheremore, it has been shown that inactivating neutrophils, macrophages or Kupffer cells prevents drug-induced hepatotoxicity (Buchweitz et al, 2002; Roth et al, 1997; Roth et al, 2003).

It is therefore reasonable to suggest that the large increase in liver susceptibility to drugs could be attributed to the H_2O_2 and/or peroxidases of the infiltrated cells or the resident Kupffer cells that catalyze the oxidation of drugs (or their P450 metabolites) to form reactive pro-oxidant radicals that are toxic to hepatocytes.

In this study, we used peroxidase activity as a useful inflammation marker for measuring the hepatic inflammatory response. Previously we described evidence indicating that peroxidase enzymes catalyzed the one-electron oxidation of phenolics, non-steroidal anti-inflammatory drugs (NSAIDs), phenothiazines or anticancer indole-3-acetic acid (IAA) derivatives, in the presence of H_2O_2, to form highly reactive free radicals which catalyzed the co-oxidation of NADH, GSH and ascorbate. Reactive oxygen species formation was shown to occur during

NADH or GSH co-oxidation but not ascorbate co-oxidation (Eghbal et al, 2004; Galati et al, 2002b; Tafazoli and O'Brien, 2004).

It was also found that addition of H_2O_2 or peroxidase/H_2O_2 to the hepatocytes to simulate an inflammatory episode markedly increased drug-induced cytotoxicity. These drugs when used in the clinic were associated with idiosyncratic liver toxicity and included troglitazone, isoniazid, hydralazine and amodiaquine (Chapters 2-5). However, addition of H_2O_2 or peroxidase/H_2O_2 did not increase the cytotoxicity of drugs or xenobiotics that did not cause liver toxicity, e.g., tribromoethanol (Avertin®), an anesthetic and acetylsalicylic acid (Aspirin®) (Tafazoli et al, 2005a) (the complete list of drugs that did not form cytotoxic pro-oxidant radicals in the hepatocyte inflammation model has been summarized in Table AI.1 (Appendix I). These results were obtained using an *in vitro* hepatocyte inflammation model, in which a continuous infusion of H_2O_2 was created by using glucose and glucose oxidase, in the presence or absence of HRP, as a model peroxidase.

In Chapter 2, the cytotoxicity of troglitazone, an α-tocopherol derivative, was compared with other α-tocopherol analogues. Even though α-tocopherol was found to be a good antioxidant, its phenoxyl radical at higher concentrations had undesirable pro-oxidant activity (Witting et al, 1999). Troglitazone was much more effective at inducing hepatocyte lipid peroxidation, GSH oxidation, and cytotoxicity when oxidized by peroxidase/H_2O_2 suggesting that the phenoxyl radical of troglitazone was much more pro-oxidant and hepatotoxic than α-tocopherol. The phenoxyl radical reactive metabolite mechanism would explain why other thiazolidinedione drugs such as rosiglitazone and pioglitazone, which have no phenoxyl radical-forming chroman ring, were not hepatotoxic. This research also showed that troglitazone cytotoxicity increased 2.5 fold by peroxidase/H_2O_2. Livers from troglitazone affected patients also had inflammatory infiltrates containing neutrophils so it is likely that peroxidase/H_2O_2 activity was increased in the liver of these patients (Fukano et al, 2000). Type 2 diabetes is also likely an inflammatory disease, as a recent prospective study showed that inflammation biomarkers could be used to predict the development of type 2 diabetes in a cohort of >27,000 U.S. women (Pradhan et al, 2001). It is not known whether patients with more advanced inflammation, e.g., those with vascular and circulatory injury, were more susceptible to troglitazone hepatotoxicity.

In Chapter 3, isoniazid-induced cytotoxicity in the hepatocyte inflammation model involved its major metabolite hydrazine. Hydrazine was shown to be 16-fold more toxic in the presence of a non-toxic H_2O_2-generating system but hepatocyte susceptibility was not further increased with added peroxidase. Acetylhydrazine, which was previously suggested as the toxic metabolite of isoniazid was much less cytotoxic than hydrazine in this model. The molecular cytotoxic mechanism of hydrazine-induced toxicity involved hydrazine activation by P450/H_2O_2 to a reactive metabolite much likely a hydrazyl radical. Cytotoxicity was also shown to be oxidative stress-mediated, as ROS and protein carbonyltion occurred before the hepatocyte toxicity ensued. Isoniazid toxicity in the inflammation model was independent from peroxidase, as added exogenous peroxidase did not affect cytotoxicity.

Chapter 4 introduced two cytotoxic mechanisms for hydralazine. Using the hepatocyte inflammation model, we found that hydralazine caused cytotoxicity by a P450/H_2O_2-catalyzed oxidative stress-mediated cytotoxic pathway (in the absence of peroxidase) or a peroxidase/H_2O_2-catalyzed cytotoxic mechanism, once peroxidase was added to the system. The peroxidase-mediated pathway most likely involved hydralazyl radicals and it involved extensive oxidative stress.

Chapter 5 further tested this hypothesis with amodiaquine. It was shown that a H_2O_2 generating system did not affect hepatocyte susceptibility to amodiaquine but susceptibility to amodiaquine increased 66-fold upon addition of peroxidase. Amodiaquine toxicity in the inflammation model also involved extensive oxidative stress and the formation of a semiquinoneimine reactive metabolite which oxidized GSH, resulted in an increase in mitochondrial membrane potential and formed protein carbonylation.

6.1.2 Hypothesis 2: *Drugs or xenobiotic radicals can increase cell vulnerability to inflammation by increasing H_2O_2 formation or by decreasing cellular resistance to H_2O_2.*

Under normal conditions, the combined activities of catalase and glutathione peroxidase handle H_2O_2 whilst maintaining normal GSH/GSSG ratio. The GSH/GSSG ratio, in turn, is dependent on the activity of glutathione reductase and the supply of NADPH from the hexose monophosphate shunt (Cochrane, 1991). Using the *in vitro* hepatocyte inflammation model, it was shown that the non-cytotoxic H_2O_2 generating system used did not affect the GSH/GSSG or the mitochondrial potential. However, addition of some of the tested drugs was accompanied by a significant increase in the endogenous H_2O_2 levels which decreased the GSH/GSSG ratio and the mitochondrial potential. The source of the endogenous H_2O_2 is not known and could result from drug radicals or the inhibition of mitochondrial respiration. This oxidative stress can result in multiple damaging effects on cell metabolism, function, and structure. H_2O_2-induced single-strand breaks of DNA have been suggested to lead to activation of poly(ADP-ribose) polymerase resulting in depletion of nicotinamide adenine dinucleotide (NAD) (Schraufstatter et al, 1986), an essential cofactor in glycolysis. It has also been shown that H_2O_2 toxicity is dependent on cellular sources of iron (Starke and Farber, 1985), thus suggesting that damage is directly inflicted by hydroxyl radicals generated from H_2O_2 through a Fenton reaction which is dependent on the availability of transition metals such as iron or copper in reduced form. The hydroxyl radical reacts site-specifically at diffusion controlled rates with most biomolecules and thus the cellular disposition of H_2O_2 and reactive iron is of great importance in oxidative stress-induced cellular pathology (Starke and Farber, 1985). This can lead to lysosomal membrane damage since secondary lysosomes are likely sites for the formation of hydroxyl radicals by Fenton reactions due to the availability of loosely bound reduced and reactive iron.

Hydrazine-induced toxicity was accompanied by a significant increase in production of H_2O_2 which resulted in lysosomal membrane damage and led to a collapse in mitochondrial membrane potential (Chapter 3). The significant increase in endogenous H_2O_2 formation could result from hydralazyl radicals and diimine oxidation products reacted with oxygen to form H_2O_2 (Misra and Fridovich, 1976; Yamamoto and Kawanishi, 1991) (Chapter 4) or in case of amodiaquine, peroxidase-catalyzed amodiaquine oxidation to semiquinoneimine radicals which reacted with oxygen to form H_2O_2 (Moridani et al, 2003; O'Brien, 1991) (Chapter 5). Increased H_2O_2 formation occurred in all cases before cytotoxicity ensued.

Furthermore, it was shown that peroxidase/H_2O_2 or P450/H_2O_2-catalyzed oxidation of hydralazine, hydrazine (isoniazid metabolite) and amodiaquine all resulted in a significant decrease in mitochondrial membrane potential as an indicator of mitochondrial toxicity due to oxidative stress. However, non-toxic, low level H_2O_2 generating system or peroxidase/H_2O_2 by itself did not affect mitochondrial membrane potential, suggesting that the collapse in mitochondrial membrane potential was ROS-mediated. This could be due to a pro-oxidant drug radical or high toxic levels of H_2O_2-mediated peroxidation of the phospholipid cardiolipin which results in the mitochondrial permeabilization and release of cytochrome *c* and other proapoptotic factors into the cytosol (Goldman et al, 1999; Kagan et al, 2005; Tyurina et al, 2006) which can trigger caspase activation and apoptosis-mediated cell death (Orrenius, 2007).

The schematic in Figure 6.1 depicts a summary of our results that answer the two hypotheses raised in Chapter 1.

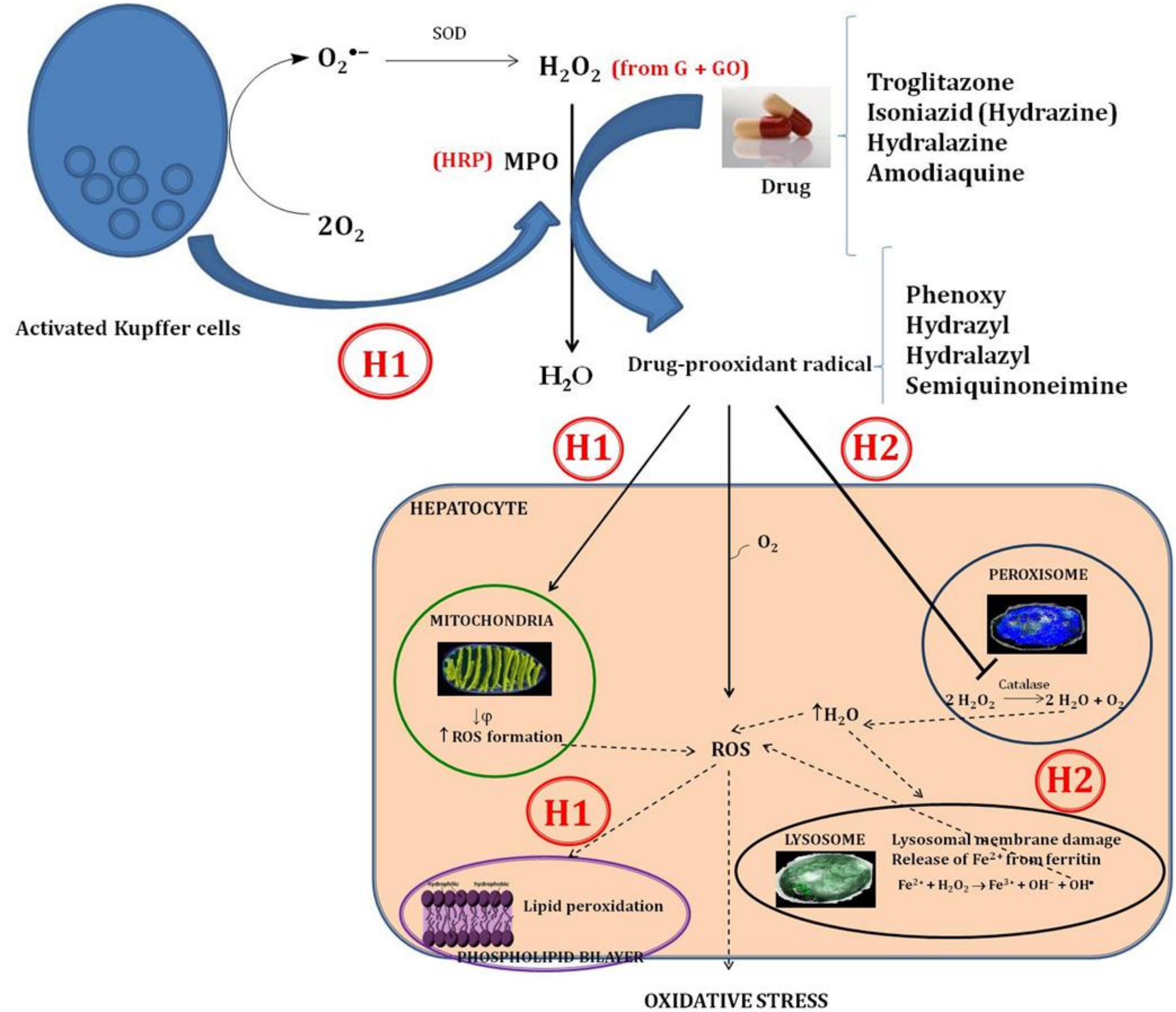

Figure 6.1 Schematic of drug-induced oxidative stress in the hepatocyte inflammation model. This illustration shows that the idiosyncratic drugs researched in the chapters of this thesis (Troglitazone, Isoniazid, Hydralazine and Amodiaquine) can be activated by the immune cell products such as H_2O_2 and peroxidase to pro-oxidant radicals which can cause oxidative stress in hepatocytes (Hypothesis 1, H1). The mechanism of the drug-induced oxidative stress involved mitochondrial toxicity, lipid peroxidation, ROS formation or lysosomal damage. The lysosomal damage led to the decreased cellular resistance to H_2O_2-induced cytotoxicity via Fenton reaction and ROS formation (Hypothesis 2, H2).

6.2. Future directions

6.2.1 An *in vivo* animal inflammation model

Using an *in vitro* or an *in vivo* animal model may clarify mechanisms to minimize injury or to determine if alternative drug candidates that do not have similar potential for toxicity would be better utilized. The ultimate goal will be to design an animal model that could predict idiosyncratic reactions to detect potential problems early in drug development and could be used to help design appropriate human clinical trials. Clearly, further exploration and validation are needed to determine how universally applicable the hypothesis is and whether predictive animal models are plausible. Such studies should include the use of a wide variety of drugs from numerous pharmacologic classes that have various propensities to cause idiosyncratic reactions in people.

A preliminary *in vivo* animal study was carried out in which *tert*-butyl hydroperoxide (*t*-BHP) was used to assess the effect of inflammation on increased hydrazine-induced hepatotoxicity. *t*-BHP, is a short chain analog of lipid hydroperoxide which is not removed by catalase and has therefore often been used as a model to investigate the mechanism of cell injury initiated by acute oxidative stress (Hwang et al, 1996; Joyeux et al, 1990). It has been shown by other laboratories that treatment of rats with *t*-BHP caused liver necrosis with inflammatory cell (neutrophils) infiltration, serum liver enzyme elevation, and liver GSH oxidation (Hwang et al, 1996; Joyeux et al, 1990). Based on these findings, *t*-BHP seemed to be a good candidate for an oxidative stress model which is also associated with inflammation. On the other hand, the chemical hydrazine has been chosen as it is a known hepatotoxin and also a major and minor metabolite of isoniazid and hydralazine, respectively (Timbrell et al, 1982; Timbrell and

Harland, 1979). Furthermore, the cytotoxic mechanism of hydrazine has already been studied in the hepatocyte inflammation model, as described in Chapter 3. The procedure and results of this preliminary experiment has been summarized in Appendix II.

In summary, the results from these preliminary experiments clearly showed that an otherwise non-toxic dose of hydrazine when administered simultaneously or after a non-toxic dose of *t*-BHP caused a significant elevation in serum alanine aminotranferease (ALT) and aspartate aminotransferase (AST) levels, as an indicator of hepatotoxicity. Furthermore, pretreatment of rats with non-toxic doses of *t*-BHP, prior to the non-toxic administration of hydrazine caused a significant decrease in the liver tissue GSH levels when compared to hydrazine or *t*-BHP alone. Further research could determine the mechanism by which toxicity may be occurring by measuring the following indicators of oxidative stress or cell susceptibility to oxidative stress: protein nitrotyrosine residues in liver homogenate, protein carbonyls or F_2-isoprostanes as an oxidative damage marker.

These preliminary results are a small step towards a bigger study required to show that the administration of non-injurious concentrations of an inflammagen (e.g., LPS) or cytokines can markedly increase hepatocyte susceptibility to some drugs or xenobiotics thereby confirming a role for inflammation in oxidative stress-induced hepatotoxicity.

6.2.2 Limitations and knowledge gaps

Using an *in vitro* or an *in vivo* animal model may clarify mechanisms to minimize drug side effects or toxicity to determine if alternative drug candidates are likely to be safer. The ultimate goal will be to design an animal model that could predict idiosyncratic reactions to detect potential problems early in drug development and could be used to help design appropriate human clinical trials. For example, a rat model of endotoxin-induced mild acute inflammation will delineate the impact of inflammation or oxidative stress at increasing drug-induced hepatotoxicity. To test this, the development of liver injury will be evaluated in rats co-treated with doses of LPS/ inflammagen and the tested drug, which were non-injurious when given alone.

Clearly, further exploration and validation are needed to determine how universally applicable the hypothesis is and whether predictive animal models are plausible. It needs to be established whether oxidative stress-enhanced drug toxicity also correlates with the hepatotoxicity of these drugs that cause idiosyncratic hepatoxicity.

However, although systemic exposure to LPS within a few hours of a xenobiotic agent appears to cause a potentiated response, LPS exposure one or two days earlier is more likely to produce tolerance to the potentially toxic agent (Calcamuggi et al, 1992). For example, people experiencing chronic inflammation might be less, rather than more, susceptible to drug idiosyncrasy due to development of tolerance. Similarly, people with bacterial infections might develop tolerance to LPS exposure before administration of an antibiotic, and this might temporarily reduce the potential for idiosyncratic responses to antibiotic drugs.

The role of polymorphism or inborn errors of metabolism may also be important as risk factors for idiosyncratic reactions. These include genes that encode for or control the expression of inflammatory factors such as cytokines, reactive oxygen species, lipid mediators, proteases, adhesion molecules or Toll-like receptors. Such genes are expected to control the magnitude of the pro-inflammatory response to a particular amount of LPS or other inflammatory stimuli. Other genes that would be expected to have important influences are those that determine target cell sensitivity to inflammatory factors. As examples, genes controlling hepatocellular glutathione or other antioxidants, and signal transduction might fall into this category. If this connection proves to be correct, then genetic differences would render some people more likely than others to develop an idiosyncratic response from the same exposure to drug and inflammagen. Looking to the future, genotypic analysis could be used to identify at-risk individuals before drug therapy is initiated.

Furthermore, the focus of this study was on hepatic idiosyncratic reactions, since the liver is the most frequent drug target. Numerous other organ targets exist (skin in case of skin rashes or bone marrow associated agranulocytois), and consideration should be given to the possibility that modest, concurrent inflammation may also underlie their involvement in idiosyncrasy.

By broadening our thinking regarding the basis for drug idiosyncrasy, doors may open to increase our understanding of toxicity mechanisms and to find ways for predicting or avoiding such untoward reactions to otherwise useful drugs.

Reference List

Agarwal, S., Gupta, U. R., Gupta, R. C., Anand, N., and Agarwal, S. S., 1988. Susceptibility of glucose-6-phosphate dehydrogenase deficient red cells to primaquine enantiomers and two putative metabolites--I. Effect on reduced glutathione, methemoglobin content and release of hemoglobin. Biochem. Pharmacol. 37, 4605-4609.

Albano, E. and Tomasi, A., 1987. Spin trapping of free radical intermediates produced during the metabolism of isoniazid and iproniazid in isolated hepatocytes. Biochem. Pharmacol. 36, 2913-2920.

Amenta, J. S and Johnston, E. H, 1963. The Effects of hydrazine upon the metabolism of amino acids in the rat liver. Lab Invest 12, 921-928.

Anari, M. R., Khan, S., Jatoe, S. D., and O'Brien, P. J., 1997. Cytochrome P450 dependent xenobiotic activation by physiological hydroperoxides in intact hepatocytes. Eur. J. Drug Metab Pharmacokinet. 22, 305-310.

Andersson, B. S., Aw, T. Y., and Jones, D. P., 1987. Mitochondrial transmembrane potential and pH gradient during anoxia. Am. J. Physiol 252, C349-C355.

Andres, D., Sanchez-Reus, I., Bautista, M., and Cascales, M., 2003. Depletion of Kupffer cell function by gadolinium chloride attenuates thioacetamide-induced hepatotoxicity. Expression of metallothionein and HSP70. Biochem. Pharmacol. 66, 917-926.

Antunes, F. and Cadenas, E., 2001. Cellular titration of apoptosis with steady state concentrations of H(2)O(2): submicromolar levels of H(2)O(2) induce apoptosis through Fenton chemistry independent of the cellular thiol state. Free Radic. Biol. Med. 30, 1008-1018.

Arai, H., Nagao, A., Terao, J., Suzuki, T., and Takama, K., 1995. Effect of d-alpha-tocopherol analogues on lipoxygenase-dependent peroxidation of phospholipid-bile salt micelles. Lipids 30, 135-140.

Aruoma, O. I., Evans, P. J., Kaur, H., Sutcliffe, L., and Halliwell, B., 1990. An evaluation of the antioxidant and potential pro-oxidant properties of food additives and of trolox C, vitamin E and probucol. Free Radic. Res. Commun. 10, 143-157.

Babior, B. M., 2000. The NADPH oxidase of endothelial cells. IUBMB. Life 50, 267-269.

Balani, S. K., Zhu, T., Yang, T. J., Liu, Z., He, B., and Lee, F. W., 2002. Effective dosing regimen of 1-aminobenzotriazole for inhibition of antipyrine clearance in rats, dogs, and monkeys. Drug Metab Dispos. 30, 1059-1062.

Basivireddy, J., Jacob, M., Pulimood, A. B., and Balasubramanian, K. A., 2004. Indomethacin-induced renal damage: role of oxygen free radicals. Biochem. Pharmacol. 67, 587-599.

Bataller, R., Schwabe, R. F., Choi, Y. H., Yang, L., Paik, Y. H., Lindquist, J., Qian, T., Schoonhoven, R., Hagedorn, C. H., Lemasters, J. J., and Brenner, D. A., 2003. NADPH oxidase signal transduces angiotensin II in hepatic stellate cells and is critical in hepatic fibrosis. J. Clin. Invest 112, 1383-1394.

Bepler, CR, Baier, HN, McCracken, S, Rentschler, CL, Rogers, FB, and Lansbury, J, 1959. A 15 month controlled study of the effects of amodiaquine (camoquin) in rheumatoid arthritis. Arthritis Rheum. 403-413.

Black, M., Mitchell, J. R., Zimmerman, H. J., Ishak, K. G., and Epler, G. R., 1975. Isoniazid-associated hepatitis in 114 patients. Gastroenterology 69, 289-302.

Bonizzi, G., Piette, J., Merville, M. P., and Bours, V., 2000. Cell type-specific role for reactive oxygen species in nuclear factor-kappaB activation by interleukin-1. Biochem. Pharmacol. 59, 7-11.

Bourdi, M., Gautier, J. C., Mircheva, J., Larrey, D., Guillouzo, A., Andre, C., Belloc, C., and Beaune, P. H., 1992. Anti-liver microsomes autoantibodies and dihydralazine-induced hepatitis: specificity of autoantibodies and inductive capacity of the drug. Mol. Pharmacol. 42, 280-285.

Boutin, J. A., Kass, G. E., and Moldeus, P., 1989. Drug-induced hydrogen peroxide production in isolated rat hepatocytes. Toxicology 54, 129-137.

Boveris, A. and Cadenas, E., 1975. Mitochondrial production of superoxide anions and its relationship to the antimycin insensitive respiration. FEBS Lett. 54, 311-314.

Bowry, V. W., Mohr, D., Cleary, J., and Stocker, R., 1995. Prevention of tocopherol-mediated peroxidation in ubiquinol-10-free human low density lipoprotein. J. Biol. Chem. 270, 5756-5763.

Brand, M. D., Affourtit, C., Esteves, T. C., Green, K., Lambert, A. J., Miwa, S., Pakay, J. L., and Parker, N., 2004. Mitochondrial superoxide: production, biological effects, and activation of uncoupling proteins. Free Radic. Biol. Med. 37, 755-767.

Bright, H. J. and Porter, D. J., Boyer PD, 1975. Flavoprotein Oxidases. 421-503.

Brown, K. E., Brunt, E. M., and Heinecke, J. W., 2001. Immunohistochemical detection of myeloperoxidase and its oxidation products in Kupffer cells of human liver. Am. J. Pathol. 159, 2081-2088.

Brownlee, M., 2005. The pathobiology of diabetic complications: a unifying mechanism. Diabetes 54, 1615-1625.

Buch, H., Buzello, W., Heymann, E., and Krisch, K., 1969. Inhibition of phenacetin- and acetanilide-induced methemoglobinemia in the rat by the carboxylesterase inhibitor bis-[p-nitrophenyl] phosphate. Biochem. Pharmacol. 18, 801-811.

Buchweitz, J. P., Ganey, P. E., Bursian, S. J., and Roth, R. A., 2002. Underlying endotoxemia augments toxic responses to chlorpromazine: is there a relationship to drug idiosyncrasy? J. Pharmacol. Exp. Ther. 300, 460-467.

Cadenas, E. and Davies, K. J., 2000. Mitochondrial free radical generation, oxidative stress, and aging. Free Radic. Biol. Med. 29, 222-230.

Calcamuggi, G., Lanzio, M., Dughera, L., Babini, G., and Emanuelli, G., 1992. Endotoxin tolerance and polymyxin B modify liver damage and cholestasis induced by a single dose of alpha-naphthylisothiocyanate in the rat. Arch. Toxicol. 66, 126-130.

Cameron, H. A. and Ramsay, L. E., 1984. The lupus syndrome induced by hydralazine: a common complication with low dose treatment. Br. Med. J. (Clin. Res. Ed) 289, 410-412.

Castell, J. V., Jover, R., Martinez-Jimenez, C. P., and Gomez-Lechon, M. J., 2006. Hepatocyte cell lines: their use, scope and limitations in drug metabolism studies. Expert. Opin. Drug Metab Toxicol. 2, 183-212.

Chan, K., Jensen, N. S., Silber, P. M., and O'Brien, P. J., 2007. Structure-activity relationships for halobenzene induced cytotoxicity in rat and human hepatoctyes. Chem. Biol. Interact. 165, 165-174.

Cheeseman, K. H., McBrien, B. C. H. and Slater, T. F., 2008. Free Radicals, Lipid Peroxidation and Cancer. 197-214.

Cheng, W. H., Combs, G. F., Jr., and Lei, X. G., 1998. Knockout of cellular glutathione peroxidase affects selenium-dependent parameters similarly in mice fed adequate and excessive dietary selenium. Biofactors 7, 311-321.

Cheng, W. H., Ho, Y. S., Ross, D. A., Valentine, B. A., Combs, G. F., and Lei, X. G., 1997. Cellular glutathione peroxidase knockout mice express normal levels of selenium-dependent plasma and phospholipid hydroperoxide glutathione peroxidases in various tissues. J. Nutr. 127, 1445-1450.

Christie, G., Breckenridge, A. M., and Park, B. K., 1989. Drug-protein conjugates--XVIII. Detection of antibodies towards the antimalarial amodiaquine and its quinone imine metabolite in man and the rat. Biochem. Pharmacol. 38, 1451-1458.

Churchill, F. C., Patchen, L. C., Campbell, C. C., Schwartz, I. K., Nguyen-Dinh, P., and Dickinson, C. M., 1985. Amodiaquine as a prodrug: importance of metabolite(s) in the antimalarial effect of amodiaquine in humans. Life Sci. 36, 53-62.

Clarke, J. and Shannon, L. M., 1976. The isolation and characterization of the glycopeptides from horseradish peroxidase isoenzyme C. Biochim. Biophys. Acta 427, 428-442.

Cochrane, C. G., 1991. Mechanisms of oxidant injury of cells. Mol. Aspects Med. 12, 137-147.

Cohen, G and Hochstein, P, 1964. Generation of hydrogen peroxide in erythrocytes by hemolytic agents. Biochemistry 3, 895-900.

Comporti, M., Saccocci, C., and Dianzani, M. U., 1965. Effect of CCl-4 in vitro and in vivo on lipid peroxidation of rat liver homogenates and subcellular fractions. Enzymologia. 29, 185-204.

Cook, S., 2006. Coronary artery disease, nitric oxide and oxidative stress: the "Yin-Yang" effect--a Chinese concept for a worldwide pandemic. Swiss. Med. Wkly. 136, 103-113.

Coon, M. J., Ding, X. X., Pernecky, S. J., and Vaz, A. D., 1992. Cytochrome P450: progress and predictions. FASEB J. 6, 669-673.

Dallner, G., 1978. Isolation of microsomal subfractions by use of density gradients. Methods Enzymol. 52, 71-82.

Davies, M. J., Forni, L. G., and Willson, R. L., 1988. Vitamin E analogue Trolox C. E.s.r. and pulse-radiolysis studies of free-radical reactions. Biochem. J. 255, 513-522.

Davila, J. C. and Morris, D. L., 1999. Analysis of cytochrome P450 and phase II conjugating enzyme expression in adult male rat hepatocytes. In Vitro Cell Dev. Biol. Anim 35, 120-130.

De Duve, C. and Baudhuin, P., 1966. Peroxisomes (microbodies and related particles). Physiol Rev. 46, 323-357.

De Minicis, S. and Brenner, D. A., 2007. NOX in liver fibrosis. Arch. Biochem. Biophys. 462, 266-272.

de Vries, S., 1986. The pathway of electron transfer in the dimeric QH2: cytochrome c oxidoreductase. J. Bioenerg. Biomembr. 18, 195-224.

Decker, E. A., 1997. Phenolics: prooxidants or antioxidants? Nutr. Rev. 55, 396-398.

Deng, X., Luyendyk, J. P., Zou, W., Lu, J., Malle, E., Ganey, P. E., and Roth, R. A., 2007. Neutrophil interaction with the hemostatic system contributes to liver injury in rats cotreated with lipopolysaccharide and ranitidine. J. Pharmacol. Exp. Ther. 322, 852-861.

Dhand, R., Gilhotra, R., Sehgal, S., and Malik, S. K., 1987. Incidence of isoniazid-induced antinuclear antibodies in patients of tuberculosis. Indian J. Med. Res. 85, 503-507.

Diaz-Cruz, A., Guinzberg, R., Guerra, R., Vilchis, M., Carrasco, D., Garcia-Vazquez, F. J., and Pina, E., 2007. Adrenaline stimulates H2O2 generation in liver via NADPH oxidase. Free Radic. Res. 41, 663-672.

Dinauer, M. C., Deck, M. B., and Unanue, E. R., 1997. Mice lacking reduced nicotinamide adenine dinucleotide phosphate oxidase activity show increased susceptibility to early infection with Listeria monocytogenes. J. Immunol. 158, 5581-5583.

Dominguez, A. M, Amenta, J. S, Hill, C. S, and Domanski, T. J, 1962. Morphologic and biochemical alteration in the kidney of the hydrazine-treated rat. Aeromed. Acta 22, 1094-1097.

Droge, W., 2002. Free radicals in the physiological control of cell function. Physiol Rev. 82, 47-95.

Eastmond, D. A., Smith, M. T., Ruzo, L. O., and Ross, D., 1986. Metabolic activation of phenol by human myeloperoxidase and horseradish peroxidase. Mol. Pharmacol. 30, 674-679.

Eghbal, M. A., Tafazoli, S., Pennefather, P., and O'Brien, P. J., 2004. Peroxidase catalysed formation of cytotoxic prooxidant phenothiazine free radicals at physiological pH. Chem. Biol. Interact. 151, 43-51.

Ekstrom, T. and Hogberg, J., 1980. Chloroform-induced glutathione depletion and toxicity in freshly isolated hepatocytes. Biochem. Pharmacol. 29, 3059-3065.

Farombi, E. O., 2000. Influence of amodiaquine treatment on microsomal lipid peroxidation and antioxidant defense systems of rats. Pharmacol. Toxicol. 87, 249-254.

Fridovich, I., 1995. Superoxide radical and superoxide dismutases. Annu. Rev. Biochem. 64, 97-112.

Fukano, M., Amano, S., Sato, J., Yamamoto, K., Adachi, H., Okabe, H., Fujiyama, Y., and Bamba, T., 2000. Subacute hepatic failure associated with a new antidiabetic agent, troglitazone: a case report with autopsy examination. Hum. Pathol. 31, 250-253.

Fukuzawa, K., Tokumura, A., Ouchi, S., and Tsukatani, H., 1982. Antioxidant activities of tocopherols on Fe2+-ascorbate-induced lipid peroxidation in lecithin liposomes. Lipids 17, 511-513.

Galati, G., Sabzevari, O., Wilson, J. X., and O'Brien, P. J., 2002a. Prooxidant activity and cellular effects of the phenoxyl radicals of dietary flavonoids and other polyphenolics. Toxicology 177, 91-104.

Galati, G., Tafazoli, S., Sabzevari, O., Chan, T. S., and O'Brien, P. J., 2002b. Idiosyncratic NSAID drug induced oxidative stress. Chem. Biol. Interact. 142, 25-41.

Gale, E. A., 2001. Lessons from the glitazones: a story of drug development. Lancet 357, 1870-1875.

Gandhi, S. and Wood, N. W., 2005. Molecular pathogenesis of Parkinson's disease. Hum. Mol. Genet. 14 Spec No. 2, 2749-2755.

Garibaldi, R. A., Drusin, R. E., Ferebee, S. H., and Gregg, M. B., 1972. Isoniazid-associated hepatitis. Report of an outbreak. Am. Rev. Respir. Dis. 106, 357-365.

Gharib, B., Abdallahi, O. M., Dessein, H., and De Reggi, M., 1999. Development of eosinophil peroxidase activity and concomitant alteration of the antioxidant defenses in the liver of mice infected with Schistosoma mansoni. J. Hepatol. 30, 594-602.

Goldman, R., Claycamp, G. H., Sweetland, M. A., Sedlov, A. V., Tyurin, V. A., Kisin, E. R., Tyurina, Y. Y., Ritov, V. B., Wenger, S. L., Grant, S. G., and Kagan, V. E., 1999. Myeloperoxidase-catalyzed redox-cycling of phenol promotes lipid peroxidation and thiol oxidation in HL-60 cells. Free Radic. Biol. Med. 27, 1050-1063.

Goldman, R., Tsyrlov, I. B., Grogan, J., and Kagan, V. E., 1997. Reactions of phenoxyl radicals with NADPH-cytochrome P-450 oxidoreductase and NADPH: reduction of the radicals and inhibition of the enzyme. Biochemistry 36, 3186-3192.

Gregus, Z., Watkins, J. B., Thompson, T. N., and Klaassen, C. D., 1983. Depletion of hepatic uridine diphosphoglucuronic acid decreases the biliary excretion of drugs. J. Pharmacol. Exp. Ther. 225, 256-262.

Griendling, K. K., Sorescu, D., Lassegue, B., and Ushio-Fukai, M., 2000. Modulation of protein kinase activity and gene expression by reactive oxygen species and their role in vascular physiology and pathophysiology. Arterioscler. Thromb. Vasc. Biol. 20, 2175-2183.

Guillouzo, A., Morel, F., Fardel, O., and Meunier, B., 1993. Use of human hepatocyte cultures for drug metabolism studies. Toxicology 82, 209-219.

Hajieva, P. and Behl, C., 2006. Antioxidants as a potential therapy against age-related neurodegenerative diseases: amyloid Beta toxicity and Alzheimer's disease. Curr. Pharm. Des 12, 699-704.

Halliwell, B and Gutteridge, J. M. C., 2002. Free Radicals in Biology and Medicine. 3rd, 936-

Halliwell, B. and Gutteridge, J. M., 1985. The importance of free radicals and catalytic metal ions in human diseases. Mol. Aspects Med. 8, 89-193.

Hampton, M. B., Kettle, A. J., and Winterbourn, C. C., 1998. Inside the neutrophil phagosome: oxidants, myeloperoxidase, and bacterial killing. Blood 92, 3007-3017.

Hansch, C., Lien, E. J., and Helmer, F., 1968. Structure--activity correlations in the metabolism of drugs. Arch. Biochem. Biophys. 128, 319-330.

Harrison, A. C., Kitteringham, N. R., Clarke, J. B., and Park, B. K., 1992. The mechanism of bioactivation and antigen formation of amodiaquine in the rat. Biochem. Pharmacol. 43, 1421-1430.

Hartley, D. P., Kroll, D. J., and Petersen, D. R., 1997. Prooxidant-initiated lipid peroxidation in isolated rat hepatocytes: detection of 4-hydroxynonenal- and malondialdehyde-protein adducts. Chem. Res. Toxicol. 10, 895-905.

Hatton, C. S., Peto, T. E., Bunch, C., Pasvol, G., Russell, S. J., Singer, C. R., Edwards, G., and Winstanley, P., 1986. Frequency of severe neutropenia associated with amodiaquine prophylaxis against malaria. Lancet 1, 411-414.

Hayashi, T., Saito, A., Okuno, S., Ferrand-Drake, M., Dodd, R. L., and Chan, P. H., 2004. Oxidative injury to the endoplasmic reticulum in mouse brains after transient focal ischemia. Neurobiol. Dis. 15, 229-239.

Hayes, J. D. and McLellan, L. I., 1999. Glutathione and glutathione-dependent enzymes represent a co-ordinately regulated defence against oxidative stress. Free Radic. Res. 31, 273-300.

He, Q., Kim, J., and Sharma, R. P., 2005. Fumonisin B1 hepatotoxicity in mice is attenuated by depletion of Kupffer cells by gadolinium chloride. Toxicology 207, 137-147.

Hissin, P. J. and Hilf, R., 1976. A fluorometric method for determination of oxidized and reduced glutathione in tissues. Anal. Biochem. 74, 214-226.

Hofstra, A. H., Matassa, L. C., and Uetrecht, J. P., 1991. Metabolism of hydralazine by activated leukocytes: implications for hydralazine induced lupus. J. Rheumatol. 18, 1673-1680.

Hofstra, A. H. and Uetrecht, J. P., 1993. Reactive intermediates in the oxidation of hydralazine by HOCl: the major oxidant generated by neutrophils. Chem. Biol. Interact. 89, 183-196.

Hsiao, G., Lin, Y. H., Lin, C. H., Chou, D. S., Lin, W. C., and Sheu, J. R., 2001. The protective effects of PMC against chronic carbon tetrachloride-induced hepatotoxicity in vivo. Biol. Pharm. Bull. 24, 1271-1276.

Hussain, S. M. and Frazier, J. M., 2002. Cellular toxicity of hydrazine in primary rat hepatocytes. Toxicol. Sci. 69, 424-432.

Hwang, J. M., Tseng, T. H., Hsieh, Y. S., Chou, F. P., Wang, C. J., and Chu, C. Y., 1996. Inhibitory effect of atractylon on tert-butyl hydroperoxide induced DNA damage and hepatic toxicity in rat hepatocytes. Arch. Toxicol. 70, 640-644.

Ingold, K. U., Burton, G. W., Foster, D. O., Hughes, L., Lindsay, D. A., and Webb, A., 1987. Biokinetics of and discrimination between dietary RRR- and SRR-alpha-tocopherols in the male rat. Lipids 22, 163-172.

Itoh, S., Ichinoe, A., Tsukada, Y., and Itoh, Y., 1981. Hydralazine-induced hepatitis. Hepatogastroenterology 28, 13-16.

Jezek, P. and Hlavata, L., 2005. Mitochondria in homeostasis of reactive oxygen species in cell, tissues, and organism. Int. J. Biochem. Cell Biol. 37, 2478-2503.

Joly, J. G., Doyon, C., and Peasant, Y., 1975. Cytochrome P-450 measurement in rat liver homogenate and microsomes. Its use for correction of microsomal losses incurred by differential centrifugation. Drug Metab Dispos. 3, 577-586.

Joyeux, M., Rolland, A., Fleurentin, J., Mortier, F., and Dorfman, P., 1990. tert-Butyl hydroperoxide-induced injury in isolated rat hepatocytes: a model for studying anti-hepatotoxic crude drugs. Planta Med. 56, 171-174.

Kaderlik, K. R., Mulder, G. J., Shaddock, J. G., Casciano, D. A., Teitel, C. H., and Kadlubar, F. F., 1994. Effect of glutathione depletion and inhibition of glucuronidation and sulfation on 2-amino-1-methyl-6-phenylimidazo[4,5-b]pyridine (PhIP) metabolism, PhIP-DNA adduct formation and unscheduled DNA synthesis in primary rat hepatocytes. Carcinogenesis 15, 1711-1716.

Kagan, V. E., Kuzmenko, A. I., Shvedova, A. A., Kisin, E. R., Li, R., Martin, I., Quinn, P. J., Tyurin, V. A., Tyurina, Y. Y., and Yalowich, J. C., 2003. Direct evidence for recycling of myeloperoxidase-catalyzed phenoxyl radicals of a vitamin E homologue, 2,2,5,7,8-pentamethyl-6-hydroxy chromane, by ascorbate/dihydrolipoate in living HL-60 cells. Biochim. Biophys. Acta 1620, 72-84.

Kagan, V. E., Kuzmenko, A. I., Shvedova, A. A., Kisin, E. R., Tyurina, Y. Y., and Yalowich, J. C., 2000. Myeloperoxidase-catalyzed phenoxyl radicals of vitamin E homologue, 2,2,5,7,8-pentamethyl- 6-hydroxychromane, do not induce oxidative stress in live HL-60 cells. Biochem. Biophys. Res. Commun. 270, 1086-1092.

Kagan, V. E., Kuzmenko, A. I., Tyurina, Y. Y., Shvedova, A. A., Matsura, T., and Yalowich, J. C., 2001. Pro-oxidant and antioxidant mechanisms of etoposide in HL-60 cells: role of myeloperoxidase. Cancer Res. 61, 7777-7784.

Kagan, V. E., Tyurin, V. A., Jiang, J., Tyurina, Y. Y., Ritov, V. B., Amoscato, A. A., Osipov, A. N., Belikova, N. A., Kapralov, A. A., Kini, V., Vlasova, I. I., Zhao, Q., Zou, M., Di, P., Svistunenko, D. A., Kurnikov, I. V., and Borisenko, G. G., 2005. Cytochrome c acts as a cardiolipin oxygenase required for release of proapoptotic factors. Nat. Chem. Biol. 1, 223-232.

Kalyanaraman, B., Darley-Usmar, V., Struck, A., Hogg, N., and Parthasarathy, S., 1995. Role of apolipoprotein B-derived radical and alpha-tocopheroxyl radical in peroxidase-dependent oxidation of low density lipoprotein. J. Lipid Res. 36, 1037-1045.

Kato, A., Yoshidome, H., Edwards, M. J., and Lentsch, A. B., 2000. Regulation of liver inflammatory injury by signal transducer and activator of transcription-6. Am. J. Pathol. 157, 297-302.

Kawahara, T., Kohjima, M., Kuwano, Y., Mino, H., Teshima-Kondo, S., Takeya, R., Tsunawaki, S., Wada, A., Sumimoto, H., and Rokutan, K., 2005. Helicobacter pylori lipopolysaccharide activates Rac1 and transcription of NADPH oxidase Nox1 and its organizer NOXO1 in guinea pig gastric mucosal cells. Am. J. Physiol Cell Physiol 288, C450-C457.

Keisari, Y., Braun, L., and Flescher, E., 1983. The oxidative burst and related phenomena in mouse macrophages elicited by different sterile inflammatory stimuli. Immunobiology 165, 78-89.

Khan, A. U. and Wilson, T., 1995. Reactive oxygen species as cellular messengers. Chem. Biol. 2, 437-445.

Khan, S. and O'Brien, P. J., 1991. 1-bromoalkanes as new potent nontoxic glutathione depletors in isolated rat hepatocytes. Biochem. Biophys. Res. Commun. 179, 436-441.

Kitazawa, M., Podda, M., Thiele, J., Traber, M. G., Iwasaki, K., Sakamoto, K., and Packer, L., 1997. Interactions between vitamin E homologues and ascorbate free radicals in murine skin homogenates irradiated with ultraviolet light. Photochem. Photobiol. 65, 355-365.

Kresse, M., Latta, M., Kunstle, G., Riehle, H. M., van Rooijen, N., Hentze, H., Tiegs, G., Biburger, M., Lucas, R., and Wendel, A., 2005. Kupffer cell-expressed membrane-bound TNF mediates melphalan hepatotoxicity via activation of both TNF receptors. J. Immunol. 175, 4076-4083.

Kretz-Rommel, A. and Boelsterli, U. A., 1993. Diclofenac covalent protein binding is dependent on acyl glucuronide formation and is inversely related to P450-mediated acute cell injury in cultured rat hepatocytes. Toxicol. Appl. Pharmacol. 120, 155-161.

Kushnareva, Y., Murphy, A. N., and Andreyev, A., 2002. Complex I-mediated reactive oxygen species generation: modulation by cytochrome c and NAD(P)+ oxidation-reduction state. Biochem. J. 368, 545-553.

LaCagnin, L. B., Colby, H. D., and O'Donnell, J. P., 1986. The oxidative metabolism of hydralazine by rat liver microsomes. Drug Metab Dispos. 14, 549-554.

Lambert, A. J. and Brand, M. D., 2004a. Inhibitors of the quinone-binding site allow rapid superoxide production from mitochondrial NADH:ubiquinone oxidoreductase (complex I). J. Biol. Chem. 279, 39414-39420.

Lambert, A. J. and Brand, M. D., 2004b. Superoxide production by NADH:ubiquinone oxidoreductase (complex I) depends on the pH gradient across the mitochondrial inner membrane. Biochem. J. 382, 511-517.

Lambeth, J. D., Cheng, G., Arnold, R. S., and Edens, W. A., 2000. Novel homologs of gp91phox. Trends Biochem. Sci. 25, 459-461.

Larrey, D., Castot, A., Pessayre, D., Merigot, P., Machayekhy, J. P., Feldmann, G., Lenoir, A., Rueff, B., and Benhamou, J. P., 1986. Amodiaquine-induced hepatitis. A report of seven cases. Ann. Intern. Med. 104, 801-803.

LeBel, C. P., Ischiropoulos, H., and Bondy, S. C., 1992. Evaluation of the probe 2',7'-dichlorofluorescin as an indicator of reactive oxygen species formation and oxidative stress. Chem. Res. Toxicol. 5, 227-231.

LeCluyse, E. L., 2001. Human hepatocyte culture systems for the in vitro evaluation of cytochrome P450 expression and regulation. Eur. J. Pharm. Sci. 13, 343-368.

Lee, E., Miki, Y., Katsura, H., and Kariya, K., 1990. Mechanism of inactivation of myeloperoxidase by propylthiouracil. Biochem. Pharmacol. 39, 1467-1471.

Lei, X. G., Cheng, W. H., and McClung, J. P., 2007. Metabolic regulation and function of glutathione peroxidase-1. Annu. Rev. Nutr. 27, 41-61.

Li, X. Q., Bjorkman, A., Andersson, T. B., Ridderstrom, M., and Masimirembwa, C. M., 2002. Amodiaquine clearance and its metabolism to N-desethylamodiaquine is mediated by CYP2C8: a new high affinity and turnover enzyme-specific probe substrate. J. Pharmacol. Exp. Ther. 300, 399-407.

Lien, E. J., Ren, S., Bui, H. H., and Wang, R., 1999. Quantitative structure-activity relationship analysis of phenolic antioxidants. Free Radic. Biol. Med. 26, 285-294.

Liochev, S. I., 1999. The mechanism of "Fenton-like" reactions and their importance for biological systems. A biologist's view. Met. Ions. Biol. Syst. 36, 1-39.

Liu, C. L., Wang, J. M., Chu, C. Y., Cheng, M. T., and Tseng, T. H., 2002a. In vivo protective effect of protocatechuic acid on tert-butyl hydroperoxide-induced rat hepatotoxicity. Food Chem. Toxicol. 40, 635-641.

Liu, Y., Fiskum, G., and Schubert, D., 2002b. Generation of reactive oxygen species by the mitochondrial electron transport chain. J. Neurochem. 80, 780-787.

Loschen, G., Flohe, L., and Chance, B., 1971. Respiratory chain linked H(2)O(2) production in pigeon heart mitochondria. FEBS Lett. 18, 261-264.

Lu, L. S., Wu, C. C., Hung, L. M., Chiang, M. T., Lin, C. T., Lin, C. W., and Su, M. J., 2007. Apocynin alleviated hepatic oxidative burden and reduced liver injury in hypercholesterolaemia. Liver Int. 27, 529-537.

Luyendyk, J. P., Lehman-McKeeman, L. D., Nelson, D. M., Bhaskaran, V. M., Reilly, T. P., Car, B. D., Cantor, G. H., Maddox, J. F., Ganey, P. E., and Roth, R. A., 2006. Unique gene expression and hepatocellular injury in the lipopolysaccharide-ranitidine drug idiosyncrasy rat model: comparison with famotidine. Toxicol. Sci. 90, 569-585.

Luyendyk, J. P., Shores, K. C., Ganey, P. E., and Roth, R. A., 2002. Bacterial lipopolysaccharide exposure alters aflatoxin B(1) hepatotoxicity: benchmark dose analysis for markers of liver injury. Toxicol. Sci. 68, 220-225.

MacRae, W. D. and Stich, H. F., 1979. Induction of sister-chromatid exchanges in Chinese hamster ovary cells by thiol and hydrazine compoudns. Mutat. Res. 68, 351-365.

Maggs, J. L., Kitteringham, N. R., Breckenridge, A. M., and Park, B. K., 1987. Autoxidative formation of a chemically reactive intermediate from amodiaquine, a myelotoxin and hepatotoxin in man. Biochem. Pharmacol. 36, 2061-2062.

Maggs, J. L., Tingle, M. D., Kitteringham, N. R., and Park, B. K., 1988. Drug-protein conjugates--XIV. Mechanisms of formation of protein-arylating intermediates from amodiaquine, a myelotoxin and hepatotoxin in man. Biochem. Pharmacol. 37, 303-311.

Martelli, A., Allavena, A., Campart, G. B., Canonero, R., Ghia, M., Mattioli, F., Mereto, E., Robbiano, L., and Brambilla, G., 1995. In vitro and in vivo testing of hydralazine genotoxicity. J. Pharmacol. Exp. Ther. 273, 113-120.

Maru, G. B. and Bhide, S. V., 1982. Effect of antioxidants and antitoxicants of isoniazid on the formation of lung tumours in mice by isoniazid and hydrazine sulphate. Cancer Lett. 17, 75-80.

Marubayashi, S., Dohi, K., Ochi, K., and Kawasaki, T., 1986. Role of free radicals in ischemic rat liver cell injury: prevention of damage by alpha-tocopherol administration. Surgery 99, 184-192.

Metodiewa, D., Jaiswal, A. K., Cenas, N., Dickancaite, E., and Segura-Aguilar, J., 1999. Quercetin may act as a cytotoxic prooxidant after its metabolic activation to semiquinone and quinoidal product. Free Radic. Biol. Med. 26, 107-116.

Miller, E. R., Pastor-Barriuso, R., Dalal, D., Riemersma, R. A., Appel, L. J., and Guallar, E., 2005. Meta-analysis: high-dosage vitamin E supplementation may increase all-cause mortality. Ann. Intern. Med. 142, 37-46.

Misra, H. P. and Fridovich, I., 1976. The oxidation of phenylhydrazine: superoxide and mechanism. Biochemistry 15, 681-687.

Mitchell, J. R., Long, M. W., Thorgeirsson, U. P., and Jollow, D. J., 1975. Acetylation rates and monthly liver function tests during one year of isoniazid preventive therapy. Chest 68, 181-190.

Mitchell, J. R., Zimmerman, H. J., Ishak, K. G., Thorgeirsson, U. P., Timbrell, J. A., Snodgrass, W. R., and Nelson, S. D., 1976. Isoniazid liver injury: clinical spectrum, pathology, and probable pathogenesis. Ann. Intern. Med. 84, 181-192.

Moldeus, P., Hogberg, J., and Orrenius, S., 1978. Isolation and use of liver cells. Methods Enzymol. 52, 60-71.

Moridani, M. Y., Cheon, S. S., Khan, S., and O'Brien, P. J., 2003. Metabolic activation of 3-hydroxyanisole by isolated rat hepatocytes. Chem. Biol. Interact. 142, 317-333.

Mount, D. L., Patchen, L. C., Nguyen-Dinh, P., Barber, A. M., Schwartz, I. K., and Churchill, F. C., 1986. Sensitive analysis of blood for amodiaquine and three metabolites by high-performance liquid chromatography with electrochemical detection. J. Chromatogr. 383, 375-386.

Muller, F. L., Liu, Y., and Van Remmen, H., 2004. Complex III releases superoxide to both sides of the inner mitochondrial membrane. J. Biol. Chem. 279, 49064-49073.

Murata, K., Hamada, M., Sugimoto, K., and Nakano, T., 2007. A novel mechanism for drug-induced liver failure: inhibition of histone acetylation by hydralazine derivatives. J. Hepatol. 46, 322-329.

Nakamura, M., 1991. One-electron oxidation of Trolox C and vitamin E by peroxidases. J. Biochem. 110, 595-597.

Nathan, C. F. and Root, R. K., 1977. Hydrogen peroxide release from mouse peritoneal macrophages: dependence on sequential activation and triggering. J. Exp. Med. 146, 1648-1662.

Neftel, K. A., Woodtly, W., Schmid, M., Frick, P. G., and Fehr, J., 1986. Amodiaquine induced agranulocytosis and liver damage. Br. Med. J. (Clin. Res. Ed) 292, 721-723.

Nelson, S. D., Mitchell, J. R., Timbrell, J. A., Snodgrass, W. R., and Corcoran, G. B., III, 1976. Isoniazid and iproniazid: activation of metabolites to toxic intermediates in man and rat. Science 193, 901-903.

Noda, A., Hsu, K. Y., Noda, H., Yamamoto, Y., and Kurozumi, T., 1983. Is isoniazid-hepatotoxicity induced by the metabolite, hydrazine? J. UOEH. 5, 183-190.

O'Brien, P. J., 2000. Peroxidases. Chem. Biol. Interact. 129, 113-139.

O'Brien, P. J., 1988. Radical formation during the peroxidase catalyzed metabolism of carcinogens and xenobiotics: the reactivity of these radicals with GSH, DNA, and unsaturated lipid. Free Radic. Biol. Med. 4, 169-183.

O'Brien, P. J., 1991. Molecular mechanisms of quinone cytotoxicity. Chem. Biol. Interact. 80, 1-41.

O'Brien, P. J., Chan, K., and Silber, P. M., 2004. Human and animal hepatocytes in vitro with extrapolation in vivo. Chem. Biol. Interact. 150, 97-114.

O'Brien, P. J., Tafazoli, S., Chan, K., Mashregi, M., Mehta, R., and Shangari, N., 2007. A hepatocyte inflammation model for carbonyl induced liver injury: drugs, diabetes, solvents, chlorination. In: Weiner, H., Maser, E., Lindahl, R, and Plapp, B. (Eds.), Purdue University Press. West Lafayette, Indiana, pp. 105-112

Olliaro, P., Nevill, C., LeBras, J., Ringwald, P., Mussano, P., Garner, P., and Brasseur, P., 1996. Systematic review of amodiaquine treatment in uncomplicated malaria. Lancet 348, 1196-1201.

Orrenius, S., 2007. Reactive oxygen species in mitochondria-mediated cell death. Drug Metab Rev. 39, 443-455.

Ortiz de Montellano, P. R., 1995. Cytochrome P450. Structure, Mechanism and Biochemistry. 2nd, Ortiz de Montellano, P. R. and Kerr, D. E., 1983. Inactivation of catalase by phenylhydrazine. Formation of a stable aryl-iron heme complex. J. Biol. Chem. 258, 10558-10563.

Ortiz de Montellano, P. R. and Mathews, J. M., 1981. Autocatalytic alkylation of the cytochrome P-450 prosthetic haem group by 1-aminobenzotriazole. Isolation of an NN-bridged benzyne-protoporphyrin IX adduct. Biochem. J. 195, 761-764.

Ostapowicz, G., Fontana, R. J., Schiodt, F. V., Larson, A., Davern, T. J., Han, S. H., McCashland, T. M., Shakil, A. O., Hay, J. E., Hynan, L., Crippin, J. S., Blei, A. T., Samuel, G., Reisch, J., and Lee, W. M., 2002. Results of a prospective study of acute liver failure at 17 tertiary care centers in the United States. Ann. Intern. Med. 137, 947-954.

Ott, M., Gogvadze, V., Orrenius, S., and Zhivotovsky, B., 2007. Mitochondria, oxidative stress and cell death. Apoptosis. 12, 913-922.

Ou, P. and Wolff, S. P., 1996. A discontinuous method for catalase determination at 'near physiological' concentrations of H2O2 and its application to the study of H2O2 fluxes within cells. J. Biochem. Biophys. Methods 31, 59-67.

Parks, D. A., Williams, T. K., and Beckman, J. S., 1988. Conversion of xanthine dehydrogenase to oxidase in ischemic rat intestine: a reevaluation. Am. J. Physiol 254, G768-G774.

Parodi, S., De Flora, S., Cavanna, M., Pino, A., Robbiano, L., Bennicelli, C., and Brambilla, G., 1981. DNA-damaging activity in vivo and bacterial mutagenicity of sixteen hydrazine derivatives as related quantitatively to their carcinogenicity. Cancer Res. 41, 1469-1482.

Pirmohamed, M., Naisbitt, D. J., Gordon, F., and Park, B. K., 2002. The danger hypothesis--potential role in idiosyncratic drug reactions. Toxicology 181-182, 55-63.

Poli, G., Albano, E., and Dianzani, M. U., 1987. The role of lipid peroxidation in liver damage. Chem. Phys. Lipids 45, 117-142.

Pradhan, A. D., Manson, J. E., Rifai, N., Buring, J. E., and Ridker, P. M., 2001. C-reactive protein, interleukin 6, and risk of developing type 2 diabetes mellitus. JAMA 286, 327-334.

Preusch, P. C., Siegel, D., Gibson, N. W., and Ross, D., 1991. A note on the inhibition of DT-diaphorase by dicoumarol. Free Radic. Biol. Med. 11, 77-80.

Quinn, M. T., Ammons, M. C., and Deleo, F. R., 2006. The expanding role of NADPH oxidases in health and disease: no longer just agents of death and destruction. Clin. Sci. (Lond) 111, 1-20.

Reed, D. J., Babson, J. R., Beatty, P. W., Brodie, A. E., Ellis, W. W., and Potter, D. W., 1980. High-performance liquid chromatography analysis of nanomole levels of glutathione, glutathione disulfide, and related thiols and disulfides. Anal. Biochem. 106, 55-62.

Reinehr, R., Becker, S., Eberle, A., Grether-Beck, S., and Haussinger, D., 2005. Involvement of NADPH oxidase isoforms and Src family kinases in CD95-dependent hepatocyte apoptosis. J. Biol. Chem. 280, 27179-27194.

Reitman, S. and Frankel, S, 1957. A colorimetric method for the determination of serum glutamic oxalacetic and glutamic pyruvic transaminases. Am. J. Clin. Pathol. 28, 56-63.

Remacle, J., Raes, M., Toussaint, O., Renard, P., and Rao, G., 1995. Low levels of reactive oxygen species as modulators of cell function. Mutat. Res. 316, 103-122.

Rhodes, E. G., Ball, J., and Franklin, I. M., 1986. Amodiaquine induced agranulocytosis: inhibition of colony growth in bone marrow by antimalarial agents. Br. Med. J. (Clin. Res. Ed) 292, 717-718.

Richter, C., Park, J. W., and Ames, B. N., 1988. Normal oxidative damage to mitochondrial and nuclear DNA is extensive. Proc. Natl. Acad. Sci. U. S. A 85, 6465-6467.

Riddles, P. W., Blakeley, R. L., and Zerner, B., 1979. Ellman's reagent: 5,5'-dithiobis(2-nitrobenzoic acid)--a reexamination. Anal. Biochem. 94, 75-81.

Ritov, V. B., Menshikova, E. V., Goldman, R., and Kagan, V. E., 1996. Direct oxidation of polyunsaturated cis-parinaric fatty acid by phenoxyl radicals generated by peroxidase/H2O2 in model systems and in HL-60 cells. Toxicol. Lett. 87, 121-129.

Robak, J. and Gryglewski, R. J., 1988. Flavonoids are scavengers of superoxide anions. Biochem. Pharmacol. 37, 837-841.

Roberts, R. A., Ganey, P. E., Ju, C., Kamendulis, L. M., Rusyn, I., and Klaunig, J. E., 2007. Role of the Kupffer cell in mediating hepatic toxicity and carcinogenesis. Toxicol. Sci. 96, 2-15.

Roth, R. A., Harkema, J. R., Pestka, J. P., and Ganey, P. E., 1997. Is exposure to bacterial endotoxin a determinant of susceptibility to intoxication from xenobiotic agents? Toxicol. Appl. Pharmacol. 147, 300-311.

Roth, R. A., Luyendyk, J. P., Maddox, J. F., and Ganey, P. E., 2003. Inflammation and drug idiosyncrasy--is there a connection? J. Pharmacol. Exp. Ther. 307, 1-8.

Rubbo, H., Radi, R., Trujillo, M., Telleri, R., Kalyanaraman, B., Barnes, S., Kirk, M., and Freeman, B. A., 1994. Nitric oxide regulation of superoxide and peroxynitrite-dependent lipid peroxidation. Formation of novel nitrogen-containing oxidized lipid derivatives. J. Biol. Chem. 269, 26066-26075.

Rubin, R. L., 2005. Drug-induced lupus. Toxicology 209, 135-147.

Runge-Morris, M. and Novak, R. F., 1993. Effects of phenelzine and hydralazine on hydrogen peroxide production and proteolysis in human red blood cells. J. Pharmacol. Exp. Ther. 267, 1401-1406.

Rwagacondo, C. E., Niyitegeka, F., Sarushi, J., Karema, C., Mugisha, V., Dujardin, J. C., Van Overmeir, C., van den, Ende J., and D'Alessandro, U., 2003. Efficacy of amodiaquine alone and combined with sulfadoxine-pyrimethamine and of sulfadoxine pyrimethamine combined with artesunate. Am. J. Trop. Med. Hyg. 68, 743-747.

Sagach, V. F., Scrosati, M., Fielding, J., Rossoni, G., Galli, C., and Visioli, F., 2002. The water-soluble vitamin E analogue Trolox protects against ischaemia/reperfusion damage in vitro and ex vivo. A comparison with vitamin E. Pharmacol. Res. 45, 435-439.

Santanam, N. and Parthasarathy, S., 1995. Paradoxical actions of antioxidants in the oxidation of low density lipoprotein by peroxidases. J. Clin. Invest 95, 2594-2600.

Saran, M., Michel, C., Stettmaier, K., and Bors, W., 2000. Arguments against the significance of the Fenton reaction contributing to signal pathways under in vivo conditions. Free Radic. Res. 33, 567-579.

Sarich, T. C., Adams, S. P., Petricca, G., and Wright, J. M., 1999. Inhibition of isoniazid-induced hepatotoxicity in rabbits by pretreatment with an amidase inhibitor. J. Pharmacol. Exp. Ther. 289, 695-702.

Sarich, T. C., Youssefi, M., Zhou, T., Adams, S. P., Wall, R. A., and Wright, J. M., 1996. Role of hydrazine in the mechanism of isoniazid hepatotoxicity in rabbits. Arch. Toxicol. 70, 835-840.

Satoh, K., Kadofuku, T., and Sakagami, H., 1997. Effect of Trolox, a synthetic analog of alpha-tocopherol, on cytotoxicity induced by UV irradiation and antioxidants. Anticancer Res. 17, 2459-2463.

Schafer, F. Q. and Buettner, G. R., 2001. Redox environment of the cell as viewed through the redox state of the glutathione disulfide/glutathione couple. Free Radic. Biol. Med. 30, 1191-1212.

Scharer, L. and Smith, J. P., 1969. Serum transaminase elevations and other hepatic abnormalities in patients receiving isoniazid. Ann. Intern. Med. 71, 1113-1120.

Scharschmidt, B. F., Lake, J. R., Renner, E. L., Licko, V., and Van Dyke, R. W., 1986. Fluid phase endocytosis by cultured rat hepatocytes and perfused rat liver: implications for plasma membrane turnover and vesicular trafficking of fluid phase markers. Proc. Natl. Acad. Sci. U. S. A 83, 9488-9492.

Schraufstatter, I. U., Hinshaw, D. B., Hyslop, P. A., Spragg, R. G., and Cochrane, C. G., 1986. Oxidant injury of cells. DNA strand-breaks activate polyadenosine diphosphate-ribose polymerase and lead to depletion of nicotinamide adenine dinucleotide. J. Clin. Invest 77, 1312-1320.

Sendo, T., Noda, A., Noda, H., Hsu, K. Y., and Yamamoto, Y., 1984. Metabolic hydrolysis of isoniazid by subcellular fractions of rat liver. J. UOEH. 6, 249-255.

Sharma, M. K. and Buettner, G. R., 1993. Interaction of vitamin C and vitamin E during free radical stress in plasma: an ESR study. Free Radic. Biol. Med. 14, 649-653.

Shatwell, K. P. and Segal, A. W., 1996. NADPH oxidase. Int. J. Biochem. Cell Biol. 28, 1191-1195.

Shaw, P. J., Hopfensperger, M. J., Ganey, P. E., and Roth, R. A., 2007. Lipopolysaccharide and trovafloxacin coexposure in mice causes idiosyncrasy-like liver injury dependent on tumor necrosis factor-alpha. Toxicol. Sci. 100, 259-266.

Sheu, J. R., Lee, C. R., Hsiao, G., Hung, W. C., Lee, Y. M., Chen, Y. C., and Yen, M. H., 1999. Comparison of the relative activities of alpha-tocopherol and PMC on platelet aggregation and antioxidative activity. Life Sci. 65, 197-206.

Singh, I., 1996. Mammalian peroxisomes: metabolism of oxygen and reactive oxygen species. Ann. N. Y. Acad. Sci. 804, 612-627.

Singh, I., 1997. Biochemistry of peroxisomes in health and disease. Mol. Cell Biochem. 167, 1-29.

Sinha, B. K., 1983. Enzymatic activation of hydrazine derivatives. A spin-trapping study. J. Biol. Chem. 258, 796-801.

Slater, T. F., 2008. Free radical mechanisms in tissue injury.

Smith, M. T., 2003. Mechanisms of troglitazone hepatotoxicity. Chem. Res. Toxicol. 16, 679-687.

Smith, M. T., Thor, H., Hartizell, P., and Orrenius, S., 1982. The measurement of lipid peroxidation in isolated hepatocytes. Biochem. Pharmacol. 31, 19-26.

Stadtman, E. R. and Levine, R. L., 2000. Protein oxidation. Ann. N. Y. Acad. Sci. 899, 191-208.

Starke, P. E. and Farber, J. L., 1985. Ferric iron and superoxide ions are required for the killing of cultured hepatocytes by hydrogen peroxide. Evidence for the participation of hydroxyl radicals formed by an iron-catalyzed Haber-Weiss reaction. J. Biol. Chem. 260, 10099-10104.

Starke, P. E., Gilbertson, J. D., and Farber, J. L., 1985. Lysosomal origin of the ferric iron required for cell killing by hydrogen peroxide. Biochem. Biophys. Res. Commun. 133, 371-379.

Straus, W., 1981. Cytochemical detection of mannose-specific receptors for glycoproteins with horseradish peroxidase as a ligand. Histochemistry 73, 39-47.

Suzuki, Y. J. and Packer, L., 1993. Inhibition of NF-kappa B activation by vitamin E derivatives. Biochem. Biophys. Res. Commun. 193, 277-283.

Tafazoli, S., Mashregi, M., and O'Brien, P. J., 2008. Role of hydrazine in isoniazid-induced hepatotoxicity in a hepatocyte inflammation model. Toxicol. Appl. Pharmacol. 229, 94-101.

Tafazoli, S. and O'Brien, P. J., 2004. Prooxidant activity and cytotoxic effects of indole-3-acetic acid derivative radicals. Chem. Res. Toxicol. 17, 1350-1355.

Tafazoli, S. and O'Brien, P. J., 2005. Peroxidases: a role in the metabolism and side effects of drugs. Drug Discov. Today 10, 617-625.

Tafazoli, S. and O'Brien, P. J., 2008. Accelerated cytotoxic mechanism screening of hydralazine using an in vitro hepatocyte inflammatory cell peroxidase model. Chem. Res. Toxicol. 21, 904-910.

Tafazoli, S., Spehar, D. D., and O'Brien, P. J., 2005a. Oxidative stress mediated idiosyncratic drug toxicity. Drug Metab Rev. 37, 311-325.

Tafazoli, S., Wright, J. S., and O'Brien, P. J., 2005b. Prooxidant and antioxidant activity of vitamin E analogues and troglitazone. Chem. Res. Toxicol. 18, 1567-1574.

Timbrell, J. A. and Harland, S. J., 1979. Identification and quantitation of hydrazine in the urine of patients treated with hydralazine. Clin. Pharmacol. Ther. 26, 81-88.

Timbrell, J. A., Scales, M. D., and Streeter, A. J., 1982. Studies on hydrazine hepatotoxicity. 2. Biochemical findings. J. Toxicol. Environ. Health 10, 955-968.

Tomasi, A., Billing, S., Garner, A., Slater, T. F., and Albano, E., 1983. The metabolism of halothane by hepatocytes: a comparison between free radical spin trapping and lipid peroxidation in relation to cell damage. Chem. Biol. Interact. 46, 353-368.

Toth, B., 1978. Tumorigenic effect of 1-hydrazinophthalazine hydrochloride in mice. J. Natl. Cancer Inst. 61, 1363-1365.

Toth, B. and Shubik, P., 1966. Carcinogenesis in Swiss mice by isonicotinic acid hydrazide. Cancer Res. 26, 1473-1475.

Tukov, F. F., Maddox, J. F., Amacher, D. E., Bobrowski, W. F., Roth, R. A., and Ganey, P. E., 2006. Modeling inflammation-drug interactions in vitro: a rat Kupffer cell-hepatocyte coculture system. Toxicol. In Vitro 20, 1488-1499.

Tyurina, Y. Y., Kini, V., Tyurin, V. A., Vlasova, I. I., Jiang, J., Kapralov, A. A., Belikova, N. A., Yalowich, J. C., Kurnikov, I. V., and Kagan, V. E., 2006. Mechanisms of cardiolipin oxidation by cytochrome c: relevance to pro- and antiapoptotic functions of etoposide. Mol. Pharmacol. 70, 706-717.

Ueda, J., Tsuchiya, Y., and Ozawa, T., 2001. Relationship between effects of phenolic compounds on the generation of free radicals from lactoperoxidase-catalyzed oxidation of NAD(P)H or GSH and their DPPH scavenging ability. Chem. Pharm. Bull. (Tokyo) 49, 299-304.

Uetrecht, J., 2005. Current trends in drug-induced autoimmunity. Autoimmun. Rev. 4, 309-314.

Valko, M., Rhodes, C. J., Moncol, J., Izakovic, M., and Mazur, M., 2006. Free radicals, metals and antioxidants in oxidative stress-induced cancer. Chem. Biol. Interact. 160, 1-40.

van den Bosch, H., Schutgens, R. B., Wanders, R. J., and Tager, J. M., 1992. Biochemistry of peroxisomes. Annu. Rev. Biochem. 61, 157-197.

Weglarz, L., Drozdz, M., Wardas, M., and Goss, M., 1989. Activities of antioxidant enzymes in fibroblasts cultured in vitro in the presence of hydralazine. Biomed. Biochim. Acta 48, 489-493.

Welinder, K. G., 1985. Plant peroxidases. Their primary, secondary and tertiary structures, and relation to cytochrome c peroxidase. Eur. J. Biochem. 151, 497-504.

Wernsdorfer, W. H., 1983. Urgent efforts needed to combat drug-resistant malaria. WHO Chron. 37, 11-13.

Whiting, R. F., Wei, L., and Stich, H. G., 1979. Enhancement by transition metals of unscheduled DNA synthesis induced by isoniazid and related hydrazines in cultured normal and xeroderma pigmentosum human cells. Mutat. Res. 62, 505-515.

Williams, D. P. and Park, B. K., 2003. Idiosyncratic toxicity: the role of toxicophores and bioactivation. Drug Discov. Today 8, 1044-1050.

Witting, P. K., Mohr, D., and Stocker, R., 1999. Assessment of prooxidant activity of vitamin E in human low-density lipoprotein and plasma. Methods Enzymol. 299, 362-375.

Wong, P. K., Poyer, J. L., DuBose, C. M., and Floyd, R. A., 1988. Hydralazine-dependent carbon dioxide free radical formation by metabolizing mitochondria. J. Biol. Chem. 263, 11296-11301.

Woo, J., Chan, C. H., Walubo, A., and Chan, K. K., 1992. Hydrazine--a possible cause of isoniazid--induced hepatic necrosis. J. Med. 23, 51-59.

Wright, J. S., Johnson, E. R., and DiLabio, G. A., 2001. Predicting the activity of phenolic antioxidants: theoretical method, analysis of substituent effects, and application to major families of antioxidants. J. Am. Chem. Soc. 123, 1173-1183.

Yamamoto, K. and Kawanishi, S., 1991. Free radical production and site-specific DNA damage induced by hydralazine in the presence of metal ions or peroxidase/hydrogen peroxide. Biochem. Pharmacol. 41, 905-914.

Yard, A. S and McKennis, H. Jr, 1955. Effect of structure on the ability of hydrazino compounds to produce fatty livers. J. Pharmacol. Exp. Ther. 114, 391-397.

Yokoyama, Y., Beckman, J. S., Beckman, T. K., Wheat, J. K., Cash, T. G., Freeman, B. A., and Parks, D. A., 1990. Circulating xanthine oxidase: potential mediator of ischemic injury. Am. J. Physiol 258, G564-G570.

Yu, B. P., 1994. Cellular defenses against damage from reactive oxygen species. Physiol Rev. 74, 139-162.

Zdolsek, J., Zhang, H., Roberg, K., and Brunk, U., 1993. H2O2-mediated damage to lysosomal membranes of J-774 cells. Free Radic. Res. Commun. 18, 71-85.

Zetterberg, G. and Bostrom, G., 1981. Mitotic gene conversion induced in yeast by isoniazid. influence of a transition metal and of the physiological conditions of the cells. Mutat. Res. 91, 215-219.

Zingale, S. B, Minzer, L, Rosenberg, B, and Lee, S. L, 1963. Drug induced lupus-like syndrome. Clinical and laboratory syndrome similar to systemic lupus erythematosus following antituberculous therapy: report of a case. Arch. Intern. Med. 112, 63-66.

Appendices

Appendix I: List of Drugs that did not Form Cytotoxic Radicals in the Hepatocyte Inflammation Model

The toxicity of the following drugs did not increase in the presence of a H_2O_2 generating system with or without peroxidase. This could be because 1) these drugs are not oxidized to radicals by peroxidase/H_2O_2 or P450/H_2O_2; 2) rapid Phase II drug metabolism; 3) radicals readily dimerize or disproportionate; 4) radicals formed are strong antioxidants or 4) the radicals formed are reduced by P450 reductases. More research is required to further determine the mechanism(s) involved.

Table AI.1 List of the drugs that did not form cytotoxic pro-oxidant radicals in the hepatocyte inflammation model

Name of the drugs tested	Therapeutic use	Dose range tested
Tribromoethanol (Avertin®)	Anesthetic	0.1 – 1 mM
Acetylsalicylic acid (Aspirin®)	Analgesic	1 - 5 mM
Ranitidine (Zantac®)	Antacid	0.5 - 2 mM
Naproxen (Naprosyn®, Aleve®)	Antipyretic/Analgesic	0.3 - 3 mM
Ciglitazone	Antidiabetic	0.1 - 1 mM
Pioglitazone (Actos®)	Antidiabetic	0.1 – 1 mM
Leflunomide (Arava®)	Anti-arthritic	0.1 – 1 mM

Hepatocytes (10^6 cells/mL) were preincubated at 37°C for 30 min in Krebs-Henseleit buffer (pH 7.4). Hepatocytes were treated with different concentrations of drugs and were then exposed to non-toxic H_2O_2 generating system (10 mM glucose and 0.5 U/mL glucose oxidase), in the presence and absence of 0.1 μM horseradish peroxidase (HRP) to mimic an inflammatory response. Cell viability was determined by trypan blue uptake.

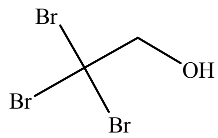

2,2,2-Tribromoethanol (Avertin)

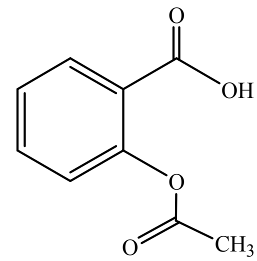

Acetylsalicylic acid (Aspirin)

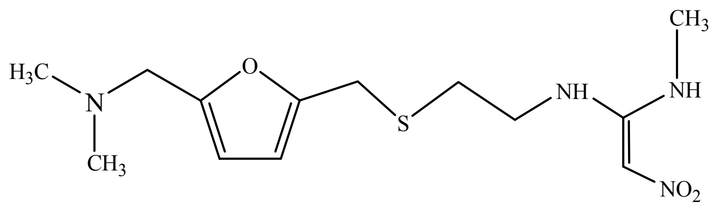

Ranitidine (Zantac)

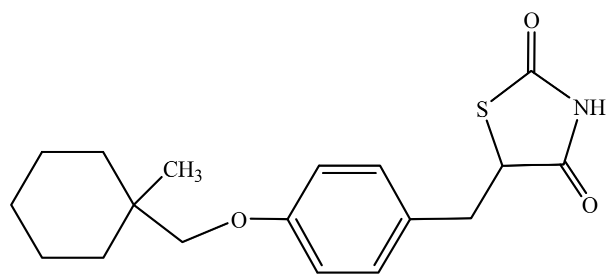

Ciglitazone

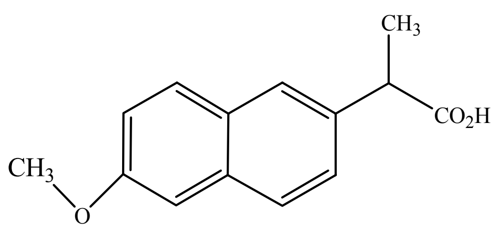

Naproxen (Aleve)

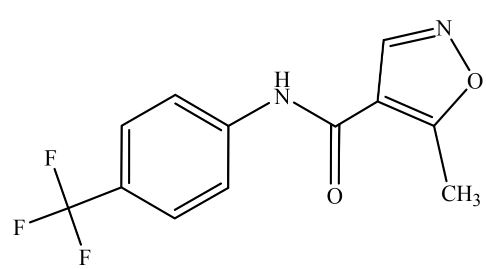

Leflunomide (Arava)

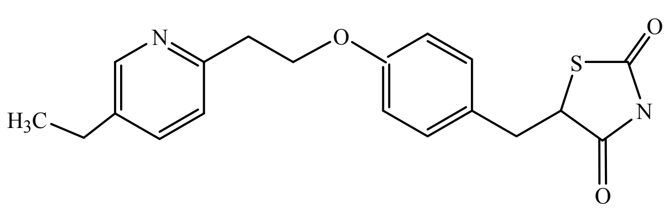

Pioglitazone (Actos)

Figure AI.1 Structure of the drugs that did not form cytotoxic pro-oxidant radicals in the hepatocyte inflammation model

Appendix II: A Preliminary *In vivo* Rat Study

The following *in vivo* animal study was carried out using *t*-BHP to assess the effect of inflammation on increased hydrazine-induced hepatotoxicity:

AII. 1 Animal treatment

Male Sprague-Dawley rats (200 ± 10g) were fed standard chow and housed in clear plastic cages. Care and treatment of the rats were in compliance with the guidelines of the Canadian Council on Animal Care, and the protocol was approved by the University of Toronto Animal Care Committee. The following environmental conditions applied throughout the course of the study; 12 h light/day cycle (lights on at 05:00 h), and an ambient temperature of 21–23 °C with a 50–60% relative humidity. The animals were allowed to acclimatize for 1 week and were fed a diet of standard rat chow and given water *ad libitum*. After 1 week the animals were randomized and divided equally into five groups of three animals each: Group A (control) received vehicle (0.9% saline solution) only. Group B was given 0.05 mmol/kg *t*-BHP (dissolved in 0.9% saline) intraperitoneally (i.p.). Group C was injected i.p. with 10 mg/kg hydrazine hydrate (dissolved in water). Group D was co-treated with *t*-BHP and hydrazine and Group E was given *t*-BHP 2 hours before hydrazine administration. Animal were then anesthetized 18 hrs later by CO_2 inhalation as described (Liu et al, 2002a) and the blood samples were collected from abdominal aorta and plasma was separated by centrifugation and was aliquoted for storage at -20 °C for later analysis. A small portion of liver was removed for the GSH assay.

AII. 2 Hepatotoxicity assessments

The hepatic enzymes, aspartate aminotransferase (AST) and alanine aminotransferase (ALT), were used as the markers for early acute hepatic damage. The serum activities of AST and ALT were determined spectrophotometrically using Infinity-ALT reagent from Thermo Electron Corp. (Louisville, U.S.A) (Reitman and Frankel, 1957), as summarized in Figures AII.1 and 2.

AII.3 GSH assay

Reduced GSH was determined as described by the method of Hissin and Hilf (Hissin and Hilf, 1976). Briefly, the liver sample was homogenized in 1 mL of 0.2 M phosphate buffer (pH 8), and the mixture was centrifuged at 12,000 × *g* for 30 min. A supernatant (0.5 mL) was mixed with 0.5 mL of 4% 5-sulfosalicylic acid, kept 5 min at 4 °C, and centrifuged again at 3000 × *g* for 10 min. The supernatant obtained (0.5 mL) was mixed with 2 mL of 0.2 M phosphate buffer and 10 mL of 10 mM Ellman's reagent, 5,5′-dithiobis(2-nitrobenzoic acid) (DTNB). The absorbance was measured at 412 nm. The procedure is based on the reaction of the thiol with DTNB to give the mixed disulfide and 2-nitro-5-thiobenzoic acid (TNB) which is quantified by the absorbance of the dianion (TNB^{2-}) at 412 nm. The molar absorption coefficient of purified TNB^{2-} at 412 nm (14,150 M^{-1} cm^{-1}) was used to calculate the concentration of GSH (Riddles et al, 1979). The results are shown in Figure AII.3.

AII.4 Statistical analysis

Statistical analysis was performed by one-way ANOVA.

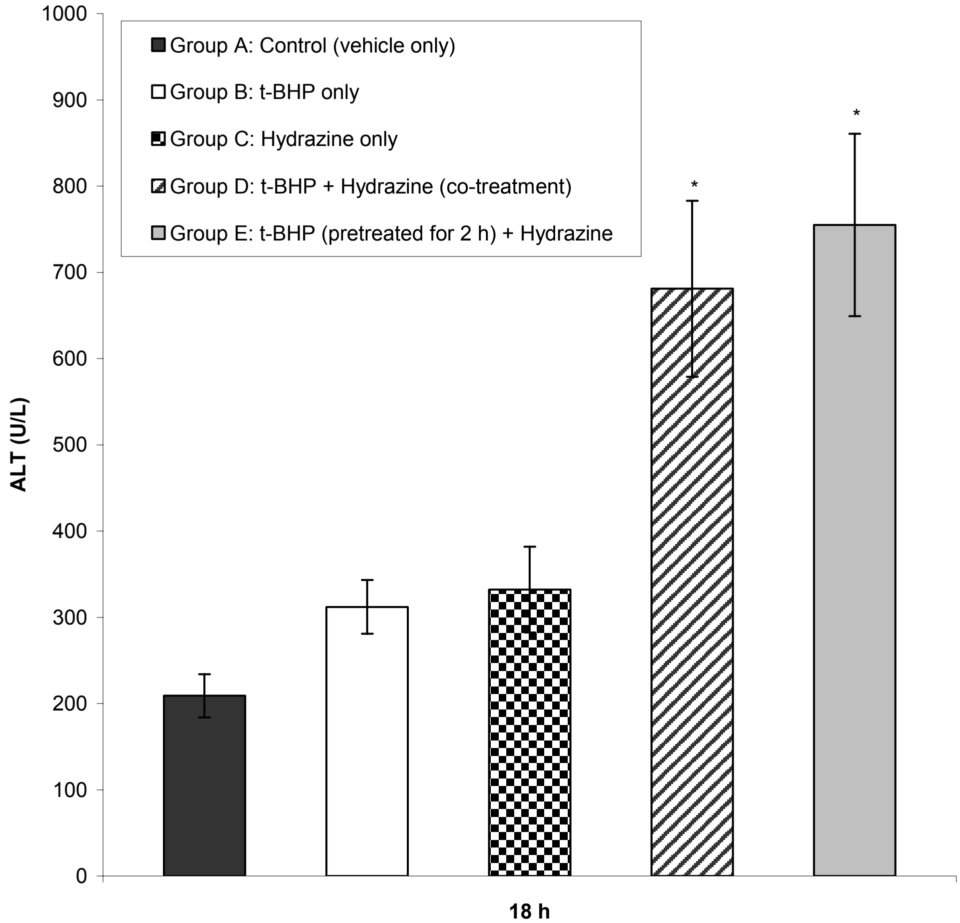

Figure AII.1 Hydroperoxide oxidative stress increased hydrazine-induced hepatotoxicity *in vivo* (using ALT as a biomarker)
Hepatotoxicity was followed by increased serum alanine aminotransferase (ALT) activity assayed spectrophotometrically using Infinity-ALT reagent. The animals were randomized and divided equally into five groups of three animals and the i.p. treatments were as follows: **Group A** (control): vehicle (0.9% saline solution) only; **Group B**: 0.05 mmol/kg *t*-BHP (dissolved in 0.9% saline); **Group C:** 10 mg/kg hydrazine hydrate (dissolved in water); **Group D**: Co-treatment with *t*-BHP and hydrazine; **Group E**: Pretreatment with 0.05 mmol/kg *t*-BHP 2 hours before 10 mg/kg hydrazine. *Significant as compared to animals treated with vehicle only ($P < 0.05$). Means ± SE of 3 animals were used.

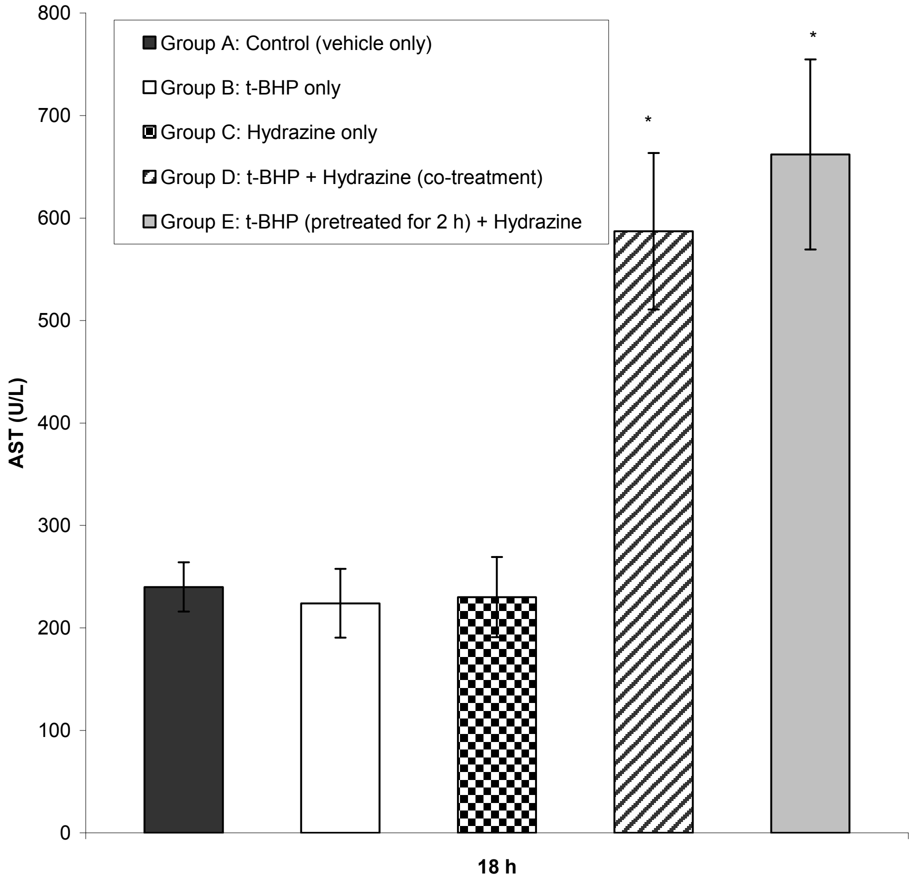

Figrue AII.2 Hydroperoxide oxidative stress increased hydrazine-induced hepatotoxicity *in vivo* (using AST as a biomarker)
Hepatotoxicity was followed by increased serum aspartate aminotransferase (AST) activity assayed spectrophotometrically using Infinity-AST reagent. The animals were randomized and divided equally into five groups of three animals and the i.p. treatments were as follows: **Group A** (control): vehicle (0.9% saline solution) only; **Group B**: 0.05 mmol/kg *t*-BHP (dissolved in 0.9% saline); **Group C:** 10 mg/kg hydrazine hydrate (dissolved in water); **Group D**: Co-treatment with *t*-BHP and hydrazine; **Group E**: Pretreatment with 0.05 mmol/kg *t*-BHP 2 hours before 10 mg/kg hydrazine. *Significant as compared to animals treated with vehicle only ($P < 0.05$). Means ± SE of 3 animals were used.

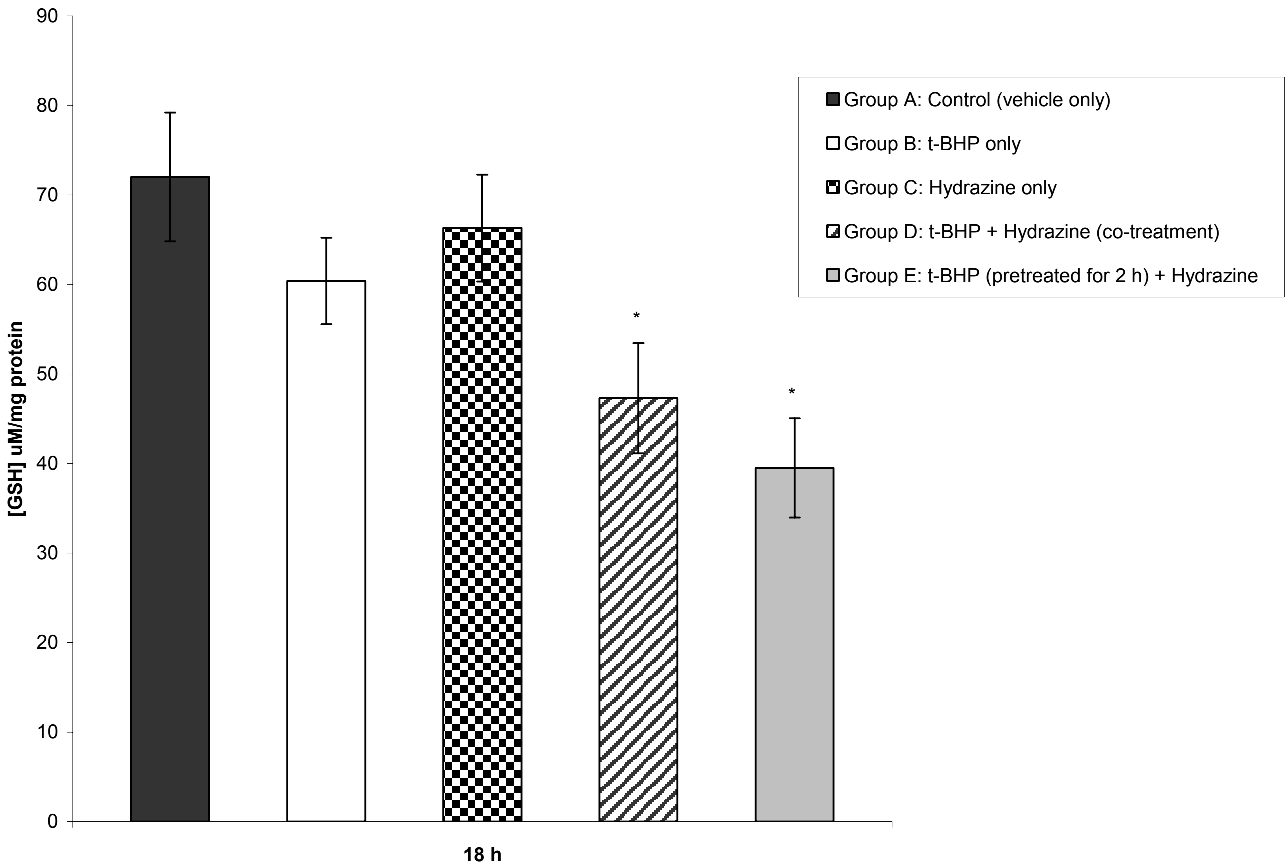

Figure AII.3 Effects of *t*-BHP and hydrazine co-treatment on hepatic levels of GSH (µg/mg protein)

The concentration of GSH was calculated by using the extinction coefficient of 14,150 M^{-1} cm^{-1} following the addition of DTNB (Ellman's reagent). The animals were randomized and divided equally into five groups of three animals and the intraperitoneally treatments were as follows: **Group A** (control): vehicle (0.9% saline solution) only; **Group B**: 0.05 mmol/kg *t*-BHP (dissolved in 0.9% saline); **Group C:** 10 mg/kg hydrazine hydrate (dissolved in water); **Group D**: Co-treatment with *t*-BHP and hydrazine; **Group E**: Pretreatment with 0.05 mmol/kg *t*-BHP 2 hours before 10 mg/kg hydrazine. *Significant as compared to animals treated with vehicle only ($P < 0.05$). Means ± SE of 3 animals were used.

Appendix III: The Cytotoxic Pathways of the Idiocyncratic Drugs Researched in the Thesis Chapters

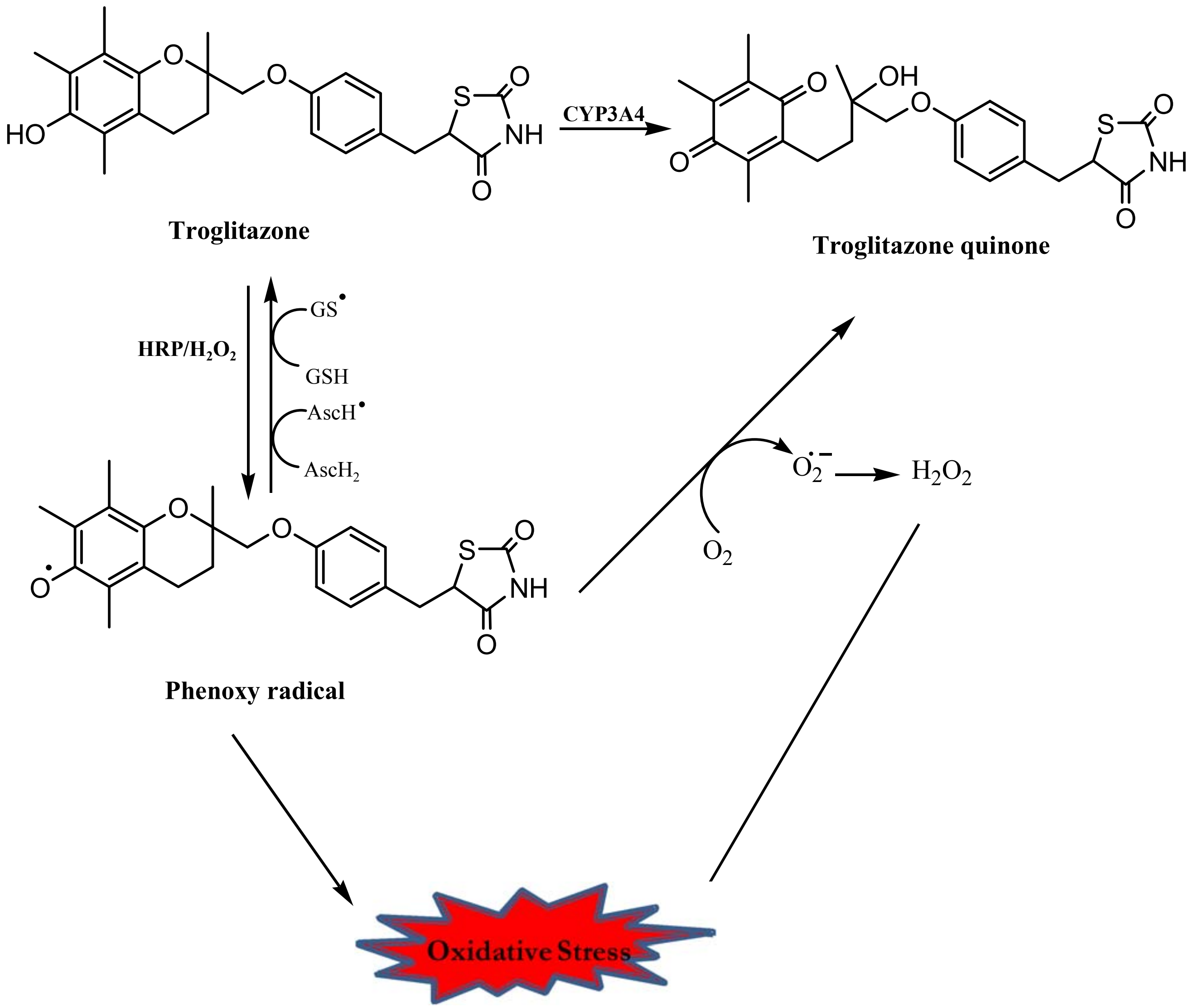

Figure AIII.1 Proposed troglitazone-induced toxicity in the hepatocyte inflammation model (*Chapter 2*)

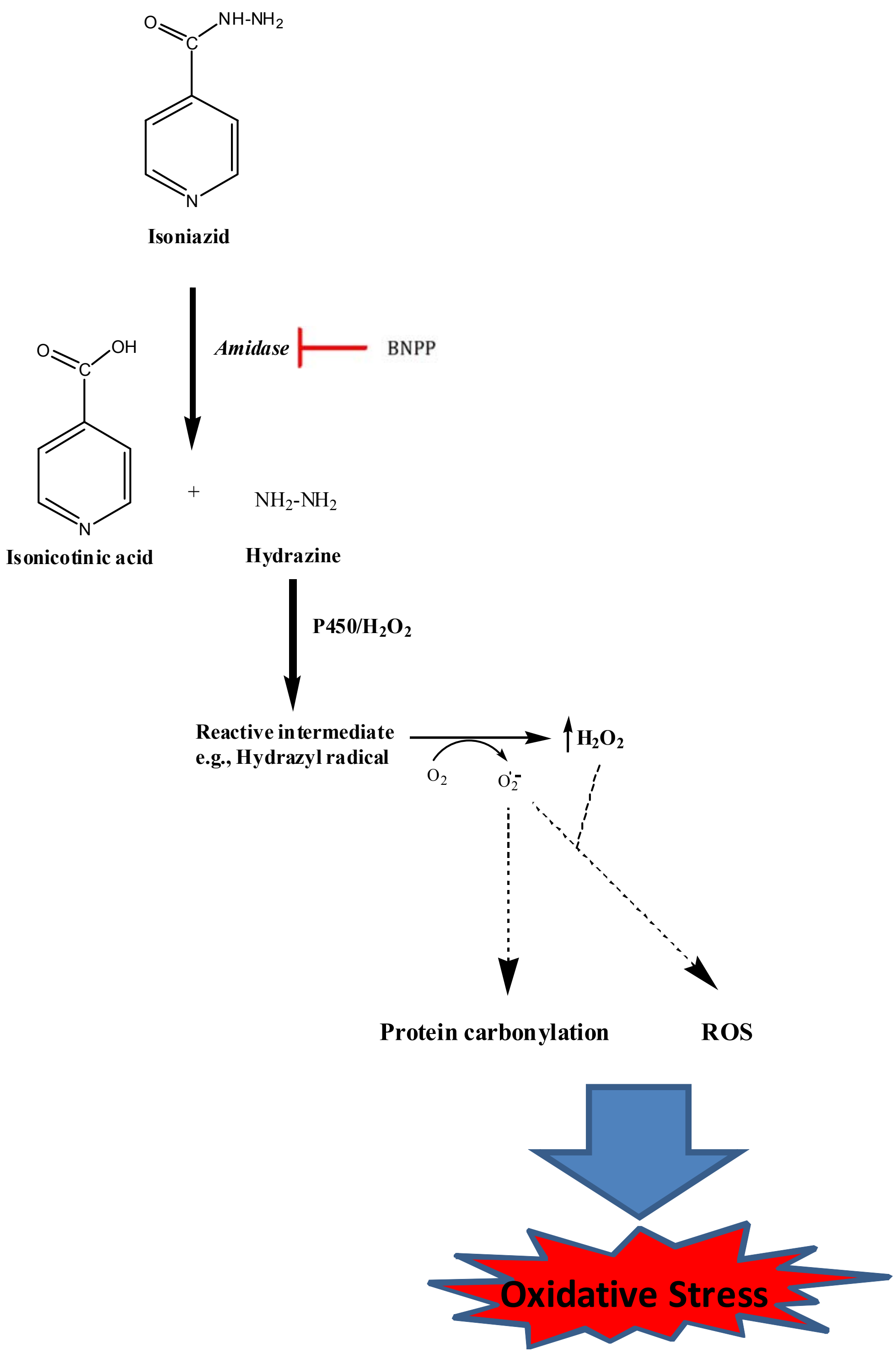

Figure AIII.2 Proposed mechanism of isoniazid cytotoxicity in the inflammation model: Role of hydrazine (*Chapter 3*)

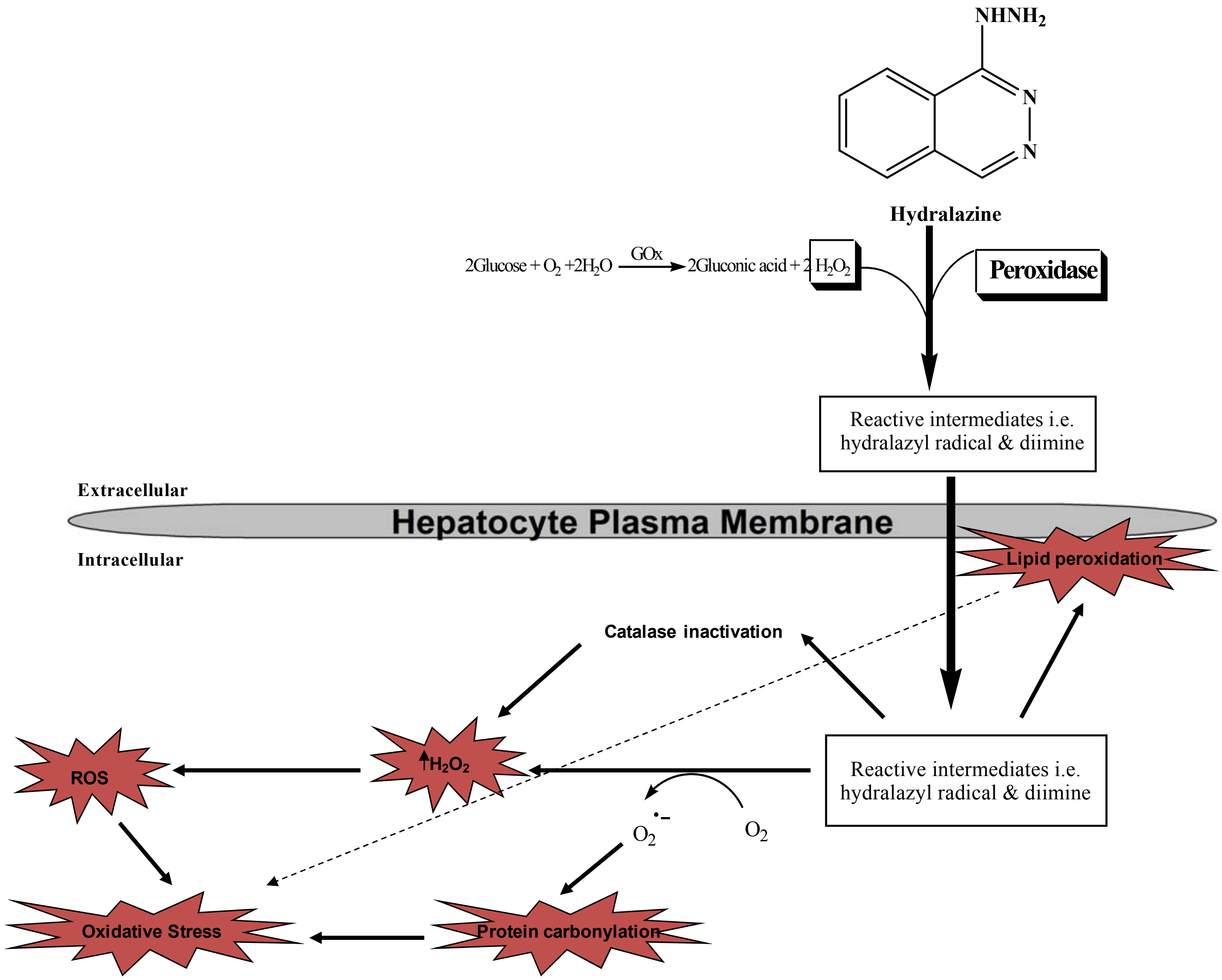

Figure AIII.3 Hydralazine-induced oxidative stress in the hepatocyte peroxidase inflammation model (*Chapter 4*)

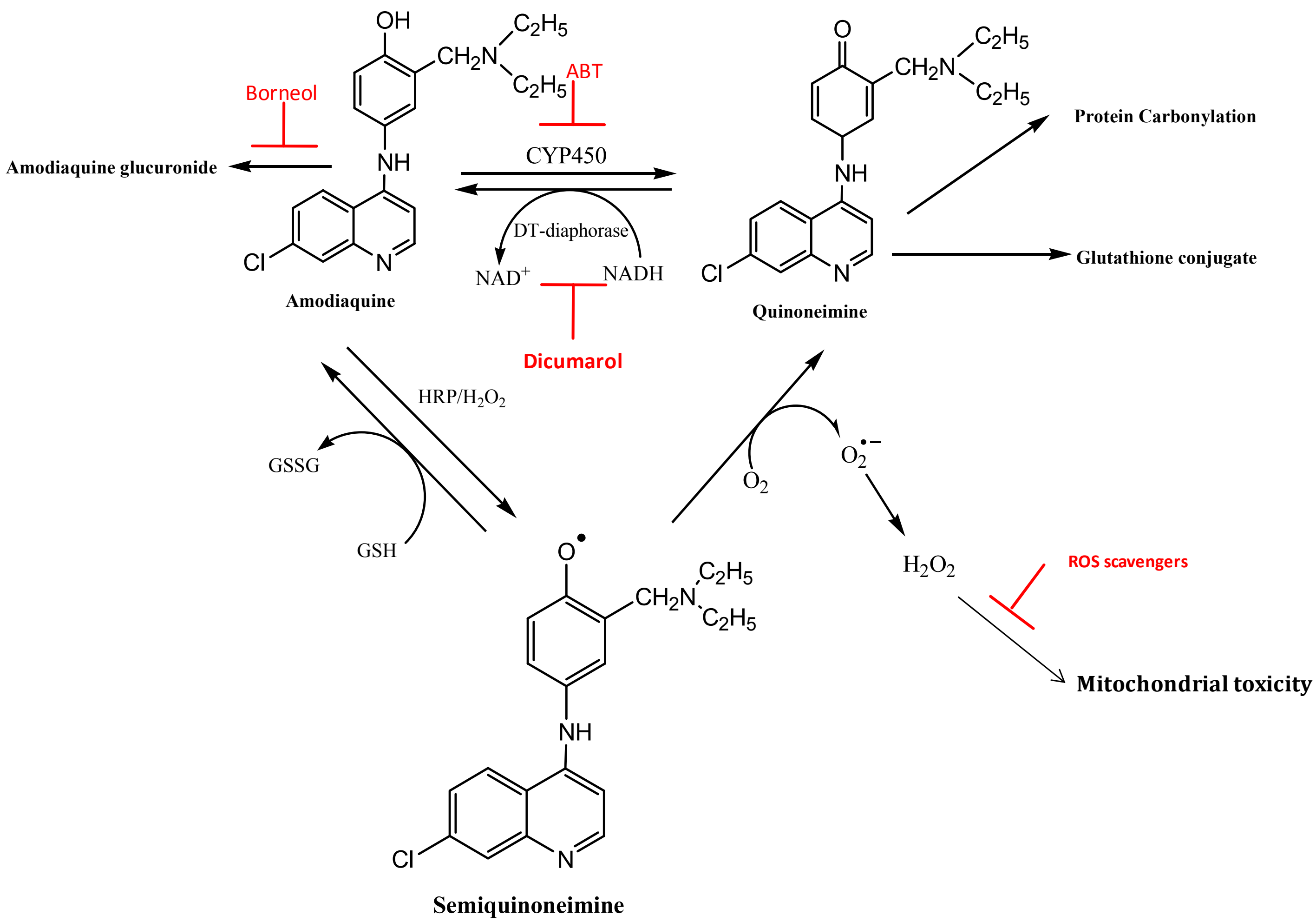

Figure AIII.4 Proposed mechanism of amodiaquine-induced cytotoxicity in the hepatocyte inflammation model (*Chapter 5)*